THE UNIVERSITY OF
SYDNEY

THE UNIVERSITY OF SYDNEY

DEVELOPMENT OF SOFT TISSUE REGENERATIVE SCAFFOLD WITH ANTIBACTERIAL ACTIVITY

VO THI DIEM THI

March 2014

A thesis submitted in fulfillment of the requirements for the degree of Master of Philosophy

School of Aerospace, Mechanical and Mechatronic Engineering, Faculty of Engineering & Information Technologies, The University of Sydney.

Supervised by

Professor Andrew Ruys

Dr Philip Boughton

Associate Professor Karen Vickery

ABSTRACT

With increasingly aging and sedentary populations, chronic wounds have been reported to be approaching pandemic proportions. Chronic wounds are defined by slow or absent healing. Accumulation of wound bacteria forms a biofilm that can inhibit wound healing and the action of antibiotics. Conventional skin grafts can readily harbor bacterial and fungal cells while excluding penetration of larger immune cells and essential neo-vascularization.

Soft tissue regenerative scaffolds with highly interconnected porosity have been developed for wound healing. In this research, scaffolds were fabricated with bioactive components to impart antibacterial activity. The interconnective porosity of the scaffold was preserved through using thermally forming composite scaffolds. Bioactive glass (45S5), bulk metallic glass (MgZnCa), and infused antibiotic (Cephazolin sodium) were utilised to form the composite eluting scaffolds.

A novel *in vivo* wound model was generated to simulate the wound environment. This consisted of perfusing media, proximal biofilm, planktonic bacteria, and bacterial cells which attached within the scaffold. A confluent biofilm of *Staphylococcus aureus* was generated on polymer coupons using a bioreactor (10^6 - 10^9 colony forming units (cfu)/ml each coupon). The coupons were placed within nutrient agar dishes (simulating tissue) underneath scaffold specimens. Gravity fed perfusion flow was set up using a drip-set kit.

The model successfully replicated the planktonic phase of the *Staph. aureus* life-cycle and infection of the scaffold from the wound model. Bacterial attachment assays were also conducted to assess the potency of bioactive component combinations. All composite scaffolds were observed to remain physically *in tact* throughout experiements.

Bioactive glass by itself did not contribute any detectable *Staph.* antibacterial activity whether on the scaffold or fused to a silicone substrate. Bioactive glass modified surfaces increased CFU measurements. When bioactive glass was present with MgZnCa and antibiotic, it appeared to contribute to a mild synergistic improvement in antibacterial activity. This strategy may facilitate soft tissue adhesion and further mitigate against bacterial infection.

Novel interconnective bioactive polymer composite scaffolds with particulate bioactive glass, MgZnCa metallic glass, infused antibiotic inhibited *Staph. aureus* proliferation within the scaffold compared to the smooth surfaced controls. This is the first instance of an *in-vitro* wound model with an infusion method and planktonic bacteria phase, applied to assess antibacterial activity synthetic scaffolds

DECLARATION OF CONTRIBUTION

- I conducted the background search based on various papers and wrote the literature survey
- I synthesised soft tissue scaffolds.
- I produced Bulk Metallic Glass coated, Bioglass infused, antibiotic infused scaffolds.
- I developed the novel *in vitro* scaffold-biofilm-wound model with the guidance of A/Prof Karen Vickery.
- I conducted bacterial attachment tests on scaffolds and antibiotic elution assays with assistance from Jessica Houang and under supervision of A/Prof Karen Vickery.
- I performed bacterial attachment tests on silicone samples and bioactive glass coated silicone samples provided by Devendra Gaire.
- I interpreted microbiological results with advice from A/Prof Karen Vickery and Dr Philip Boughton.
- I performed visual analysis on scanning electron microscope and fluoroscopic images taken by Alex Baume.
- I analysed and processed data attained from experiments, induced by discussion with my supervisor Prof Andrew Ruys and Dr Philip Boughton.

The above represents an accurate summary of the student's contribution

Thi Vo	Prof. Andrew Ruys
Student	Supervisor

ACKNOWLEDGEMENTS

First of all, I owe my supervisors Prof. Andrew Ruys a debt of gratitude for all he has done for me. He understood my difficulties inside and outside university as I am an international student and help me overcome obstacles from the very first stage of this study. I would like also take this opportunity to thank Dr. Philip Boughton for his attempt to give me an opportunity to conduct experiments in a state-of-art laboratory. Thank you to Drs.Philip and Elizabeth Boughton for their advice for writing the thesis. Their continued guidance and encouragement from the beginning to the end has been significantly precious.

I extend my sincere thanks to Jessica Houang, who has assisted me with work at Australian School of Advanced Medicine (ASAM) at Macquaire University (MQ). She shared a lot of time and effort to help me with language barrier I encountered. Many thanks must also be given to A/Prof Karen Vickery and Dr. Helen Hu, MQ, for their knowledge, guidance and assistance with laboratory work at ASAM. Without both of them, much of the biological experiments done would be impossible. Special thanks should be delivered to Ben Chow for his help with antibiotic experiments and good advice throughout this part.

I would also like to thank Helen Ma, Peter Lok, Alex Baume and Luthfi for their advice in scaffold production and writing, especially Alex for his help in SEM imaging. Thanks also to Micheal Rolph for his proofreading work.

I appreciate the help from all my close friends; especially Edward, Linda for sorting out my technical problem and console me during the most difficult phases of this degree. Thanks to another special friend Dinh for his continual support in student life.

With sincerity, this thesis is dedicated to my loving parents and my brother who gave me financial supports and encouragement to move ahead. In particular, I wish to thank my mother for her endless love and care from my hometown all the time.

TABLE OF CONTENTS

LIST OF FIGURES

LIST OF TABLES

CHAPTER 1

LITERATURE REVIEW

1.1 ANATOMY AND PHYSIOLOGY OF SKIN

The functionality of the skin is based on the integrity of its two primary tissue layers: the epidermis and dermis, which are shown in Figure 1.1.

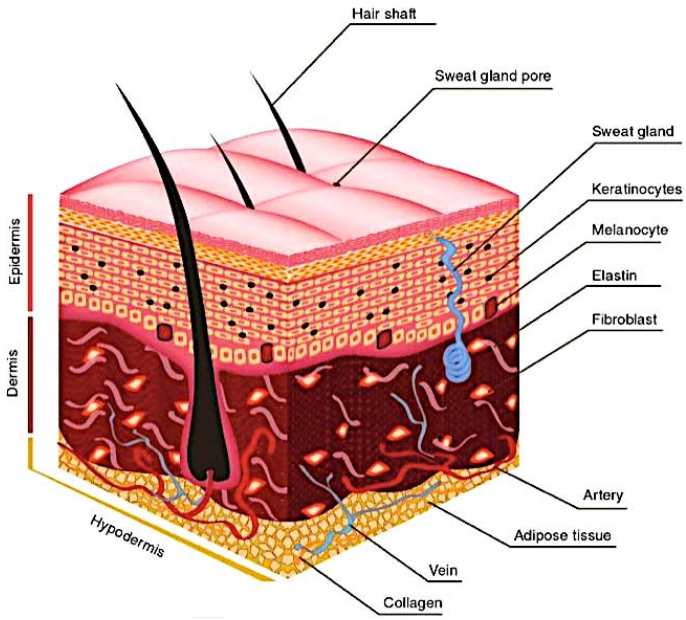

Figure 1.1: Skin structure showing two main layers, the skin appendages and the main cellular components.[1]

1.1.1 Epidermis

The epidermis is the outermost layer of the skin, forming a 0.06 – 1.4mm protective layer. This layer is impermeable, mechanically strong and enzyme resistant. The main cell type in the epidermis is the keratinocyte, which synthesises and deposits keratin which forms the stratum corneum [2]. When damage occurs to the corneum, pathogens are recognised by Langerhan cells, T-cells and Natural Killer- T cells and the immune response is triggered [3, 4].

Another prominent cell type in the epidermis is Merkel cells, which are pressure sensitive proprioceptors. In addition, melanocytes secrete the pigment melanin, which protects the body against ultraviolet radiation. Sebum is secreted by sebaceous glands, considered to be the surface film which protects against entry of microorganisms [5]. Furthermore, these

surface microorganisms are removed with dead keratinocytes which are regularly shed when new cell layers form on the skin surface [6].

1.1.2 Dermis

The dermis is the secondary layer of the skin, which is a 0.3- 3mm thick layer composed of blood vessels, sensory nerves, connective tissue and hair follicles. This layer is responsible for structural strength, hydration, thermoregulation and nutrient supply. The main components of the dermis are collagen, elastic fibers and extrafibrillar matrix, which provide resistance to force in all directions. This is particularly important for tensile strength, to prevent skin tearing in response to massive stretching [7]. One of three critical type cells in the dermis is the fibroblast, which can synthesise extracellular matrix, including collagen, elastin and plays a critical role in wound healing [8]. Other cells in the dermis involved in wound healing include endothelial cells in vessels and various immune cells [6]

1.1.3 Skin Function

In general, the roles of skin include:

- Serving as an anatomical barrier to physical, chemical and biological assaults from the external environment. The skin is the first line of defence system against infection. [9]
- Injury sensory perception from the external environment via a variety of nerve endings in the skin.
- Controlling evaporation to regulate internal body temperature.
- Storage of lipids and water.
- Contribute to the endocrine system by releasing hormones, growth factors and cytokines.
- Excretions from sweat, sebaceous and apocrine glands.

When the skin barrier is disrupted, its ability to perform its essential functions is impaired. It is therefore vital to restore its integrity as soon as possible. A wound is defined as a break in the epithelial integrity of the skin. However, the disruptions can also go deeper, extending to the dermis, subcutaneous fat, fascia, muscle and even bone. Skin can be lost due to burns, ulceration and postsurgical and posttraumatic wounds. A lack of sufficient donor tissue and the high cost of bioengineered skin mean there is a need for readily available and cost-effective synthetic skin grafts.

1.1.4 The Natural Wound Healing Process (Acute Wound)

Mammalian skin is able to recover from injury. The process occurs in four overlapping phases: haemostasis, inflammation, proliferation and remodeling, as shown in the following figure. [1].

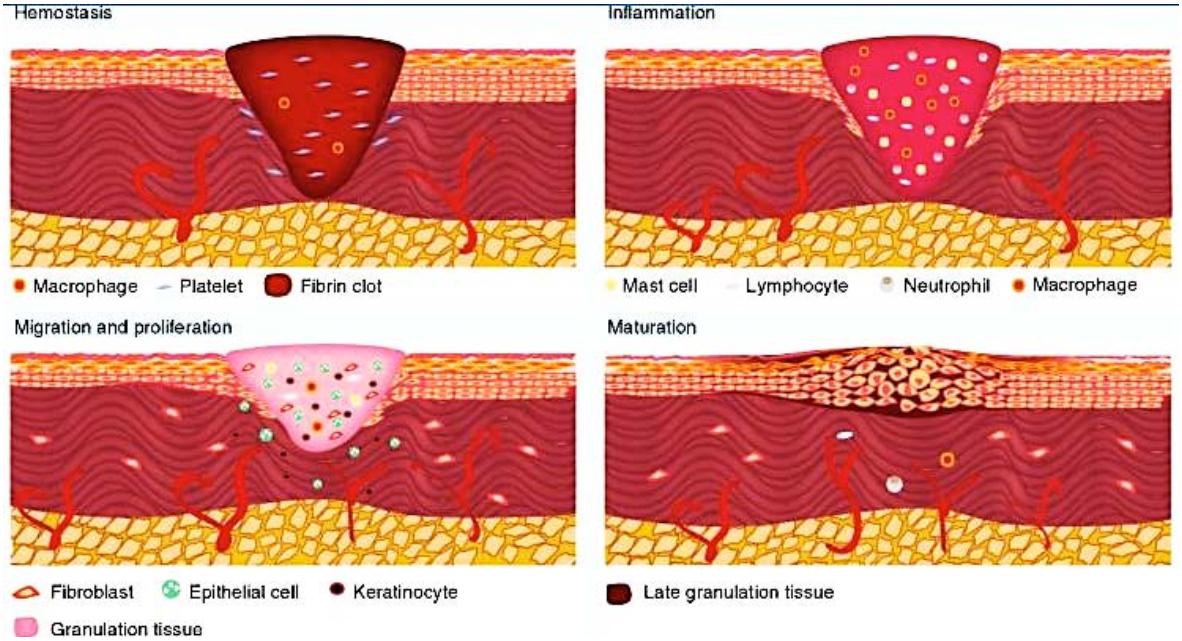

Figure 1.2: Phases of the wound healing process: haemostasis, inflammation, migration and proliferation, and maturation [1].

1.1.4.1 Haemostasis

This phase occurs in the moments immediately following injury. The wounded area fills with a clot to stop bleeding and prevent external contamination. In the later phases of healing, this clot will act as a temporary matrix, particularly its fibrin and platelet components, for the cells involved in reconstruction of the dermal tissue

1.1.4.2 Inflammation

The inflammation phase occurs almost simultaneously with haemostasis. In this phase, the cells responsible for wound cleaning—neutrophils, macrophages and lymphocytes, migrate to the wound site and produce inflammatory mediators. These cells contain any microorganisms and activate fibroblasts and epithelial cells for tissue repair. The immune cells and other cells involved in tissue repair increase vascular permeability to facilitate further infiltration of immune cells.

1.1.4.3 Proliferation and Migration Phases

In this phase, epithelial cells and fibroblasts synthesise the constituents of the extracellular matrix, leading to the formation of granulation tissue. New connective tissue forms and generates new skin and vasculature.

1.1.4.4 Maturation

During this stage, there is a remodeling of the granulation tissue. This results in a change in the composition and properties of the tissue. The skin regains up to 80% of its original strength. A scar forms where collagen and extracellular matrix reshape and are deposited in the wound.

1.2 CHRONIC WOUNDS

1.2.1 Infection in Deep Chronic Wounds

A chronic wound can be defined as one that fails to heal within 3 months. Tarnuzzer and Schultz indicated that the major pathobiological causes of wound chronicity are advanced age, repeated trauma, local tissue ischemia with reperfusion injury, and high numbers of bacteria are the major pathobiological causes of wound chronicity [10]. The impaired healing in chronic wounds is due to a failure of the basic processes of acute wound healing. In chronic wounds, there is a significant increase in tissue levels of proteases and collagenases, both of which can degrade matrix proteins and growth factors. The reduced level of these growth factors impairs cellular proliferation and chemotaxis, which are crucial processes for natural wound healing. It is not clear what influence bacteria have on this process, although the direct release of bacterial proteases and the indirect effect of protease release from phagocytic cells are both relevant (Figure 1.3).

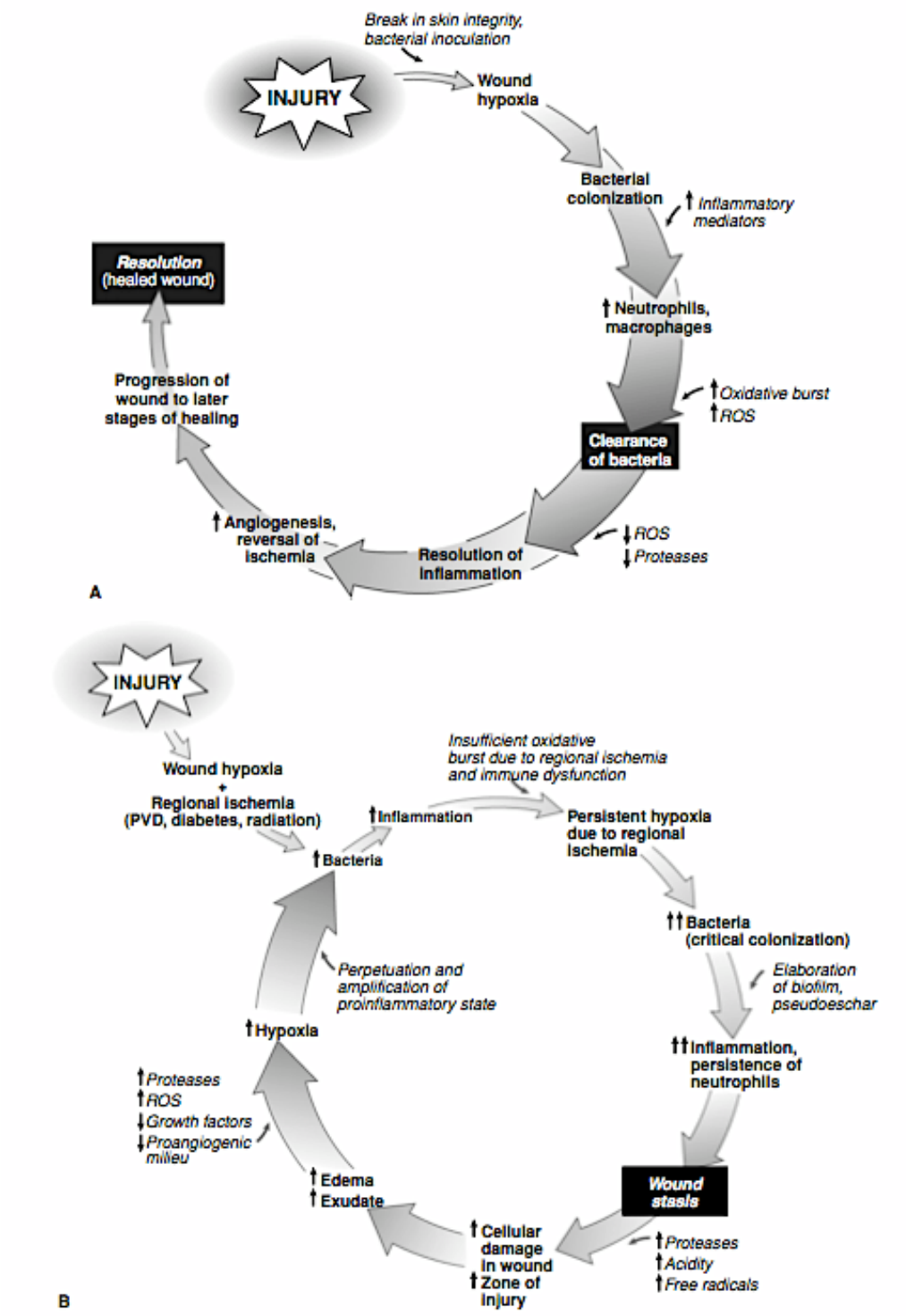

Figure 1.3: The normal inflammatory cascade of wound healing and non-healing (A) in a healthy patient and (B) in a patient suffering chronic wounds [11].

(A) At the wound bed, there is an early neutrophil-derived burst of reactive oxygen species (ROS) can kill bacteria. Once bacterial numbers decline, the oxidative burst decreases, thereby lessening damage to the surrounding tissue. The inflammatory phase of healing enables angiogenesis with resolution of wound hypoxia, and the wound proceeds to the latter stages of healing. However, in areas of regional ischemia (B), bacteria are not efficiently cleared, partly because of an ineffective oxidative burst (which requires oxygen). Local ischemia can result from conditions such as diabetes and aging, in which tissue oxygenation is impaired as a result of poor vascular supply. Bacteria can then multiply until a critical level of colonization is reached. Unless effective debridement and therapy takes place, bacteria continue to gather in a biofilm, causing an amplified and/or prolonged inflammatory response with wound stasis. This persistent inflammatory reaction and cellular damage will eventually result in the vicious cycle described.

1.2.2 Bacterial Colonisation of Chronic Wounds

1.2.2.1 Bacterial Invasion

Within one month after wounding, the Gram-positive organisms streptococci and corynebacterium begin to invade in the wound beds. In the case of non-healing ulcers, a broader-spectrum of organisms appears, including Gram-negative microbial such as coliforms, *Klebsiellae, Proteus spp.* and *Peptostreptococcus sppq* [12]. Numerous bacterial species come together to form biofilms in prolonged chronic wounds [13].

1.2.2.2 Biofilm Formation

A biofilm is defined as adherent microorganisms within a polymer matrix. Colonies can adhere to both organic and inorganic sites. This biofilm also contains water channels inside. Biofilms are formed by a wide range of bacterial species. The bacteria has a high level of resistance to antibacterial agents. Biofilms also induce chronic inflammation that delays healing [14, 15]. The mechanism for the resistance be effect of innate and induced factors, but this view is still controversial [16].

Furthermore, within the biofilms, the genotypic resistance of mutant cells can be enhanced by genetic transfer to other cells. As the consequent, resistant ability is improved, so the biofilm is further protected [15, 17]. Table 1.1 lists some common bacteria found in wounds. These have been isolated from patients in three recent studies.

Table 1.1: Bacterial species isolated from wounds [13, 18]

	Type of wound (specimen)					
	Mixed[a]		Venous ulcers (tissue specimens)[b]		Chronic wounds[c]	
Bacterial genus	Chronic (tissue)	Acute (biopsy)	Healers	Nonhealers	Swab culture	Tissue PCR
Staphylococcus	65	60	100	100	28	68
Enterococcus	62	80	…	…	12	18
Pseudomonas	35	20	88	70	32	28
Proteus	24	20	25	30	126	…
Citrobacter	24	20	…	…	8	28
Enterobacter	24	20	…	…	…	…
Streptococcus	22	0	25	60	…	…
Micrococcus	…	…	25	90	…	…
Escherichia	14	0	…	…	…	…
Morganella	8	0	…	…	…	…
Klebsiella	5	0	…	…	…	…
Acinetobacter	5	0	…	…	…	…
Serratia	3	0	…	…	…	…
Corynebacteria	…	…	…	…	0	68
Anaerobes	…	…	50	40	0	70

As shown in this table, there is a diversity of bacteria found in wounds. *Staphylococcus* spp. appears prominently in many types of wound. The most common variety of *Staphylococcus aureus* [19], an non motile, Gram-positive cocci, which attach to surfaces via adhension proteins on their cell wall [20] Therefore, in the current model, we seeded scaffolds with *Staphylococcus aureus*. Our motivation was to investigate treatments for *Staphyloccocus aureus* in the wound environment.

1.2.2.3 Antibiotics for Treating Bacteria

Antibiotic treatment can be effective in some situations. For example, many venous stasis ulcers develop a cellulitis that is difficult to control without antibiotic therapy.

Indications of infection include: (1) decrease in rate of healing, (2) increased pain and (3) straw-colored “oozing” of wound exudate from the skin. Coloured exudate is likely to be evidence of an underlying *Staphylococcus* cellulitis or lymphangitis.

Any patient with significant lymphedema and an open wound should be considered for antibiotic therapy. Antibiotics should also be used in contaminated wounds (oral flora, animal bites), as well as in patients with mechanical implants.

Systemic antibiotics can be delivered to tissues which have a good blood supply. For other tissues, topical antibiotics and/or removal of bioburden by cleansing are even more critical [21]. Table 1.2 lists some common antibiotics.

Table 1.2: Some common antibiotics for clinical treatment of infected wounds [22].

Product & Formulation	Bacterial spectrum	Advantages	Disadvantages	Refs
Neomycin Powder Cream:0.5% Ointment:0.5%	Gram-negatives except *P.aeruginosa* Gram-positives: S.auereus Not streptococci	Low cost May enhance re-epithelialisation	Potential for systemictoxicity Hypersensitivity with chronic use Bacterial resistance (staphylococci and Gram negative bacilli)	[56-60]
Bacitracin Ointment: 500units/g Powder	Gram-positives: Aerobic staphylococci &streptococci, corynebacteria, anaerobiccocci	No cross-resistance with other antibiotics Minimal absorption	Hypersensitivity with chronic use Bacterial resistance	[56-59]
Polymixin	Gram-negatives: including P.aeruginosa	Low cost Minimal potential for allergic eactions	Limited spectrum of activity	[56, 61]

These antibiotics can also be used combination, the most common being neomycin, bacitracin and polymixin. Using a combination allows a wider spectrum of bacteria to be treated [22].

1.2.2.4 Cephalosporin

Cephalosporin is mainly used to treat bacterial infections of the skin [23]. It is clinically effective against infections caused by Staphylococci (except methicillin-resistant *Staphylococus aureus*) and Streptococci of Gram-positive bacteria. These organisms are common on normal human skin. Resistance to cephalosporin is seen in several species of bacteria.

Cephazolin sodium, the first generation of cephalosporin, is used extensively as a prophylaxis antibiotic before wide range of surgical operations. This antibiotic interfere with the synthesis

of cell-walls, causing cell to rupture and die [24] Due to it's common use in clinic, in the current study we decided to incorporate cephazolin sodium into soft tissue regenerative scaffold, in order to treat bacteria present in skin wounds. Cephazolin sodium (Sandoz, Novartis) was the chosen antibiotic to load onto the scaffolds. This was to complement the chosen test bacteria of *Staphylococcus Aureus*. Their established binding affinity to hydrophobic sites made it a suitable choice for attaching to similarly hydrophobic polyester scaffolds [25]. The maximum absorbance peak of Cephazolizsodium was found at 270nm wavelength [26]

1.3 TREATMENTS FOR CHRONIC WOUNDS

Wound healing can be promoted by adherence to the following principles [27]:

- Overall health care such as control of diabetes, weight control and nutritional balance
- Wound debridement and treatment of infection
- Maintenance of a moist wound environment and stable temperature
- Restore arterial flow and allow wound exudates to drain freely
- Minimisation of scarring and restoration of function
- There are a number of techniques commonly used for treatment of wounds:

1.3.1 Negative Pressure Therapy (NPWT)

NPWT uses negative pressure to create a suction force that promotes wound healing by increasing blood flow and cellular activity, stimulating granulation tissue formation and reducing the likelihood of oedema [28].

This treatment has the advantages of a low complication rate [29] and the ability to treat chronic wounds caused by some rare diseases (e.g., complex reconstructions in plastic surgery) [30]. However, its efficiency in curing chronic wounds has not yet been definitively proven [29].

1.3.2 Wound Debridement

The process of preparing the wound bed for wound healing by reducing the bioburden is known as debridement. Without adequate debridement, a wound is persistently exposed to cytotoxic stressors and competes with bacteria for scarce resources such as oxygen and nutrients. Debridement step is a crucial step, as most problematic wounds afflict aged patients and occur in the setting of ischemia. Although non-surgeons and wound-product manufacturers have rediscovered the importance of debridement in the care of both acute and chronic wounds, many surgeons do not fully appreciate the importance of adequate

debridement. That many surgeons still allow wounds to heal under a “biologic dressing” or eschar suggest an under appreciation of the deleterious side effects that occur during the process of eschar formation.

Types of debridement include surgical, autolysis, enzymatic and mechanical. Autolysis is when debridement occurs through the action of leukocytes. Enzymatic and proautolytic agents prevent the crosslinking of exudated components and impede the formation of bacteria-sequestering pseudoeschar and biofilms from forming. Some dressings (notably hydrocolloid dressings) have the ability to rehydrate partially dehydrated and hardened scab tissue, which can then be phagocytosed by wound leukocytes.

A particularly useful mechanical debrider is the pressurized water jet (VersaJet, Smith & Nephew, Largo, FL), which has the ability to penetrate into microcrevasses in the wound bed to flush out entrapped particulate matter and bacteria. A Waterpik (Waterpik Technologies, Fort Collins, CO), or even a handheld shower spray, is a low-tech device that patients can use at home. Similarly, a syringe with a 20- gauge needle will generate the 15 psi necessary to reduce bacterial load in tissue.

Another means of achieving wound debridement is through the use of maggot therapy, which can be remarkably efficacious in removing devitalized material while sparing viable, well-perfused tissue. Some centers use this form of biologic debridement extensively.

1.3.3 Skin Substitutes

Skin substitute can be used to provide permanent protection of a wound area. Split skin and grafts from other areas have also shown good promise. Advantages of skin substitutes are the availability to treat large wound areas and to diminish the risk of infection or immunologic issues. However, their drawbacks include they are painful and relatively expensive compared to other methods[31]. Entrenched deep infection may still persist after the graft is deployed when antibiotic resistant bacteria or fungal infection is involved. In 2003, a paper described an individual with neuropathic joint and tarsometatarsal joints of the left foot who was successfully treated with skin cultured from neonatal foreskin tissue [32].

1.3.4 Free Flap

The term free flap means tissue transfer from a donate site to wound site. This method accelerates the healing of wound site and corrects scar contractures [33]. However, it contributes to morbidity and lack of donor sites. It is estimated that the ratio between wound site and donor site is 1:1 for split graft and 1:1.4 for full length graft [34]. Therefore, this method is not available for large wound area.

1.3.5 Tissue Engineering

Tissue engineering scaffolds play a vital role in providing ancillary support for tissue repair at sites of injury or disease [35].Tissue scaffolds, or matrices, are used for regenerative treatment where both the form and function of the native tissue are restored to healthy conditions [36]**.** This approach marks a shift from replacement of tissues as provisioned in prosthetic devices [28, 36-38]**.** Increasing the life-span of medical implants is a critical area of development, particularly as society seeks strategies to cope with an aging population [39].

The chief aims of tissue engineering approaches are therefore to:

(1) Improve the integration of implants within the body,

(2) To improve the health of damaged tissue by addressing underlying pathological issues and

(3) To be completely replaced and eliminated from the body in the long term.

Approaches to improve the attachment of tissue to medical devices have included the incorporation of bioactive materials and modulation of the implant shape/surface [40, 41]**.** Bioactive scaffolds which promote tissue regeneration have great potential for improving healing outcomes for a wide range of tissue types and conditions [42]. This will be discussed in more details in the later part of the chapter.

1.3.6 Bioengineered Skin Substitute

Table 1.4 describes the features of some commercially available skin substitutes.

	Commercial product	Company	Layers
Cellular epidermal replacement	Epicel®	Genzyme Corp.	Cultured epidermal autograft (autologous keratinocytes grown in the presence of murine fibroblasts)
	Epidex™	Euroderm GmbH	Cultured epidermal autograft (autologous outer root sheet hair follicle cells)
	Myskin™	Celltran Ltd.	Cultured epidermal autograft (autologous keratinocytes grown in the presence of irradiated murine fibroblasts)
	ReCell®	Clinical Cell Culture (C3), Ltd.	Autologous epidermal cell suspension
Engineered dermal substitute	AlloDerm®	LifeCell Corp.	Acellular donated allograft human dermis
	Dermagraft®	Advanced BioHealing Inc.	Bioabsorbable polyglactin mesh scaffold seeded with human allogeneic neonatal fibroblasts
	Integra®	Integra LifeSciences Corp.	Thin polysiloxane (silicone) layer; cross-linked bovine tendon collagen type I and shark glycosaminoglycan (chondroitin-6-sulfate)
	Matriderm®	Dr. Suwelack Skin & Health Care AG	Bovine dermal collagen type I, III, V and elastin
Engineered dermo-epidermal substitutes	Apligraf®	Organogenesis Inc.	Human allogeneic neonatal keratinocytes; bovine collagen type I containing human allogeneic neonatal fibroblasts
	OrCel®	Forticell Bioscience, Inc.	Human allogeneic neonatal keratinocytes on gel-coated non-porous side of sponge; bovine collagen sponge containing human allogeneic neonatal fibroblasts

Figure 1.4: Commercially available tissue engineering solutions for dermal injuries [4, 43-48].

1.4 DRUG DELIVERY SYSTEM (DDS)

Drug Delivery System (DDS) refers to a method or process to convey drugs to target places and manipulate drug release through pharmacokinetics and bio-distribution of drugs. Controlled DDS can provide an excellent method to delivery drugs to wound sites to promote healing process as well as supressing endless inflammatory reaction [49]. However, there is little literature applying long term DDS to wound healing [49]

Conventional drug delivery involves delivering a high concentration of drug instantly, in a burst. This might lead to toxicity, and to the drug being used up within a short period of time. This means that the drug may not able to reach its target site. Even it does, the concentration may be below the lowest efficient concentration. This kind of problem inhibits drug efficacy for chronic wounds.

To overcome this problem, one approach is to increase the dosage of the medication by increasing the number or concentration of treatments. However, this approach may raise the

risk of potential side effects. In addition, some drugs can only be effective after they overcome obstacles on their way to target site, such as digestion in the stomach, the brain-blood barrier or biofilm in the wound site. Unfortunately, conventional drug delivery does not provide any protection or way for drugs to pass through those obstacles, causing the efficacy of the drug to reduce. Therefore, a new and more effective method of drug delivery is needed.

Over the last three decades, DDS has been increasingly drawing scientists and engineers' interests for its significant advantages. One advantage is the controlled and sustained release of drugs. With the help of DDS, drug concentration *in vivo* can be maintained within a desirable time period without triggering any side effects, reducing the essential amount of drug for each dose and increased the efficiency of the drug. In addition, DDS can provide protection for the drug to en route to the target site. With the help of modern technologies, including micro-/nano-technology and surface technology, DDS allows the localised delivery of a drug. Releasing the drug at the target site without it being flushed away to irrelevant parts of the body ensures efficacy and safety. Improving safety and efficiency of "old" drugs is the goal of many researchers today. This is done by altering drug delivery behavior, including controlling the delivery rate, a slow and sustained delivery, and targeted delivery [50]. Certain biomaterials bond to both soft tissue and hard tissue [51]. This provides a convenient way to localise the DDS. DDS allow lengthy periods of drug action, extending to weeks or even months [52].

Drug release mechanisms for DDSs are usually controlled through diffusion, solvents or chemical means [53].

1.4.1. Diffusion-Controlled Delivery System

A diffusion-controlled DDS is often made of non-biodegradable materials (usually polymers). Diffusion-controlled system include "reservoir" or "matrix" approaches.

1.4.1.1 Reservoir System

The drug can be stored within core, known as s "reservoir system". The drug release rate of a reservoir system depends on the thickness and porosity of its membrane [53].

1.4.1.2 Matrix System

Alternately, the drug can be homogenously stored in a "matrix" [54].

For hydrophobic matrix, the diffusion rate is controlled by molecule structure of polymer, such as degrees of crosslink, crystallinity, branching and overlapping [55]. The release rate of lipophilic matrix is governed by hydrophobicity of the polymer.

When compared to biodegradable DDS, diffusion DDS has more controlled and longer drug release period [56]. The most common disadvantage of diffusion mechanism is the inability to achieve a constant release rate ("zero order release kinetics"). The release rate is initially high and decline rapidly [57].

1.4.2. Solvent Controlled Delivery System

Solvent - controlled systems can be controlled by swelling or osmosis.

1.4.2.1 Swell Controlled Systems

Swell control refers to drug release due to dimension change of hydrophilic polymer matrix after water absorption [58]. The matrix swells after absorbing water without dissolving. Once the water concentration reaches high enough to low down the glass-to-rubber transition below environmental temperature, the system relaxes [58]. As a result of that, drug leaches into the surrounding tissue.

The drug release rate mainly depends on characteristics of matrix, such as the degree of water absorption, level of hydration and degree of cross-link [58-60]. In addition, when the system contain ionic networks, the kinetics are governed by mass transfer limitations, including ion exchange and interaction [59, 60].

Generally, materials used in this approach are polymers, mostly hydrogels. These materials are biocompatible and easy to be tailored into variety of different physical forms, including slabs, micro-particles, nanoparticles, coatings, and films [61]. They can also withstand harsh environment such as low pH, high temperature, high ionic strength, and high electric fields [61]. The drug release rate of some swelling-controlled DDS can be triggered due to a change in pH [62]. However, they are not able to cope with drugs which are unstable in intestinal or colonic environment and low solubility at high pH environment [63].

1.4.2.2 Osmosis Controlled Systems

Osmosis-controlled DDS involves a semipermeable membrane, which allows permeation of water but not drug. When water is pushed into drug container by difference of osmotic pressure, volume of the container increase [64], leading to drug be pumped out through delivery orifice.

The drug release rate of the Osmosis-controlled DDS is mainly determined by: (1) thickness of semi-membrane,(2) level of leachable component of the membrane, (3) the osmotic pressure difference between inside and outside membrane [65]. However, Tobias et al. argues that for a large orifice, the diffusion rate is the dominant factor [66]

A key feature of osmosis controlled DDS is that performance is independent on external variables, such as pH, hydrodynamics of the external dissolution medium, stirring [67-69]. This system is suitable for delivering substances which are difficult to administrate due to their rapid degradation and poor absorption in the gastrointestinal tract [70]. In addition, literatures point out that most of osmosis-controlled DDSs can achieve a constant rate of drug release [68, 70].

Unfortunately, numerous challenges constrain the development of the DDS, including concentration polarization, membrane fouling, reverse solute diffusion and the requirement for membrane development [71]. Furthermore, the membrane may have a relatively low permeability. Therefore, the system cannot suit low aqueous solubility drugs [69, 72].

1.4.3 Chemical-Controlled Delivery System

Chemical control mechanisms include conjugation and biodegradation.

1.4.3.1 Conjugation Systems

Matrix-drug conjugation is the DDS where drug molecule binds with matrix via conjugation .This bond is cleaved through hydrolysis or enzyme cleavage when the matrix reaches its target site. The drug release kinetics of conjugation system depends on the concentration of cleaving agent or enzyme at target site [73]. Other influencing factors include molecule space condition of matrix, types of side chains [74], pH and temperature at the target site [75].

These systems can be tailored for drugs, with low solubility, low permeability, poor absorption and instability [75, 76]. Because the material matrix is usually polymer, backbone and side chain are easily modified [77]. The matrix can be designed to sensitive to external simulations such as pH, temperature, light and enzyme [77, 78]. Those features give a potential method for the DDS to suit various drugs and target different sites. Most importantly, published results indicate that this mechanism readily allows drugs to be delivered through the blood-brain barrier (BBB) [79, 80].

This approach can make pharmacokinetics controllable and greatly reduce the minimum requirement of drug dosage. However, there are still some disadvantages of Matrix-drug conjugation DDS. Firstly, it is not easy to find a perfect matrix for a drug. Kosasih [81] describes that an ideal system should satisfy requirements for chemical stability, non-toxicity and, not changing properties of the drug. It is not easy to find a matrix can meet all of those requirements. Furthermore, large molecules of some drugs are not suitable for the DDS because of limited matrix space. Since a matrix has to attach a lot of side chains, such as drug and targeting moiety, there are not many spaces for large molecules. Space conditions of a

matrix could also affect the chemical process of bond cleavage [74]. Environmental vectors also play a major influence on system reliability [75].

1.4.3.2 Biodegradation System

With biodegradable DDS systems, the drug is released during biodegradation of the matrix. Two common types of matrix materials are bioceramics and polymers. Drugs are released from polymer systems via cleavage or hydrolysis of enzyme sensitive bonds [82]. Drug release from bio-ceramic is through absorption of mineral elements such as calcium, phosphorous, strontium, zinc and iron [83].

The factors affecting drug elution rates vary between matrix materials. For polymers sensitive to hydrolysation, elution depends on matrix erosion, including bulk and surface erosion. Both behaviors can happen simultaneously. The varying degrees of each is still unclear [84]. Literature indicates erosion behavior may depend on the diffusivity of water inside matrix [84-86]. If hydrolysis is slower than penetration of water, it goes to bulk erosion, otherwise it leads to surface erosion [85]. When a constant, controlled drug release rate is required, surface erosion is more effective degradation method than bulk erosion of the matrix [84]

Furthermore, properties of a polymer system, also determine the ability of water accessing inside of matrix. A high glass transition temperature (Tg) indicates relatively limited molecular motion and less space available for water molecule penetration. Similarly, high degree of crystallinity means the polymer chain is tight and ordered, preventing water from ingress [87].

On the other hand, for enzyme sensitive polymer systems, the erosion rate is influenced by factors similar to matrix-drug conjugation DDS, but dominated by the concentration of specific enzymes [88].

1.5 BIODEGRADABLE MATERIALS FOR BIOENGINEERING

Biodegradable controlled DDS has drawn extensive research interest in the last two decades owing to overcoming obstacles of previously mentioned systems.

1.5.1 Biopolymers

Early DDSs were polymer-based non-degradable system. One of the first DDS systems was comprised of silicon rubber [89]. Drugs can be physically encapsulated into DDSs allowing for localised pharmacological activity when the delivery vector is injected or implanted into human body. However, this approach does not suit slowly diffuse ionic species or molecules whose relatively molecular mass are greater than 400. This is due to the polymer matrix acting as a interference factor for large molecules reducing the rate of diffusion [89]. To

address that problem, Davis [90] developed a new polyacrylamide (PAA) method. The use of PAA allowed the diffusion of large molecules, such as protein drugs, and prolonged the total release time to a few weeks. Langer et al. pointed out that this method has high risk of triggering inflammation in animals [91].

Since then, polymer-based degradable systems have been designed using biocompatible materials such as poly-(glycolic acid) and poly-(lactic acid) [52]. However, DDS derived from these polymers tend to have a reduced total release period. For instance, poly-(lactic acid) DDS with relatively molecular weights between 150,000 and 450,000 containing sulphadiazine only spends 90 days to release about 80% of the drug [52]. Conversely, drugs with a short life time, including luteinizing hormone, can be incorporated into these systems [89]. Nevertheless, the bulk erosion behaviour of polymer DDS need to be considered as it can have a major effect when developing a DDS with consistent release. In Table 3, common polymer material candidates are listed with their features and applications.

Table 1.3: Types of Polymer materials used in Drug Delivery System Applications

Polymer	Features	Applications	Refs
Poly-(glycolide)	Excellent fibre-forming ability; good initial mechanical properties	Bone internal fixation devices; drug delivery system	[82, 92]
Poly-(L-lactide) (PLLA)	Good tensile strength; low extension and a high modulus; ability to form high strength fibers	Load bearing applications; scaffold for ligament replacement;	[82]
Poly(DL-lactide) (PDLLA)	Compared to PLLA- much lower strength; faster degradation rate	Drug delivery systems; low strength scaffold	[82] [93]
Poly(lactide-co-glycolide) (PLGA)	Properties vary depending on the composition; variety of structures and forms; controllable degradation rates	Multifilament sutures; skin replacement materials; duramater substitutes; 3D scaffolds; space preservation; drug delivery system	[82, 94]
Polycaprolactone (PCL)	Hydrolytic degradation; high permeability; non-toxic; extremely high elongation; excellent biocompatibility	Long-term delivery system	[82, 95]
Poly(trimethylene carbonate) (PTMC)	Excellent flexibility	Soft tissue regeneration; drug delivery systems; suture materials	[82]

1.5.2 Polycaprolactone (PCL)

The scaffolds manufactured from biodegradable polymer polycaprolactone (PCL) has a slower degradation rate and as other biodegradable polymers. Therefore, they have a reduced inflammatory response than other materials commonly used in tissue engineering such as PLGA [96]. PCL scaffolds can be easy and affordable to manufacture and have an excellent shelf-life. These qualities mean PCL may be a suitable candidate for making scaffolds as a leave-in dressing for chronic wounds. In research conducted by our research group but not yet published, PCL-based scaffolds showed vascularisation throughout the scaffold after 2 weeks in a subcutaneous murine model. The scaffold has unique macro and microstructural characteristics and >95% porosity. Figure 1.5 shows some configurations of PCL which have been published in scientific literature.

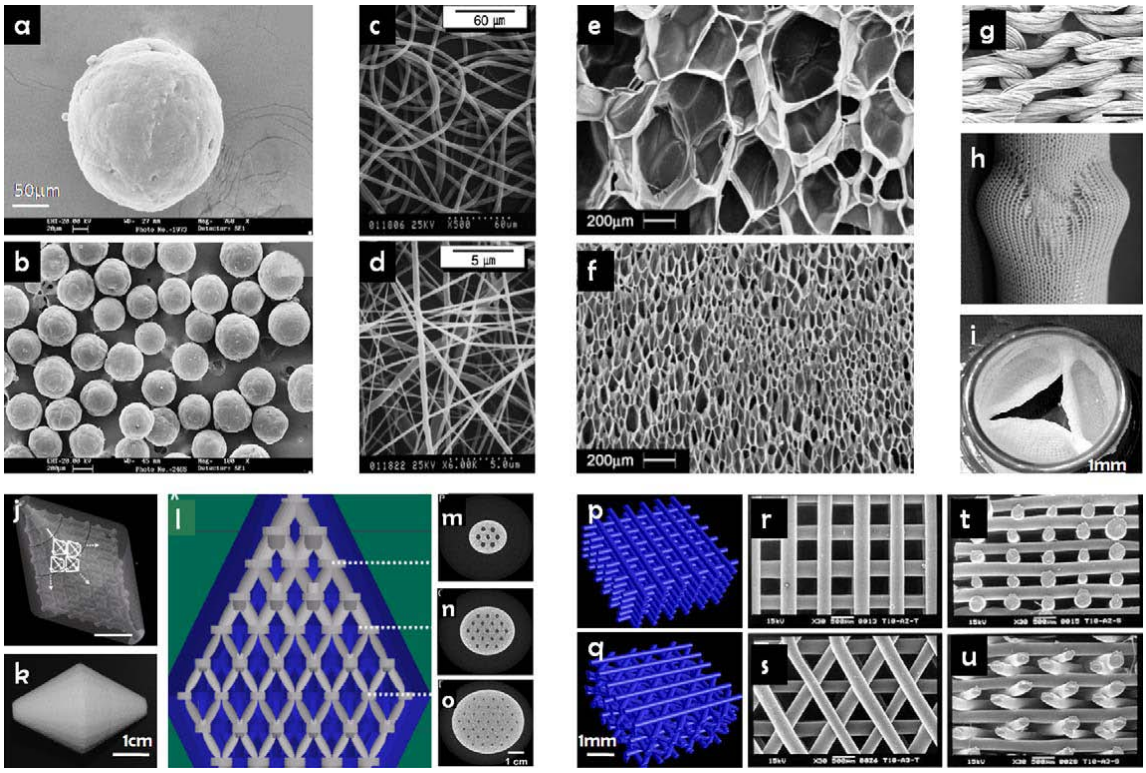

Figure 1.5: Structures made from PCL: Nanospheres (a,b). Nanofibres (c,d). Foams (e,f). Knitted textiles (g,h,i). Selective laser sintered scaffold (j-o). Fused deposition modeled scaffolds (p–u)[97].

1.5.2 Bioactive, Bioresorbable Bioceramics

Bioactive bioceramics have been used clinically since the 1970's [98]. Traditionally, they have been used as bone fillers, but more recently they have been common as implant coatings for their capacity to bond with bone [99]. They can be produced almost completely inert or with varying degrees of interaction with the physiological environment. This is known as "bioactivity". Bioceramics with a high level of bioactivity are completely bioresorbed by the body, forming products such as silica, calcium and phosphorus. Metallic or polymer surfaces can be rendered bioactive through the incorporation of ceramics of glass-ceramics.

Bioceramics include calcium phosphates (e.g. hydroxyapatite, tricalcium phosphate), calcium silicates (e.g wollastonite, hardystonite, sphene) and silica-based bioactive glasses (e.g. Bioglass). Compared to the more stable hydroxyapatite, calcium phosphates exhibit a greater degree of bioactivity and are completely absorbed into the body [100]. The incorporation of silicon results in a further increase in bioactivity by leading to the formation of Si-OH groups on the surface, thus improves bone binding by triggering the nucleation and formation of apatite layers on the surface. Silicon can be incorporated into calcium phosphate, and SiO_2 is the network former of silica-based bioactive glasses.

1.5.2.1 Calcium Phosphates

One of the most popular bioceramics is hydroxyapatite (Ca_{10} $(PO_4)_6(OH)_2$), HA), due to its biocompatibility and having the same chemical composition as bone mineral. Hydroxyapatite coatings have been used since the late 1980's, and excellent clinical results on total hip replacement 15 years+ after implantation [101]. These coatings remove the need for bone cement, while providing a seal against wear debris. Hydroxyapatite and TiCaP coatings have also been used clinically for coatings for spine implants (e.g. NuVasive) [102, 103] Fibrous encapsulation was avoided by a particulate hydroxyapatite coating on a nucleus replacement implant (ultra-high-molecular weight polyethylene woven mesh) [102, 103]. This coating encouraged good tissue integration and physiological motion during the first 6 months. However, progressive stiffening occurred as scar tissue calcified to form bone.

1.5.2.2 Calcium Silicates

Calcium silicates ($CaO\text{-}SiO_2$) were developed in the 1990s for biomedical applications, particularly by De Aza and co-workers [104]. They are highly bioactive, with a faster rate of hydroxyapatite formation then glass ceramics. Their bending strength is close to human cortical bone (50-150MPa). Calcium silicates as yet are not widely used clinically, but due to their high degree of osteoinductivity they have been investigated for their potential as bone fillers, implant coatings and incorporation into tissue scaffolds [104].

1.5.3 Bioactive Glasses

Many silica-based bioactive glasses are highly biocompatible, bioactive and biodegradable. The original formulation, 45S5, was based on the SiO_2-CaO-Na_2O-P_2O_5 system. It was developed by Larry Hench in the 1970s and commercialised under the name "Bioglass**"**[37]

Bioactive glassed have been used for many years as implant coatings (e.g. for titanium alloys), and shown excellent bonding to both hard and soft tissue without any intervening fibrous layers [99, 105]**.** Bioactive glass-coated titanium alloy was implanted in a pig bone model for 6 months, and showed the formation of a thin Ti_5Si_3 layer [106]. The bone matrix in the vicinity of the bone-implant interface of the coated implants had changed to mature lamellar-type bone, while the uncoated implants remained with woven-type bone. In addition to improving osseointegration, bioactive glass coatings also improve the corrosion resistance of implants. The role of the coating is twofold: (1) Protect the metal against corrosion from the body fluids, and (2) Protect the tissue from the corrosion products of the alloys.

Bioactive glasses are also widely used for root canal therapy [107] and bone filler [108].

Bioactive glass granules are available commercially as a synthetic bone graft (Perioglas, Novabone, US Biomaterials), and can be made into composites using the patient's own bone. The bending strength of bioactive glass is 2-3x less than calcium silicates. The brittleness of bioactive glass has limited it's clinical use as a bulk material for bone tissue engineering, although some researchers have developed porous glass scaffolds [42, 109].

1.5.3.1 Silicate Bioglass

The major constituents of Bioglass are SiO_2, Na_2O and CaO. Properties of Bioglass depend on the ratio of those three components [37]. For example, in Figure 1.6, the best area for bone bonding exists in area A.

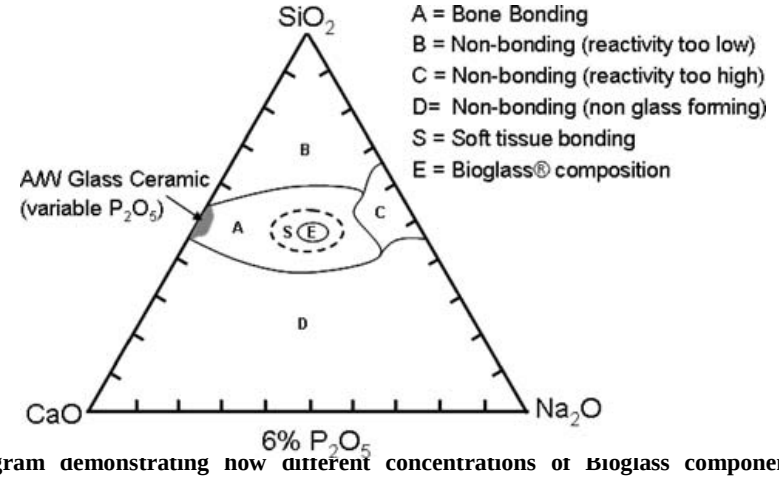

Figure 1.6: Diagram demonstrating how different concentrations of Bioglass components affect the bioactivity [37]

Researchers found that constraining proportion of Bioglass ingredients to area S facilitate bonding between implant and soft tissue. In 1977, professor Ulrich Gross and his colleagues found that 45S5 (45 representing 45 wt% SiO_2, being the network former and 5 representing the ratio of CaO to P_2O_5, based on glass-ceramic with small addition of K_2O and MgO, will produce a strong mechanical bonding [37]. Furthermore, adding multi-valent cations, such as Ti and Ta, further improves bonding [37]. What is more important is discovering of a unique processing method for producing a very fine-grained glass-ceramic composed of very small apatite and wollastonite crystals bonded by a Bioglass interface [37].

Another benefit is 45S5 Bioglass had a strong antibacterial effect against the bacteria and different effect for gram-negative and gram-positive bacteria. Research suggested that both the high pH and needle-like Bioglass debris on the surface of bacteria might be the possible mechanisms of the antibacterial effect. 45S5 Bioglass particulates caused the damage of cell walls and inactivation of bacteria [110]. Moreover, to improve inhibitory effect on bacterial growth of Bioglass, some researchers has showed the composite with silver containing bioactive glass proved to have bacterial effect (on Gram-negative *Escherichia coli* and Gram-positive *Staphylococcus epidermidis)* [111-113]

Although Bioglass 45S5 is a promising candidate for DDS, it still has some limitations. It can be relatively difficult to process and degrades slowly [106]. A range of glasses with varying properties have been developed. Bioactive glass 13-93 contains a higher percentage of SiO_2 along with K_2O and MgO. As a result, it can be sintered to high density without crystallization showing no marked difference in osteoblastic proliferation and differentiation *in vivo* study when comparing with 45S5[106]. However, 13-93 degrades even slower than 45S5 [106].

1.5.3.2 Borate Bioactive Glass

Borate glass is also considered a bioactive material. However, chemical instability of some borate bioactive glasses lead to faster degradation than 45S5 and 13-93. Toxicity is the issue need to concern because of the borate ions, (BO3)3- [106]. Borate containing scaffolds of 13-93B3 were found to be toxic to murine MLO-A5 osteogeneic cells during in vitro study [106]. However, the same scaffolds did not show toxicity to cells in vivo and supported new tissue infiltration when implanted subcutaneously in rats. The boron concentrations in the rat blood remained below the toxic level [106].

1.5.3.3 Phosphate Bioactive Glass

Phosphate glasses have also been developed for biomedical use. They consist of ions which are present in the organic mineral phase of bone [106]. Therefore, these glasses have a chemical affinity with bone.

1.5.4 Bulk Metallic Glass (BMG)

Bulk metallic glass (BMG) was discovered in 1960s. It is a type of metallic alloy with an amorphous structure that is currently being researched as a biomaterial. Its molecular formula is $Mg_{60}Zn_{35}Ca_5$. BMG possesses high strength, elasticity, corrosion resistance and biocompatibility, but because of its metastable nature it has not been well adopted for wide commercial application. Current research into BMG has focused on using the material to produce bone screws, pins or plates. Unlike other metals such as titanium, BMG bioresorbs in the body at a rate of approximately 1mm per month. The speed of degradation can be adjusted by varying the zinc content [114, 115]. It has also been shown to have good biocompatibility with higher cell viabilities compared to pure magnesium [115]. In addition, the degradation products of BMG have been shown to have antibacterial properties [116, 117]. However, small concentrations of calcium and magnesium ions have indeed been shown to be required for *S. aureus* growth. [118].

1.5.5 Polymer/Bioactive Glass Composites

Further improvement of Bioglass was driven by the dissatisfaction of its mechanical properties, including poor tensile strength and brittleness [119]. Composites of Bioglass with metal or polymer have been developed. Degradation rate and drug release kinetics were altered by selecting different polymer or/and glass materials.

1.5.5.1 Protein-Based Polymer/Ceramic Composites

Collagen and gelatine are the most commonly used proteins for this kind of composite because collagen is the most abundant protein inside human body and is easily to be obtained. Meanwhile, gelatin is a cheap and commercially available biomaterial.

Degradation rates of proteins are decided by chemical crosslinking of proteins which makes collagen or gelatin less accessible for proteolytic degradation [119]. Addition of bioceramic can make the degradation rate controllable.

Porous gelatin/collagen and ceramic particles scaffold can be fabricated via freeze-drying process [119]. However, the mechanical properties of the scaffold are not much improved. Furthermore, highly cross-linked gelatin/collagen is desired due to it’s good stability [119].

By using this kind of scaffold for DDS, drug releasing will be more sustained. Kim et al. added gentamycin to a HA/Gelatin and found results that increasing crosslinking density leads to a higher drug entrapment as well as a decreasing initial drug releasing concentration [120].

1.5.5.2 Carbohydrate-Based Polymer/Ceramic Composites

Carbohydrate polymer, such as chitin and chitosan, has drawn interest. Carbohydrate polymers are biodegradable by lytic enzymes and they have good mechanical properties matched by those of bone [119].

Carbohydrate polymers are often added into ceramic cement to improve cohesion in water as well as mechanical properties (increasing flexural strength and failure loading)[119].

When this kind of scaffold is used in a DDS, there is no significant improvement in adjusting drug releasing rates [119].

1.5.5.3 Natural polymers

Within natural polymers, a number of substances derived from various biologic tissues are included. Among these are collagen, chitosan, gelatine, thrombin, and autologous blood clot. Collagen has been studied most extensively because of relative biocompatibility, low costs and easy availability [121], and has been commercially available for over 20 years. Collagen fleeces are produced from bovine skin or tendon. Since collagen is a major component of connective tissue, it is bio-compatible and non-toxic. Degradation of collagen usually takes place within 8 weeks [122], although the speed partially depends on the method of sterilization used [123]. Degradation speed however, plays only a small role in the release rate of incorporated antibiotics as the antibiotics diffuse faster out of the collagen than its degradation speed.

1.5.5.4 Incorporating bioactive components into polymers

Polymer-ceramic composites have been used for tissue engineering approaches such as bone fillers, coatings and scaffolds. They are an attractive class of materials due to their biocompatibility, good handing properties, their capacity for long-term drug delivery and their capacity to reproducibly control their physical properties such as stiffness, strength and degradation rate.

Properties of biomedical composites are strongly affected by a number of factors [124], some of which are listed:

1. Reinforcement shape, size, and size distribution
2. Reinforcement properties and volume percentage;

3. Bioactivity of the reinforcement (or the matrix)
4. Matrix properties (molecular weight, grain size, etc.)
5. Distribution of the reinforcement in the matric; and
6. Reinforcement-matrix interfacial state.

   A large number of polymers have been used clinically, which are candidates for inclusion with bioactive ceramics [125].

1.6 DELIVERY OF THERAPEUTIC AGENTS FROM SCAFFOLDS

Conventional delivery routes for therapeutic agents include orally, intravenously or via injection. Although injection of therapeutic agents provides a bolus dose which can aid tissue repair, these factors are unable to maintain their effectiveness throughout the remodeling phase of wound healing. This occurs weeks/months after the injury.

1.6.1 Benefits of 3D Scaffolds

Three-dimensional scaffolds have the ability for short, medium or long-term localized delivery of factors beneficial for tissue regeneration. Scaffolds have the potential to deliver a higher concentration to a local area, compared with systemic delivery. In addition, lower costs can be incurred as less therapeutic is used when it is delivered locally and in a controlled way. Scaffolds have the potential to release drugs, natural factors (e.g. cytokines, hormones, proteins), plasmid DNA [126] or antibiotic agents. These agents are used to stimulate cellular adhesion, proliferation and differentiation, and/or to address infection and other tissue conditions. The challenge for engineers is to direct the release of multiple growth factors at various time intervals from a scaffold as to stimulate and enhance the natural healing process [127].

1.6.2 Factors Affecting Drug Delivery from Scaffolds

Several points need to be considered when incorporating therapeutic agents for release from scaffolds [128]

- Loading capacity –defined as the amount of therapeutic that can be mixed into the scaffolds.
- Load distribution – the therapeutic needs to be dispersed evenly throughout the scaffold;
- Bing affinity – defined as how tightly the therapeutic binds the scaffold; this binding affinity must be sufficiently low to allow release;
- Release kinetics-need to be controlled to allow the appropriate dose of growth factor to reach the cells over a given period of time and

- Long-term stability- the stability of the therapeutic when incorporated within the scaffolds at physiological temperature; therapeutics need to maintain their structure and activity over a prolonged period of time

DDSs applying scaffolds form an architectural extracellular matrix containing drugs, antibiotics and molecules provides afore mentioned advantages. Drug release kinetics can be controlled through scaffold properties; size, hydrophobicity and porosity [129].

There are three general categories: cell-based strategies, growth factor-based strategies and matrix-based strategies. However, two or more of these strategies are frequently combined to implement a solution. The criteria of scaffold vary from target sites. Generally speaking, biocompatibility and site suitability should be considered priority [130].

There is a growing interest in adding substance (growth factor etc.) or changing environment signals (light, pressure, temperature etc.) at target sites to simulate cells to migrate or/and generate to trigger healing process.

1.6.3 Key Functions of a Tissue Scaffold

Fully functional tissue is less likely to become a locus for infection and should be the ultimate goal of any tissue engineering approach [131]. A scaffold should perform several important roles to facilitate vascularized tissue repair [132]

These include:

- Offer a 3D framework in which cells can migrate, attach and proliferate
- Keep space for hierarchical tissue formation and remodeling
- Protect developing tissue from stresses such as high compressive forces and infection
- Promote good integration with the surrounding tissue
- Accelerate the transport of wound fluid and blood through scaffold
- Facilitate the transfer of force to the developing tissue
- Address underlying tissue pathologies through delivery of therapeutic factors

These key functions of a scaffold are like those of a house. Similar to the role of a house, scaffold designs should provide a protective function, while also facilitating connection to the surrounding environment. Scaffolds should provide protection from deleterious forces and yet still allow physiologic stress to be transferred to the tissue within the scaffold [40, 133]. If these concepts are not incorporated into the scaffold design, excessive displacement or forces can lead to tissue necrosis and hinder vessel development.

Instead, controlled levels and directions of force transfer are important to enable mature, vascularized tissue to develop [134].

Ideal scaffolds should also be designed to induce stasis or inhibition of bacterial colonization and biofilm formation. This can be achieved through materials selection, removal of vacant space and localized, long-term therapeutic delivery from the scaffold. Nutrient delivery to the cells and extraction of waste products should be facilitated via good mass transfer and competent vascularization throughout the scaffold. The scaffold must also provide a good connection with the surrounding tissue, so that the cells within the scaffold are not isolated via the formation of scar tissue.

Scaffolds play an important role in providing space for tissue regeneration [135]. This concept has been clinically confirmed through the use of guided tissue regeneration membranes for dental surgery. These non-biodegradable membranes were effective for space making and in the prevention of scar tissue ingrowth. In many clinical examples, scaffolds increase the speed and quality of tissue compared to the absence of a scaffold [136].

1.6.4 Methods of Imparting Bioactivity to Scaffolds

Bioactivity refers to the capacity of a material to be “tissue inductive”. Bioactive materials can facilitate cellular attachment and even gene modulation. A stable interfacial bond can form between the material and the surrounding tissue. Both bioceramic coatings and porous surfaces contribute to the level of bioactivity of an implant [38]. Coatings are considered bioactive when they facilitate the formation of a bone-like hydroxyapatite (calcium phosphate) crystallite layer on their surface, after submission in simulated body fluids.

Hench and Polak identified three classes of materials, depending upon the response they elicit from the biological environment [38, 137]. First generation materials are permanent and bioinert (e.g. alumina, stainless steel). Second generation materials are bioactive or biodegradable (e.g. poly-ε-caprolactone, tri-calcium phosphate). Third generation materials are those, which are both bioactive and biodegradable (e.g. hydroxyapatite, bioactive glass).

1.6.5 Surface Modification

Scaffolds provide the substrate for cell attachment and their subsequent growth and proliferation. However, instead of binding to scaffolds directly, cells attach on proteins absorbed on surface of scaffold [138]. Therefore, those proteins on surface of scaffold are crucial to efficacy of scaffold. Approaches, such as protein coating, photochemical modifications and plasma technique, had been done to use growth factors and peptide to mimic proteins. The concentration, local duration and spatial distribution of those proteins

affect performance of scaffold. Furthermore, the surface topography of the scaffold material has also been shown to be significant cells proliferation, differentiation as, immune system respond and inflammatory process [139].

1.6.5.1 Protein Coating

This approach is to coat surface of scaffold with cell adhesive molecules (fibronectin, heparin, collagen and gelatin), small peptides fragments of amino acid arginine-glycine-aspartic acid) or other functional groups (chitosan, poly (Llysine)-grafted-polyethylene glycol) [140].

In 2006, Chen et al. [138] did an experiment to determine the effect of surface modification on hydroxyapatite (HA) formation. Bioglass scaffolds were synthesised using a sol-gel process followed by attachment of 3-AminoPropyl-TriethoxySilane (APTS) and gluteraldehyde (GA) protein coupling agent [138]. The results indicated that the surface modification improved formation of HA.

1.6.5.2 Photografting Modification

Topographical modification has been shown to improve protein bonding. One method of accomplishing this is by photografting. In 2002, Gao et al. improved the cytocompatibility of polyurethane (PU) porous scaffolds through photo-oxidation of the scaffolds and UV light treatment. It also indicates that photografting technique is possible for porous scaffolds [141].

However, because degradable polymer materials are sensitive to solvent and low head stability, conventional modification methods such as high-energy irradiation, photografting, oxidation or etching will damage structure of polymer chain to some extent [139]. Researchers recently presented a solvent-free photografting technique for topography modification without destructive of polymer chain. They applied vapour-phase grafting technique to create topography surface modification of degradable polymers scaffold (Poly-(N-vinylpyrrolidone), PVP).

1.6.5.3 Plasma Treatment

Plasma treatment is a technology for tailoring surface properties via exposing them to an electrical discharge or plasma [142]. With this kind of technology, wettability and absorbable ability is improved. Thus, proteins can more easily attach to surface of scaffold and biocompatibility is improved. Ho et al. in 2005 immobilized RGDS (Arg-Gly-Asp-Ser) on PLLA scaffolds via plasma treatment [143]. The results demonstrated that this kind of modification can render PLLA scaffolds more suitable for culture of osteoblast-like cells and for generation of bone-like tissues.

Furthermore, mineral coating sputtered via Plasma has been shown to improve wettability, adsorption and adhesion abilities of scaffold [144]. Suárez-González et al. indicate that mineral coating (carbonate, HCO3) affect the release kinetics of growth factors [145].

1.6.6 Antibiotic Delivery

1.6.6.1 Controlled Antibiotic Release from Composite Scaffolds

Antibiotics are chemicals, which inhibit the growth of microorganisms such as bacteria which can cause infection. Scaffold composition and form have been shown to alter the rate of the release of antibiotics. Nandi and co-workers [146, 147] observed delivery of the antibiotic cefuroxime axetil over a period of 6 days, when incorporated into a porous bioactive glass block. Zhang and co-workers [148] created composite pellets from chitosan, bioactive glass particles and teicoplanin (antibiotic) powder, and found it provided an effective treatment for osteomyelitis induced by *Staphylococcus aureus*. Implantation of the pellets into a rabbit tibia osteomyelitis model resulted in the detection of teicolpanin in the blood for about 9 days.

Another group, Zhang and co-workers [149] loaded gentamicin sulphate onto chitosan/calcium phosphate scaffolds via dipping in an antibiotic/PBS solution. *In vivo*, these scaffolds showed a sustained release for more than 3 weeks, as compared with the burst-release exhibited by the pure chitosan scaffolds. Chang and co-workers [150] loaded gentamicin sulphate onto PCL matrices via suspension of the antibiotic particles in the PCL solution, prior to forming scaffolds using precipitate casting. They demonstrated the vitro release of 80% of the gentamicin sulphate over 11 weeks, with low levels of antibiotic being measured up to 20 weeks. Further it was possible to increase the amount of drug loaded onto the PCL by cooling the PCL solution to 4^0C prior to casting.

1.6.6.2 Ideal Antibiotic Carrier

An ideal antibiotic carrier is:

- Characterized by good biocompatibility,
- Controllable degradation kinetics,
- The ability to incorporate and release any antibiotic desired for treatment for an - extended period at adequate levels prevent further infection [151, 152]
- Preferably with a zero-order release kinetics (constant drug release
- overtime)

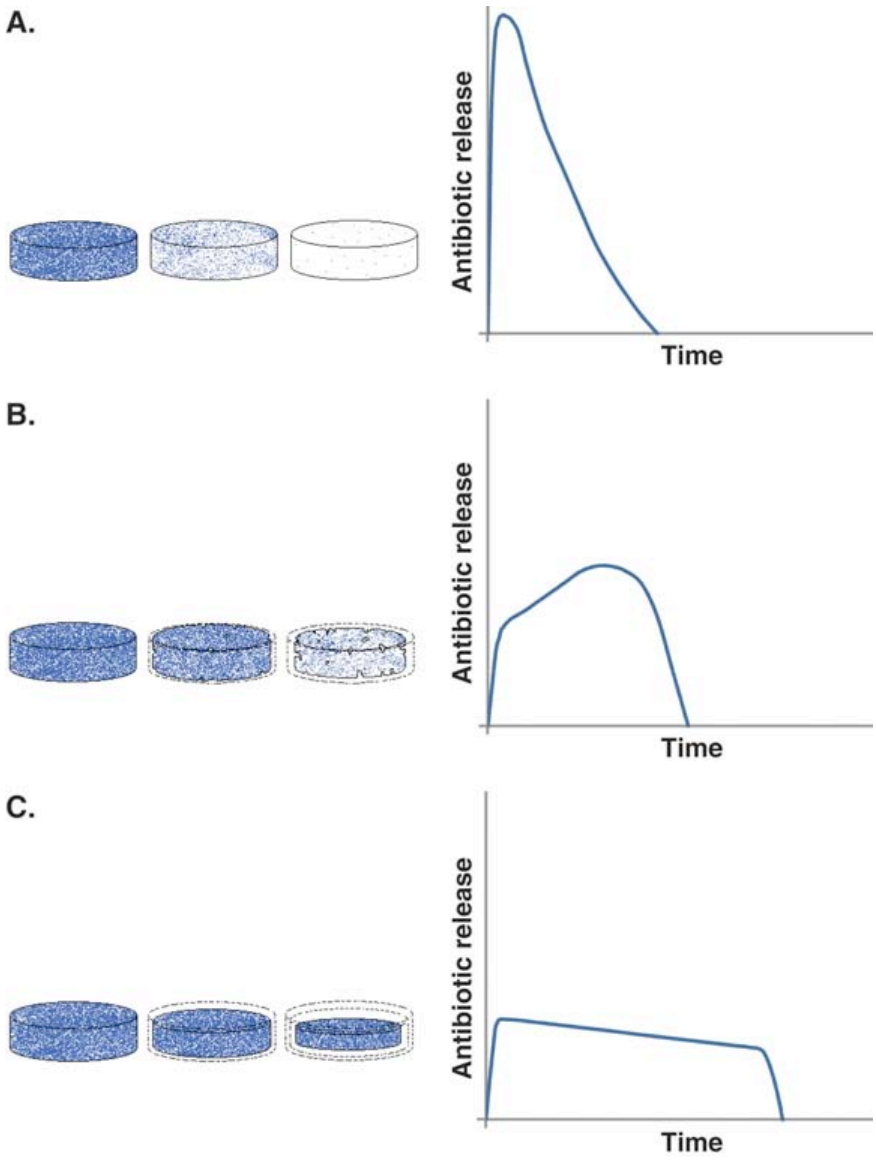

Figure 1.7: Possible antibiotic release kinetics from degradable carriers. A. Diffusion-based release from slowly degrading carrier materials. B. Bulk eroding carrier materials. C. Surface eroding carrier materials [153].

1.7 *IN VITRO* WOUND MODELS

In vitro wound models attempt to replicate the *in vivo* environment as closely as possible. *In vitro* wound models have been used to examine the physiological and biological characteristics of wounds [154, 155], and wound treatment [155, 156].

Due to importance of *in vivo* testing, different wound models have been developed. The simplest was an incised cell monolayer [154]. In order to investigate the infected chronic wound, a biofilm should be added into the model. Woods et al used a drip-flow reactor model, in which a polycarbonate membrane served as platform for biofilm growth. This membrane was located on top of an absorbent pad through which nutrients were wicked (Figure 1.8, Left) [157]. In this model, nutrient flow is constant.

Hill and coworkers used constant depth film fermenters (CDFF) to generate biofilms (Figure 1.8, Right) [158]. The model consisted of plug inserts on a rotating turntable. In order to conduct tests on wound dressings, the plug inserts were inverted onto the dressing within a broth-containing petri dish. No dynamic nutrient flow was used here.

A study by Sun et al simply used media-filled test-tubes to contain the pipette tip, previously used to inoculate the medium, as a surface on which biofilm was grown [159]

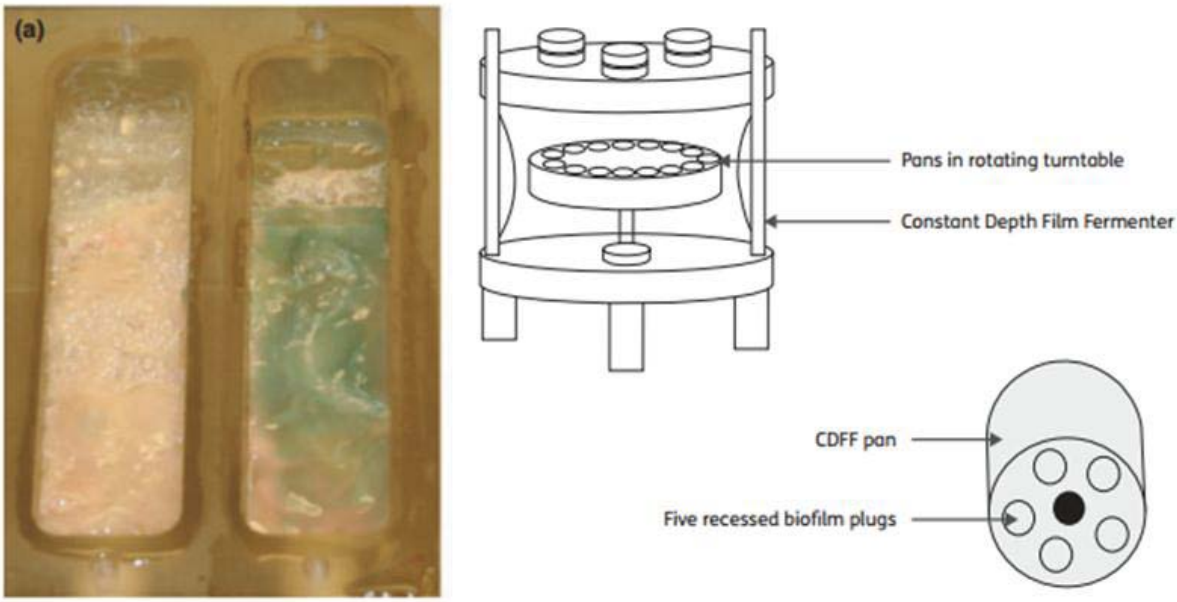

Figure 1.8: Left: Drip-flow reactor model (Woods et al.) Right: CDFF with plug inserts (Hill et al) [158].

Assadian et al. investigated the effect of topical negative pressure on bacterial inhibition by using a vacuum [160]. These systems must have appropriate dressings and coverings, so slightly more complex.

While these studies have made valid and clinically relevant discoveries, these wound model systems vary mostly in their protocols and specifications. As such, any combining of data or cross comparisons must be done with experimental variations, a mission which may be impossible in some cases.

Ideally, a standardized protocol should be used. The most recent *in vitro* wound model had been developed and established by Ngo et al [161]

However, there are currently no configurations that can adjust for all testing purposes. Therefore, the development of a standardized wound modeling protocol is necessary, which is suitable for a range of testing protocols and contain physiologically relevant wound characteristic as much as possible.

CHAPTER 2

THESIS AIM AND DESIGN REQUIREMENTS

2.1 THESIS AIM

There remains a need to develop a competent soft tissue regenerative scaffold with demonstrated antibacterial activity.

The strategy for achieving this objective included the incorporation of antibacterial coating and antibiotic into a proven biocompatible soft tissue scaffold without any adverse changes to the interconnected porous structure. The fabricated composite scaffolds were required to maintain structural integrity, be verified using microscopic analysis and spectrophotometry methods, and be subject in vitro microbiological testing. To assess the antibacterial activity of the scaffolds the assay should replicate *in vivo* condition as closely as possible.

2.2 DESIGN REQUIREMENTS

2.2.1 Design Aim

Design has to address these risks

- Blood or immune cells infusion into graft or scaffold is inhibited
- Graft or scaffold harbours bacterial or fungal infection better than granular tissue
- The system causes cytotoxic response
- The system causes chronic inflammation.
- The graft or scaffold mechanically unsuitable (too stiff or too weak)

2.2.2 Design criteria

1. Need blood and granular tissue to infuse into scaffolds to fight infection => improve interconnected attach bacteria

2. Need to combine suitable bioresorable and biocompatible materials in one unit.

3. At least one of these biomaterials needs to have inherent antibacterial activity

4. Allow infusion of antibiotic into scaffold biomaterial without inhibiting antibiotic potency.

2.2.3 User requirements:

1. Soft tissue biocompatible
2. Remain soft yet supported
3. Able to be sutured
4. Able to be inserted into a deep wound
5. Wound conforming
6. Interconnected porosity
7. Bioactive coating to facilitate soft tissue attachment
8. Antibacterial coating has potential to disrupt biofilm and bacteria cells.
9. Be compatible with antibiotic infusion and delivery.

CHAPTER 3

SYNTHETIC POLYMER SCAFFOLDS

Our group produces novel polymer scaffolds from polycaprolactone. These scaffolds can then be modified by infusing or coating with bioactive molecules to increase their effectiveness. This section describes the manufacturing protocol for these scaffolds. The modified scaffolds need to be evaluated in terms of quantity and quality.

3.1 SYNTHESIS OF SCAFFOLD

These scaffolds have a highly interconnected porous polymeric structure, composed primarily of high molecular weight aliphatic polycaprolactone (PCL) polyester, CAPA6800. Scaffolds formed from PCL are suitable for manufacturing due to their low melting temperature of 58-60°C, biocompatibility and resorbability [162]. The scaffolds can thus be used in a laboratory environment with standard laboratory safety guidelines and standard personal protective equipment.

3.1.1 Manufacturing Protocol

The general procedure for manufacture of the scaffolds follows a batch polymer coagulation process. This not only allows much more efficient manufacturing, but also improves product consistency. The procedure consists of four main processes, which are modular and can thus be individually optimised. This manufacturing protocol was thus the basis on which the new scaffolds were designed and fabricated.

This protocol describes the formation of the scaffolds using the polymer batch coagulation process.

Step 1: Solution was prepared by mixing PCL pellets in acetone. The mixture was agitated and heated to 60^0C and kept at that temperature over 24 hrs until a homogenous solution formed.

Step 2: Precursors were prepared as a template for scaffold formation. The precursors consisted of leachable particles that fill space in the scaffold, leaving pores behind once removed.

Step 3: Precursors were completely submerged in the PCL solution, heated and agitated.

Step 4: Precursors were picked up separately and washed in a water bath for 30 seconds. The membrane on the surface of each precursor was peeled off carefully and collected.

Step 5: The scaffolds were rinsed with water to remove all chemicals left inside. Each peeled scaffold was located in a separate compartment in the water bath. The arrows in the figure show the flow of water. The water was continuously recycled through the scaffolds until all the precursors had leached out. Scaffolds without precursors floated to the surface.

Step 6: The precursors were centrifuged to remove the remaining water. The spun scaffolds were collected in a clean container for the next step.

Step 7: The scaffolds were categorized and collected into groups with the same qualities before being packaged.

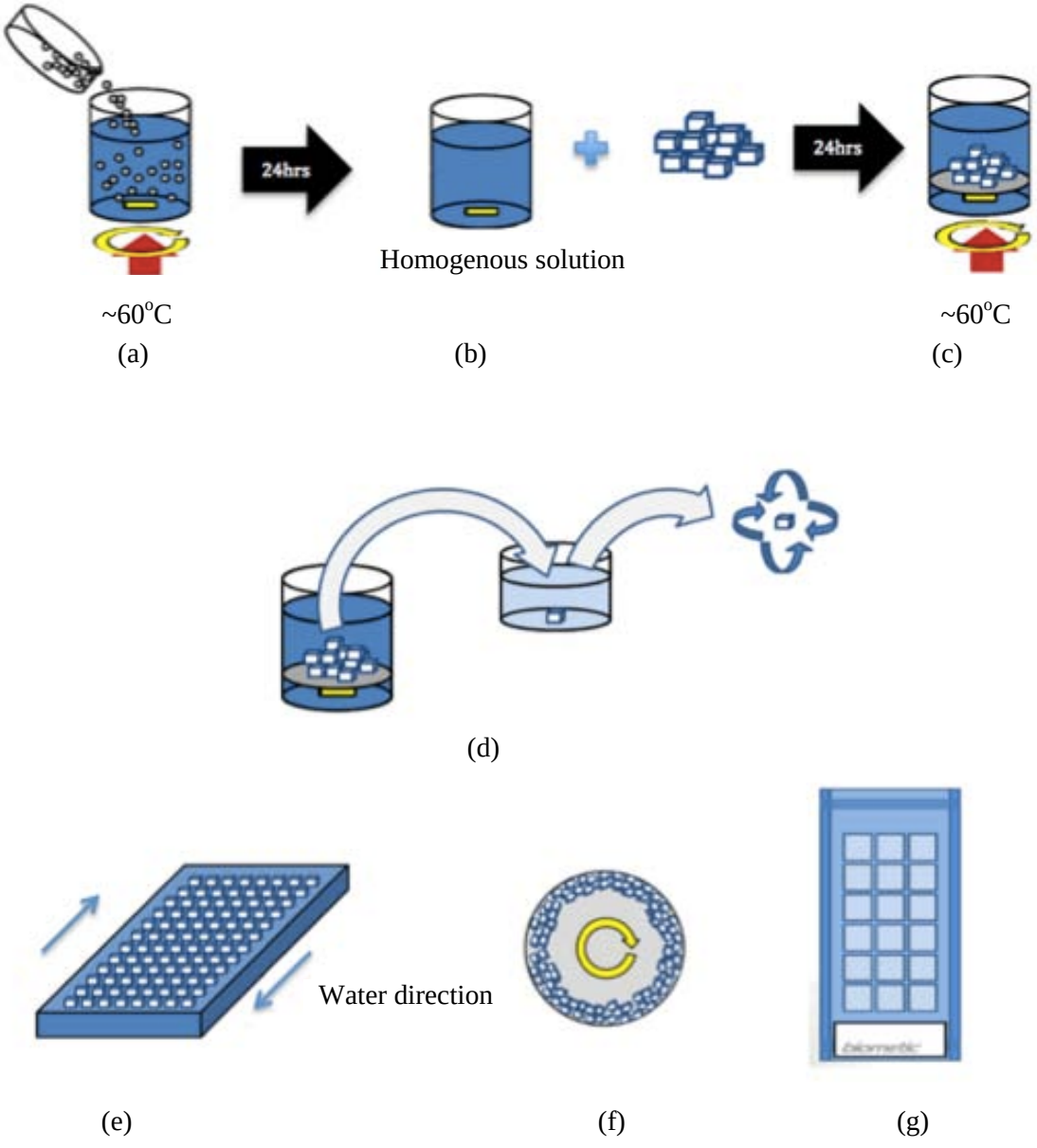

Figure 3.1: Process to make scaffolds: (a) Polymer solution preparation, (b) Addition of precursor, (c) Infusion, (d) Peeling (membrane removal), (e) Leaching, (f) Drying, (g) Packaging.

3.1.2 Key mechanisms in the main steps of production of soft tissue regenerative scaffold

Further details of the mechanisms involved in each step are given in Table 3.1.

Table 3.1: Steps in the production of the scaffolds

Fig	Stage	Description
(a)	Precursor Preparation	The precursor can be considered as a template in which the scaffold interconnections can be formed. The dimensions, level of interconnectivity and pore size of the scaffolds can be adjusted by changing the characteristics of the precursor
	Solution Preparation	The solution is a solvent which dissolves PCL and assists PCL getting inside the porogen matrix. The solvent evaporates after the polymer struts form.
(b)	Precursor Infusion	The polymer solvent solution is infused into the precursor at a specific temperature so that polymeric struts can form.
(c)	Membrane Removal	This instant step controls the surface quality of the scaffold to prevent the PCL solvent solution from forming membranes and sealing pores inside. Therefore, this step is modified individually to find out the best time to peel off the membrane.
(d)	Batch Coagulation	The polymeric beams are produced in this step. The porogen is fully dissolves in water, leaving empty space as pores. A porous and interconnected structure is obtained.

3.2 SCAFFOLD WITH BIOACTIVE PROPERTIES

Although basic scaffolds can provide supportive struts to promote tissue ingrowth and vascularization, their ability to encourage soft tissue attachment and kill microbes at the damaged skin site can be improved. Therefore, soft tissue regenerative scaffolds with potential antimicrobial potential were designed, synthesised and tested. Chapter 5 describes experiments to test the efficacy of these modified scaffolds in a wound model. This wound model may be used in the future as an alternate to preliminary animal experiments.

Plain scaffolds were manufactured, as described in section 3.1. These scaffolds infused and/or coated with a variety of bioactive substances. These included Bioglass 45S5, BMG and antibiotics. Scaffolds were made with dimensions of 6 x 6 x 5mm in order to fit the dimensions of coupon used in wound model testing.

3.2.1 Bioactive Glass 45S5 Infusion

One of the methods chosen to manufacture the composite scaffolds was through infusion of the bioactive glass component. 45S5 Bioglass was chosen for infusion into scaffolds due to it's antimicrobial ability, as mentioned in section 1.5.3.1 [163, 164]. In addition, Bioglass can promote attachment of hard and soft tissue to the polymer scaffolds. From this point, the rate of vascularization will be increased. These features are all advantageous in relation to wound healing [165].

3.2.1.1 Materials

45S5 Bioglass granules were obtained from Biometic^{TM}. The formulation contained 35% (w/w) silica (SiO_2), 31% (w/w) soda ash (Na_2CO_3), 24% (w/w) calcium carbonate (Ca_3CO_3), and 10% (w/w) tricalcium phosphate ($Ca_3(PO_4)_2$). The final Bioglass product was an ultra-fine powder, ground using a mortar and pestle. The grain diameter after grinding was $\leq$30 μm.

3.2.1.2 Method

Bioglass powder was added into the PCL/acetone solution during the first step of scaffold synthesis (Fig 3.1a). This allowed Bioglass to be directly inserted within the porous structure of the scaffold, as shown in Figure 3.2. The following steps for scaffold synthesis were as described in section 3.1.

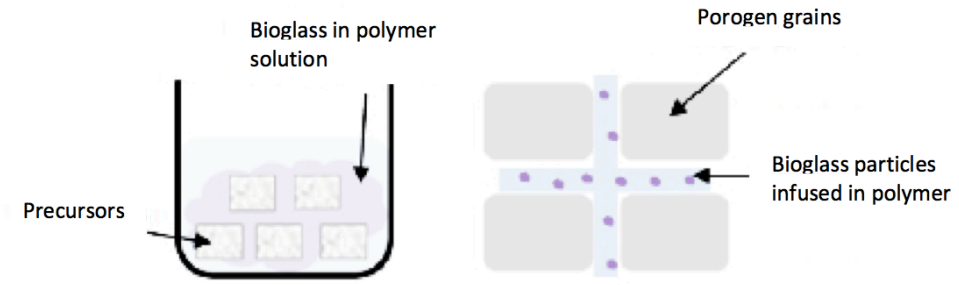

Figure 3.2 Schematic diagrams of Bioglass incorporation during the infusion process and the embedded particles in the scaffold struts.

3.2.2 Bioactive Glass 45S5 Coating

Coating with a bioactive component is another method for modifying the properties of the scaffold. It was hypothesised that coating with Bioglass could improve the healing capacity of the scaffold. This could lead to a better outcome when treating wounds on which bacterial biofilms are present.

3.2.2.1 Materials

Ultra-fine Bioglass 45S5 was used for coating.

3.2.2.2 Method

Each of the plain scaffolds was put in a sealed sterile container containing 2 g of Bioglass 4S5S. The container was agitated to obtain a full covering of Bioglass 4S5S on the surface of scaffolds. The packages were placed in an oven, with rotation and heating to 52°C for 10 minutes, to enhance thermal adherence of the Bioglass 45S5 to the scaffold. This process is depicted in Figure 3.3. The scaffolds were then moved into sterile packages (Medipack, Medipack Medical Packaging Mfg. Co.). Nine scaffolds were produced using this procedure.

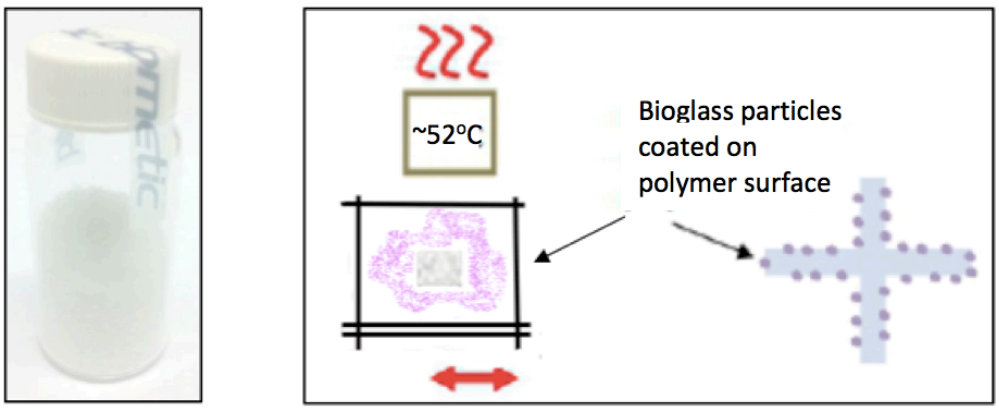

Figure 3.3: Bioglass coating with heat treatment, resulting in particle adhesion to the scaffold surface.

3.2.3 Bulk Metallic Glass Coating

As previously indicated in the literature review, bulk metallic glasses show resistance to bacterial infection, due to elements including magnesium, zinc, and calcium. This property makes bulk metallic glass coating a promising approach for incorporation of anti-bacterial activity in to skin implants. BMG also has the advantage of being biocompatible and bioresorbable [143].

3.2.3.1 Materials

Several pieces of BMG (approximately 3g) were ground with a mortar and pestle to create a fine BMG powder of 50-100μm diameter (Figure 3.4). The powder was kept in a sterile plastic jar prior to use.

3.2.3.2 Method

One scaffold was transferred to each jar containing BMG powder. The cap was closed the jar was agitated for 5 seconds with the aim of maximizing coating of the scaffold. Excess powder was shaken off and removed using a sieve. The coated scaffolds were removed from the jars using forceps and transferred to sterile Medipacks, with three scaffolds per compartment (Figure 3.4). The packaged scaffolds were rotated at 38-42°C for 30 minutes. This heat treatment step was expected to increase physical attachment of the BMG powder to the scaffold struts.

Scaffold mass change was verified by weighing of the scaffolds before and after the coating process using high precision scales.

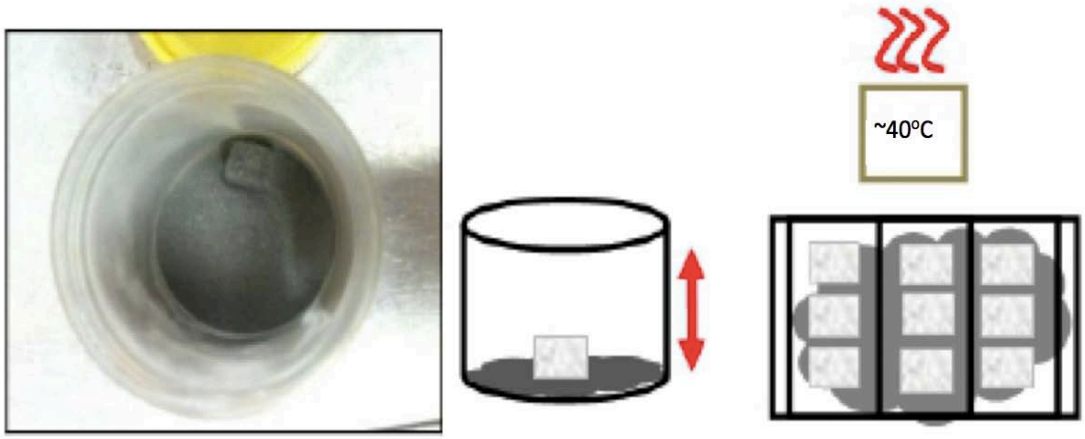

Figure 3.4: Left panel: Pot containing BMG powder and coated scaffold. Right panel: Depiction of coating process.

3.2.4 Scaffold Verification of Coatings

3.2.4.1.Optical Microscopy and Mass Change

The scaffolds were observed visually using a Leica DMRXE Optical Microscope. The scaffolds were weighed before and after coating using high precision scales and the mass change calculated.

3.2.4.2. Scanning Electron Microscope (SEM)

SEM uses a focused beam of high-energy electrons to generate a variety of signals at the surface of solid specimens. The signals reveal information about the sample including external morphology (texture), chemical composition, and crystalline structure and character of materials making up the sample [166]

The following protocol for preparation and SEM imaging of the scaffolds was carried out by Alex Baume (USYD) at the Australian Centre for Microscopy & Microanalysis (ACMM)

Three cycles of 5 minute washing was carried out in 0.1M PBS. Post-fixation was achieved with 1% osmium (OsO_4) in 0.1M PBS for 1 hour, followed by OsO_4 removal by three 5 minute washing cycles in Milli-Q water. Samples were then dehydrated in ethanol solutions at 50%, 70% and 95% (2x 5minute cycles), then at 100% (2 x 10minute cycles). A 3 minute immersion in 100% hexamethyldilazane (HMDS) allowed chemical drying, followed by transfer into a desiccator for overnight HDMS evaporation. Specimens were mounted onto aluminium stubs using carbon paint and sputter coated with 10nm gold. Images were taken on the EVO SEM with EHT set at 10kV and WD at 26mm.

3.3 RESULTS & DISCUSSION

3.3.1 Soft Tissue Regenerative Scaffolds

Plain scaffolds were synthesised as shown in Figure 3.6.

Figure 3.5: Shape of scaffolds.

Nine types of scaffolds were produced using combinations of the additive substances. The iteration and abbreviation of each type is shown in Table 3.2.

Table 3.2: Description of scaffold modification with their abbreviations.

No	Scaffold Modifications	Abbreviation
1	Plain; no modifications	Plain
2	Bioglass infused only	BG-infused
3	Bioglass coated only	BG-coated
4	BMG powder coated only	BMG-coated
5	Antibiotic infused only	Ab-infused
6	Bioglass infused and BMG coated	BG-infused + BMG-coated
7	Bioglass infused and antibiotic infused	BG-infused + Ab-infused
8	BMG and antibiotic infused	BMG-coated + Ab-infused
9	Bioglass infused and BMG and antibiotic infused	BG-infused + BMG-coated +Ab-infused

3.4 VERIFICATION OF MODIFIED SCAFFOLDS

3.4.1 Verification of BG and BMG Coating

The scaffold coatings were verified qualitatively (visually) and quantitatively (mass change). A colour change was observed for the BMG scaffolds, as the scaffolds took on a grey metallic colour (Figure 3.4). BMG particles were also verified by reflective optical microscope imaging (Figure 3.6). Scaffolds with BG infusion have no colour difference from the plain scaffolds. When being cut, these scaffolds were stiffer than the plain scaffolds, but could tear more easily.

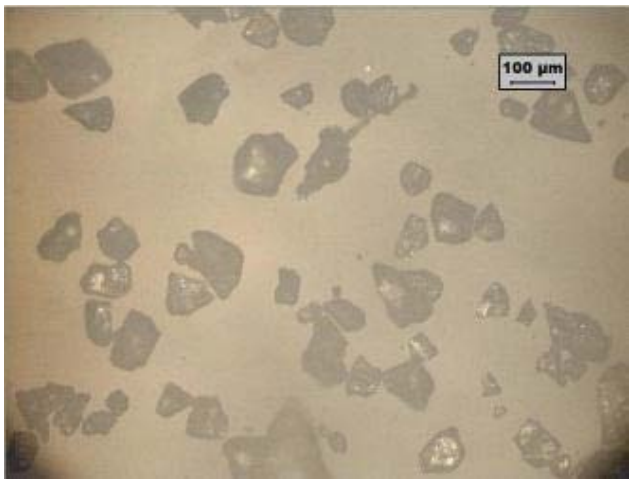

Figure 3.6: Ground BMG particles (10x) viewed under a reflective optical microscope.

Scaffold mass change was verified by weighing of the scaffolds before and after the coating process using high precision scales.

The quantitative method based on mass verification, whereby the scaffolds were weighed before and after the coating process. We use an enclosed sieve and put on a vibrating bench top for 10 minutes High precision scales were used for excess BG or BMG powder, where an average mass increase of 4.95mg was found for individual plain scaffolds, and 1.24mg for BG-infused scaffolds. Raw data can be found in the Appendix.

3.4.2 SEM Imaging

Imaging with SEM demonstrated the scaffolds were successfully coated with bioactive components. Plain scaffolds are depicted in Figure 3.7a. Figure 3.7b shows scaffolds which have been infused with Bioglass and coated with BMG. In Figure 3.8, BMG-coated scaffolds are visualized.

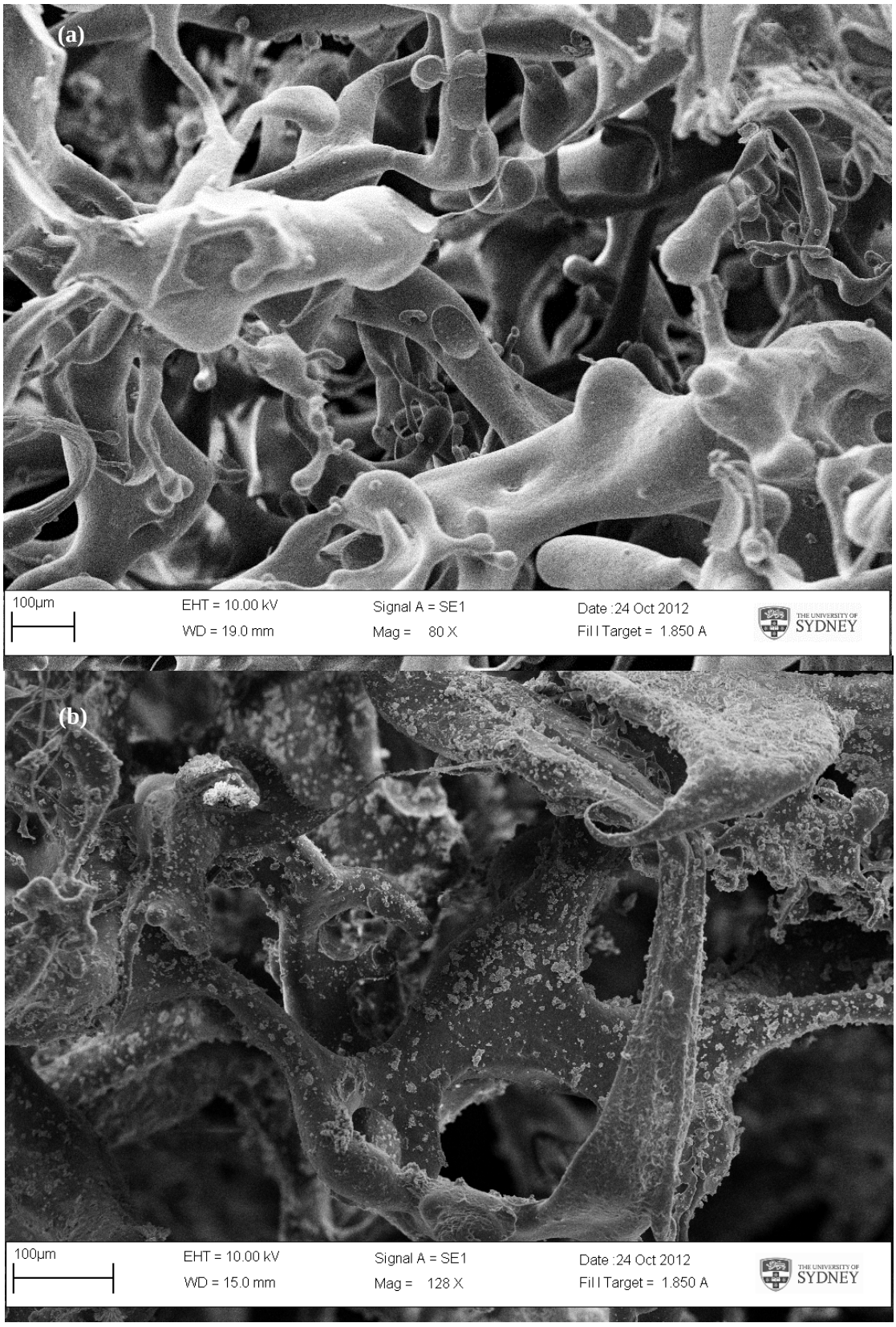

Figure 3.7: Visualisation of scaffolds with Scanning Electron Microscopy (a) Plain PCL scaffold (b) BMG coated PCL scaffold

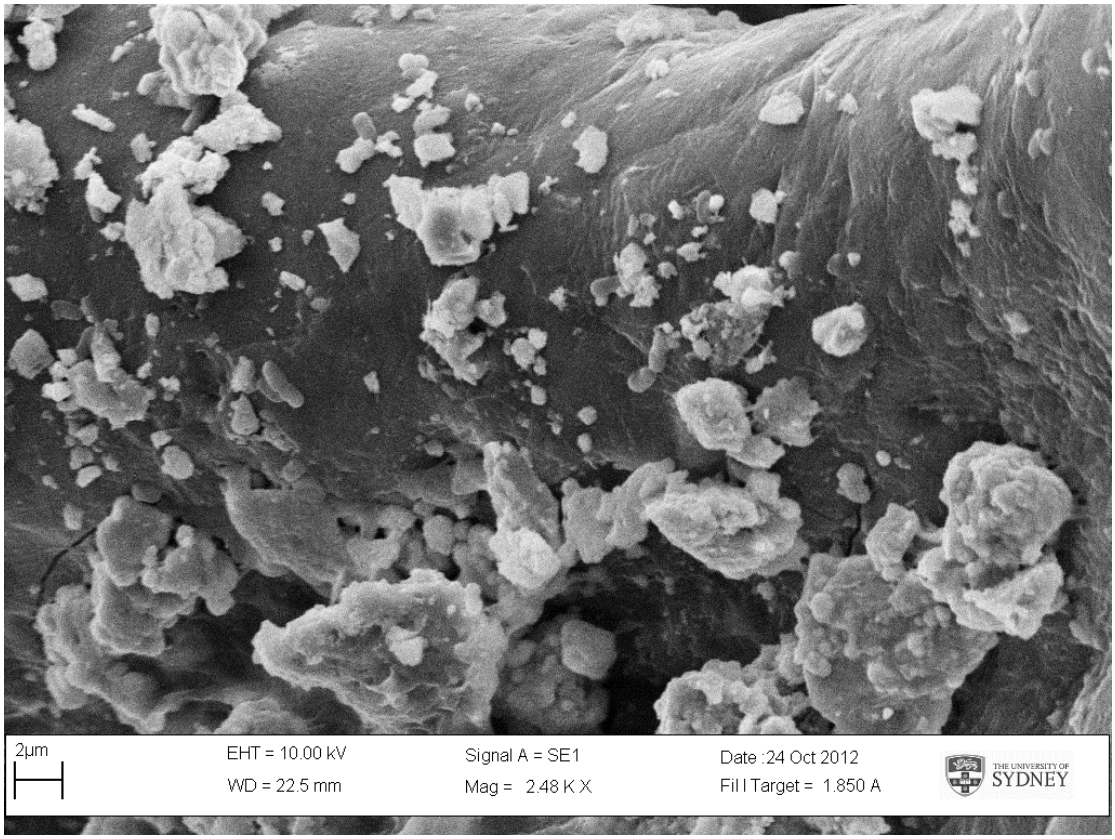

Figure 3.8: Visualisation of BG infused + BMG-coated scaffolds with Scanning Electron Microscopy

3.5 DISCUSSION

Various types of scaffold were produced for further testing. Although the plain scaffolds were sterilized, the other types were not. The modified scaffolds need to be sterilized for biological testing. Each scaffold was cut into quarters for biological testing (chapter 5).

From SEM results, our scaffolds were successfully seeded with BG and BMG. These antibacterial particles still stick on scaffolds after removing excess particles by shaking. Moreover, SEM images of scaffolds showed an interconnected structure and no damage inside modified scaffolds. These characteristics help blood vessel and immune cells get through wound and accelerate healing process. Preliminary verification findings do suggest successful modifications. Furthermore, for enhancing antibacterial effects of scaffolds, other experiments with scaffold antibiotic infusion were conducted.

CHAPTER 4

SCAFFOLD ANTIBIOTIC INFUSION AND DELIVERY

4.1 ANTIBIOTIC LOADING OF SCAFFOLDS

Cephazolin sodium (Sandoz, Novartis) was chosen to load onto the scaffolds. This antibiotic was selected to treat *Staphylococcus aureus* infection, as discussed in section 1.2.2.2. The established binding affinity of cephazolin sodium to hydrophobic sites [25] and its clinical common use made it a suitable choice for attaching to the hydrophobic scaffolds.

The antibiotic coating was the final modification of the scaffolds, performed after infusion and coating other bioactive particles on the polymer surface.

4.1.1 Materials

Cephazolin sodium powder (Figure 3.4) was dissolved in sterile deionized water to make a 5 mg/mL antibiotic solution, followed by vortexing to ensure the antibiotic was completely solubilized. The solution was stored in sterile plastic jars before use, in order to maintain maximum antibiotic activity.

4.1.2 Method

Each plastic specimen jar was filled with 12 scaffolds of a single type. Four types of scaffolds were placed in separate jars: plain scaffolds, Bioglass-infused scaffolds, Bulk Metallic Glass-coated, and Bioglass-infused + Bulk Metallic Glass-coated scaffold.

Due to the lack of research into the capacity of the scaffolds to absorb cephazolin sodium, it was not clear what concentration of antibiotic should be used so an estimation was made. 12 scaffolds were placed into 18 mL antibiotic solution to achieve an exposure ratio of one scaffold to 1.5 mL solution (average 7 mg antibiotic). This volume was chosen to ensure that each scaffold was fully submerged in antibiotic solution.

The coated scaffolds were left at room temperature in 24 hours and dried in a vacuum centrifuge (Concentrator 5301, Eppendorf). The drying was done in three separate ‘runs’ of 5, 10 and 15 duration, with the scaffolds being transferred to new Eppendorf tubes after each ‘run’. The scaffolds were stored in sterile petri dishes until use.

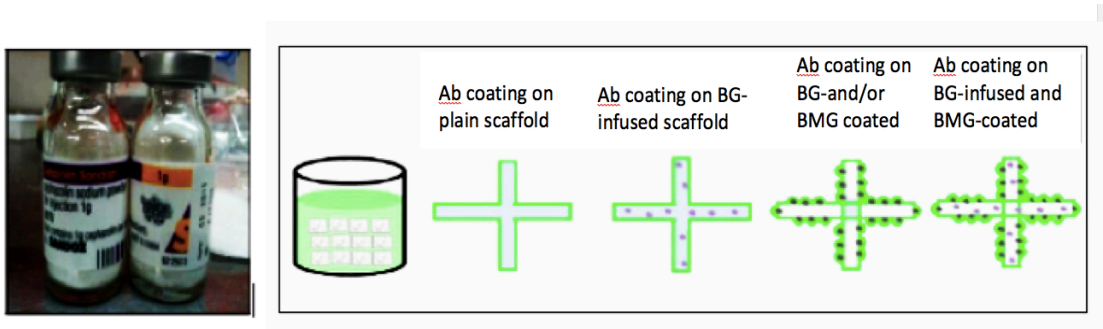

Figure 4.1: Left: Vials of cephazolin sodium. Right: The different types of antibiotic-coated scaffolds.

4.2 OPTICAL DENSITY MEASUREMENTS FOR ANTIBIOTIC VERIFICATION

To ensure scaffolds contain antibiotic for testing, we measured absorbance of antibiotic solution release by using a spectrophotometer (DU 800 Spectrophotometer, Beckman Coulter) to quantify concentration of antibiotics infused into scaffolds. Disposable cuvettes were consumed, to avoid contamination due to previously used curvettes.

4.2.1 Cephazolin Sodium Absorbance Spectrum

An absorbance spectrum of the cephazolin sodium supplied was initially determined to detect the suitable wavelength at which to make measurements for all antibiotic infused scaffolds.

A 5mg/mL stock antibiotic solution was made. A pipette was used to transfer a 10μL sample to a cuvette. Cuvettes were filled with sterile de-ionized water until the required volume was reached for the spectrophometer to work properly. The sample was tested with several different wavelengths, in order to detect the maximal absorbance peak of cephazolin sodium. This wavelength finally found at 286nm, instead of 270nm as literature review mentioned [26]. This result was depicted in Figure 4.2. This wavelength was used in subsequent tests.

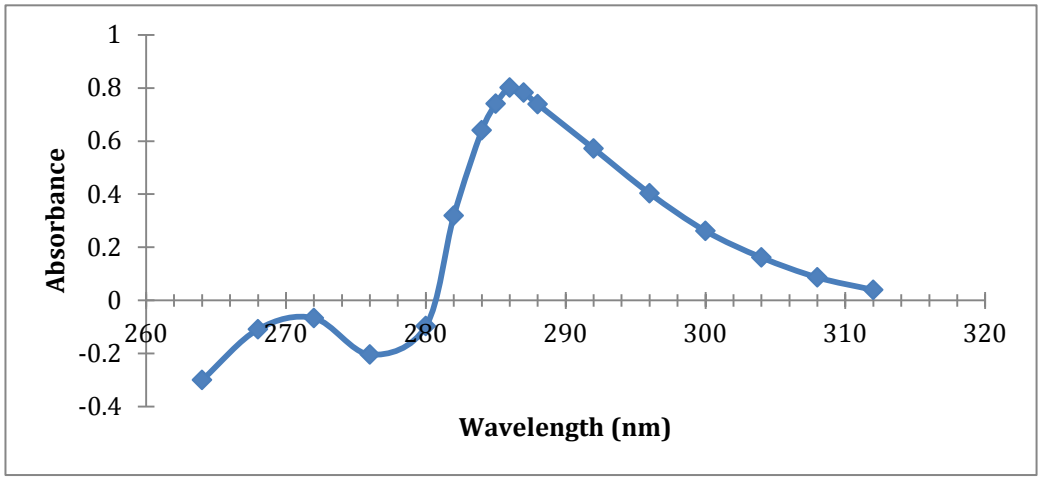

Figure 4.2: Absorbance spectrum for cephazolin sodium in wavelength range. Highest absorbance peak for reading was at 286nm.

4.2.2 Cephazolin Sodium Standard Curve

The standard curve for cephazolin sodium was found using a 1mg/mL antibiotic solution. Absorbances were measured for a range of antibiotic solution concentrations including; 0, 5, 10, 20, 40, 50, and 100µg/mL. The results are shown in Figure 4.3. The data points formed a trendline with equation y=0.0109x with an R^2=0.9718. This indicates a good linear tend. From this, the calibration coefficient for chloramphenicol is 0.0109.

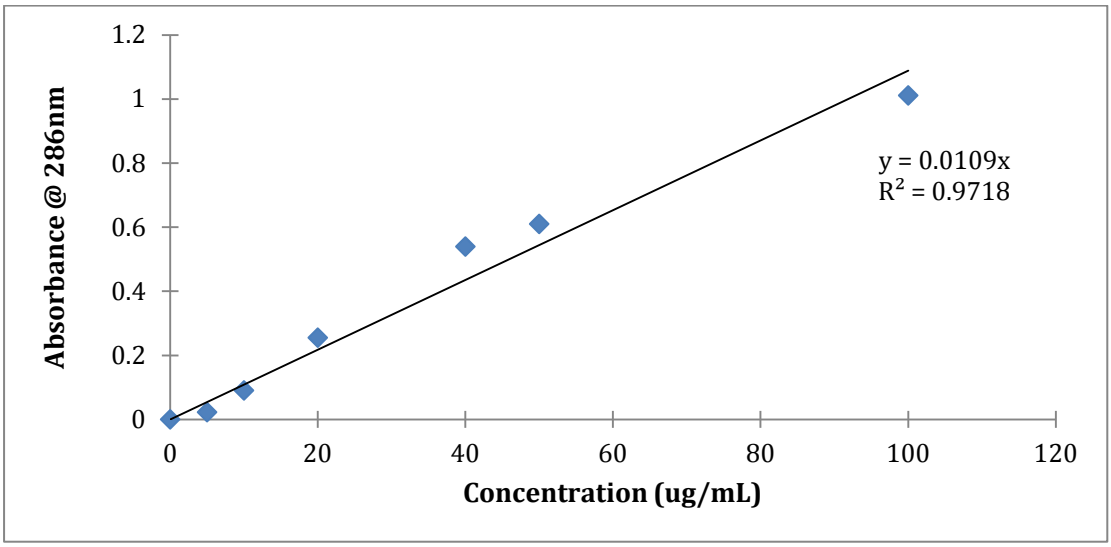

Figure 4.3: Cephazolin Sodium Calibration Curve

4.3 ANTIBIOTIC LOADING CAPACITY

This experiment was designed to confirm the attachment of cephazolin sodium to the various scaffold types. There is a lack of previous research indicating threshold loading capacities for similar antibiotics on scaffolds.

4.3 1. Methods

Three scaffold types were tested:

- Plain
- BG-infused
- BMG-coated

The antibiotic solutions were made using the following protocol.

Three 5mL plastic specimen vial of antibiotic solutions were made. 2mL of cephazolin sodium was placed in each vial at a concentration of 2.5mg/ml. The negative control was sterile deionised water and the positive control was the antibiotic solution only. The negative control aids to confirm false negatives, where negligible absorbance values were expected.

The positive control supported a reference point to compare with antibiotic concentration of test samples.

One scaffold was soaked in each vial. The vials were wrapped in foil to prevent UV exposure for degradable antibiotic inside. The vials were agitated on a platform rocker (model no: 8040, Bioline) on a medium setting. This step made the liquid go through scaffolds well and helped the concentration of the antibiotic through the scaffold to remain constant. Samples were tested in triplicate.

A small volume of liquid was taken from each plastic vial to check whether the concentration was different from the initial concentration. A 20µL sample volume and 980µL of water were mixed together in a cuvette for spectrophotometric measurements at 286nm. Sample was taken at the following time-points: 0min, 10mins, 30mins, 90mins, 3hrs, 6hrs, and 24hrs.

4.3.2 Results & Discussion

An antibiotic loading capacity test can confirm whether antibiotic attached to scaffolds. The concentration in the sample taken to spectrophometer is expected to decrease time by time. However Figure 4.4 reveals an opposite trend.

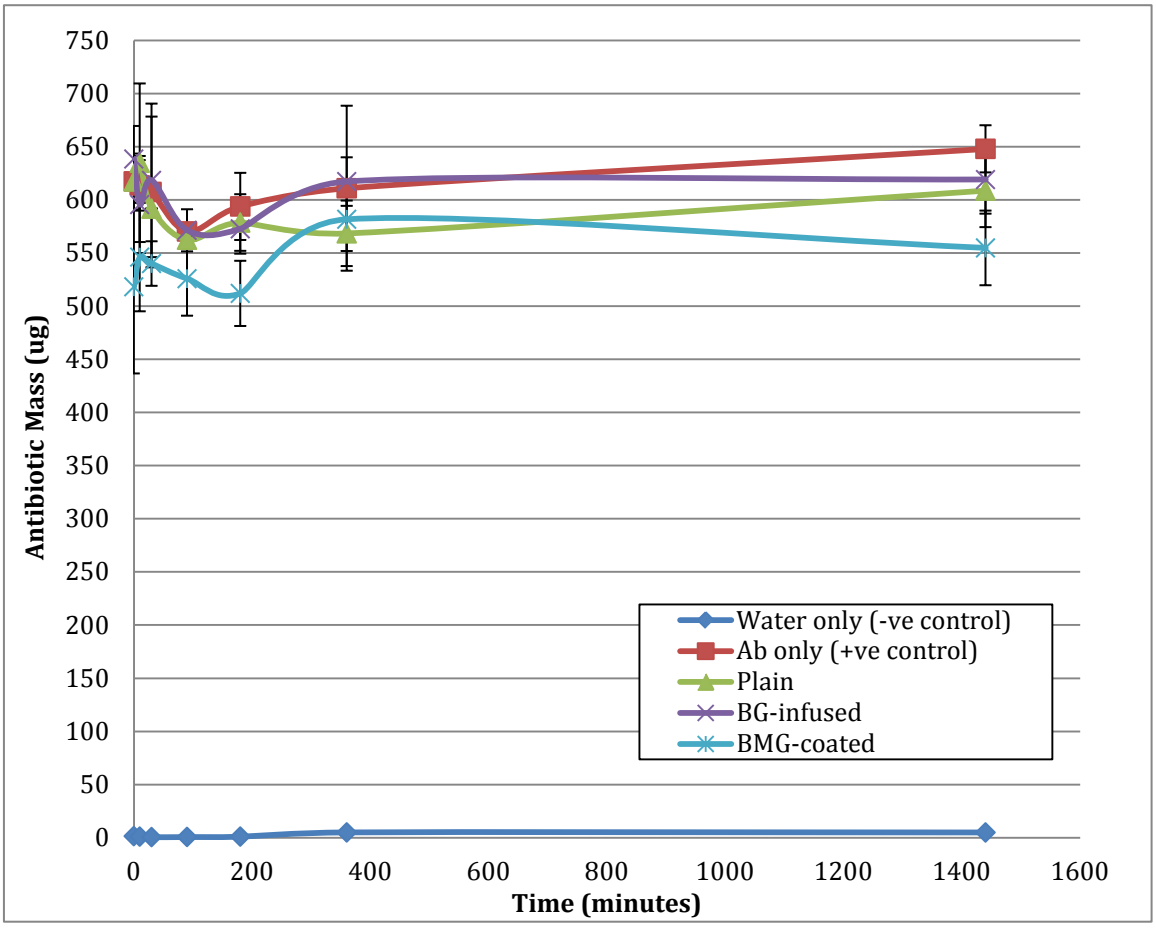

Figure 4.4: Profile showing the level of antibiotics remaining in the vials over a 24 hr period. This indicates the amount of antibiotic which had not been taken up by the scaffolds.

As seen from the figure, the level of antibiotic remaining in the vials for the different types of samples was similar after 24hrs of soaking. The decrease in the early time period may indicate loading of antibiotics onto scaffolds. However, the positive control displays a similar profile. This suggests the cephazolin attached to the plastic vial wall, despite keeping samples on a rocker platform to prevent this. Therefore, the true concentration of antibiotics is not known accurately and cannot used to calculate the amount of antibiotics that may have attached onto the scaffold. The amount of antibiotic loaded onto the scaffold could perhaps be estimated by analysing the differences in concentration between positive control and test samples (Figure 4.5). This figure shows that there may have been 3x antibiotics loaded onto the BMG-coated scaffolds, compared to the BG-infused scaffolds. However, the large standard deviation gives doubt about how accurate these trends are.

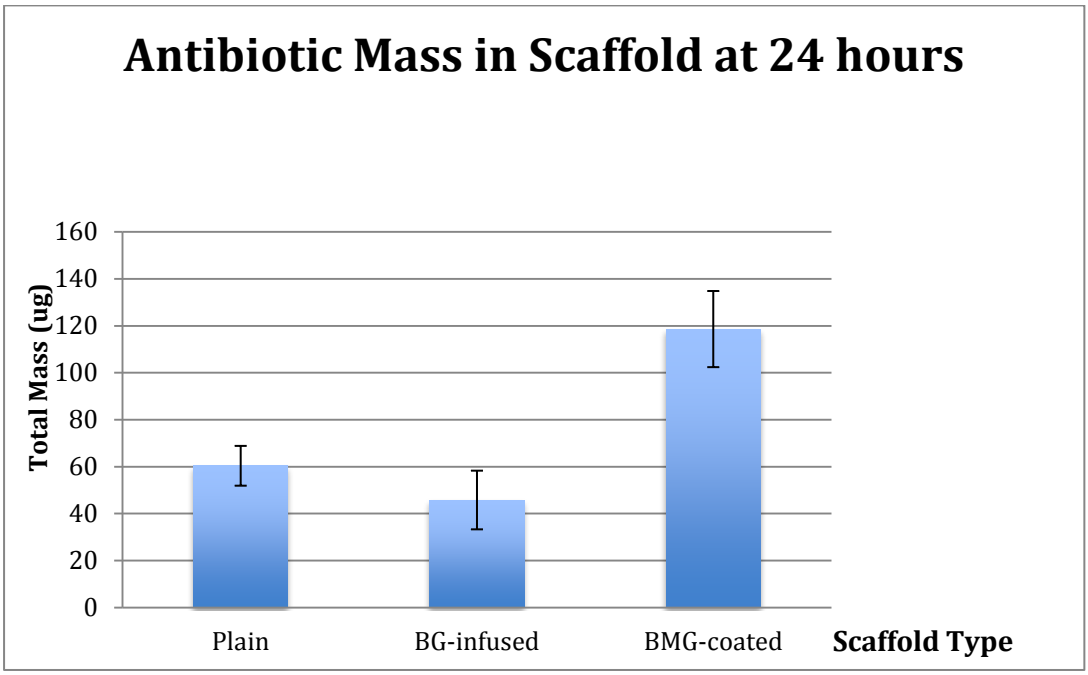

Figure 4.5: Average mass of antibiotic presumed to be in scaffold after 24 hours submersion.

These results could be explained by degradation of the antibiotic. Further experiments conducted by Ben Chow showed little degradation occurred [167].

4.3.4 Antibiotic Elution Profile

No references could be found describing the elution of cephazolin sodium from scaffolds. Figure 4.6 shows an ideal antibiotic elution profile [167]. This figure indicates the ideal curve is described by two phases, the initial burst phase, followed by a prolonged antibiotic release. The burst phase is expected to release the most antibacterial activity with its high concentration. This phase is essential for treating bacterial in wound beds instantly and then the sustained release phase continued, whereby can prevent further infections [151, 152]

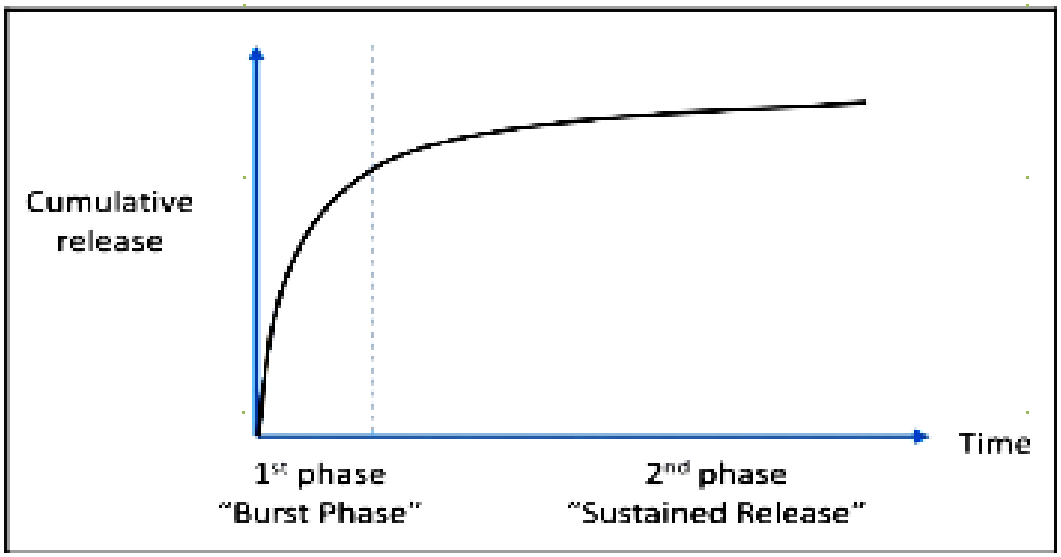

Figure 4.6: The ideal antibiotic elution profile, consisting of an initial burst phase, followed by a secondary sustained release [121].

4.3.4.1 Methods

Four scaffold types were tested for their antibiotic elution properties, including plain, BG-infused, BMG-coated and BG-infused + BMG-coated. Each type of scaffolds was coated with antibiotic. Each scaffold was put separately into plastic specimen vials and wrapped in foil. In each vial, 3mLdeionised water was added. Vials were agitated on a platform rocker.

At specified timepoints, a 200µL sample was taken from each vial for testing. Absorbance measurements were conducted at 286nm, at the same time-points as for the loading capacity time-course. The first time point was taken as the first contact point for the water and scaffold. The negative control used was plain scaffold to ensure that any absorbance readings were antibiotic, not due to other eluted scaffold particulates. Samples were examined in triplicate.

4.3.4.2 Results & Discussion

The resulting elution profiles are shown in Figure 4.7. These profiles clearly deviate from the 'ideal curve'. Positive eluted antibiotic amounts were recorded for plain and BG-infused scaffolds only. However, BMG-coated and BG-infused + BMG-coated scaffolds may have also eluted antibiotics, but were not detected given that the values for the negative control are also below zero.

This error may be equipment related, given the uncharacteristic negative control values. Alternately, the presence of BMG particles may have reacted with and broken down antibiotic molecules, either prior to or during elution profiling.

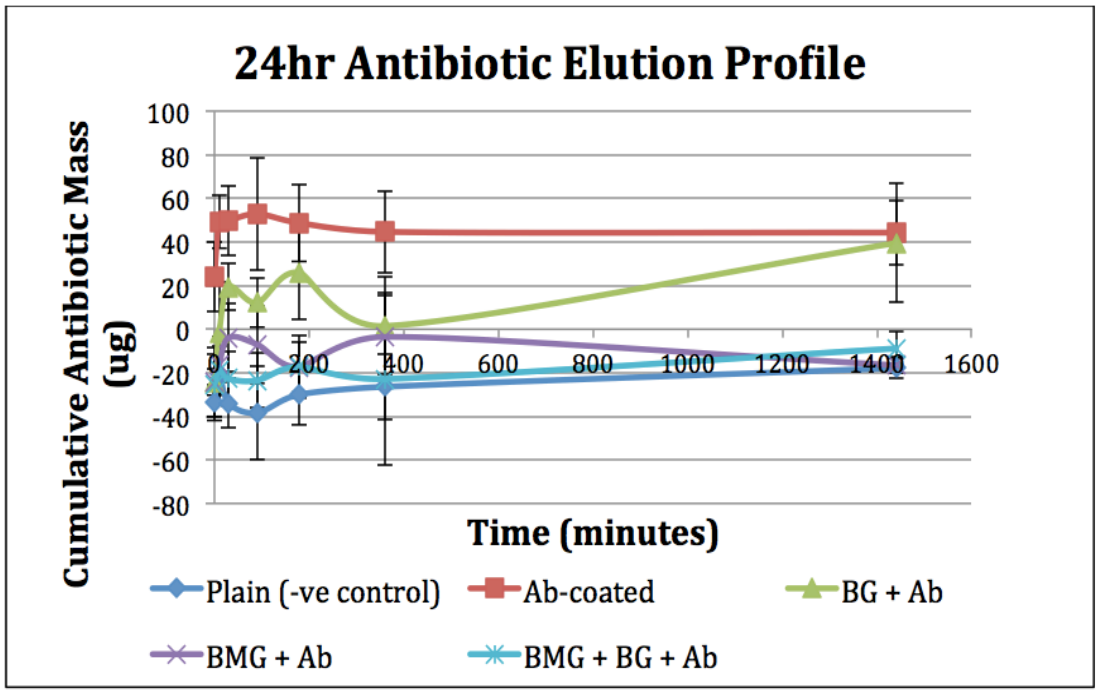

Figure 4.7: Elution of cephazolin sodium over 24 hours.

Despite these results, the possibility of successful antibiotic attachment should not be rejected. It is a possibility that antibiotic elution from BMG-coated scaffolds are prolonged and thus cannot be detected within 24 hours.

Basically the data are indicating that the cumulative antibiotic mass was essentially zero for the plain, BMG+Ab and BMG+BG+Ab specimens, whereas the cumulative antibiotic mass was significant for Ab-coated and BG+Ab.

There is no current literature on the interaction between BMG and cephazolin sodium, particularly on a hydrophobic surface such as the PCL scaffold. As such, further investigations into their use are required. In the future, larger samples could be used to ensure detection of smaller eluted antibiotic amounts.

4.3.5 Summary of Antibiotic Loading Capacity

The uncertainty surrounding antibiotic coating on a BMG-coated scaffold remains to be resolved. Preliminary verification findings do suggest successful modifications. However, main unknown is the interaction between these substances and their antibacterial effect, especially, in an *in-vivo* environment. Next chapter designed to determine whether modified scaffolds inhibit bacteria.

The data demonstrate that the elution rate of BMG-coated scaffolds was lower than for the control, while the Bioglass-infused scaffold had about the same elution rate as the control.

This is a new and significant finding. However, as this is the first time such a study has been done, there is nothing in the literature with which these results can be compared. Therefore, it should be noted, that the present findings are based on a number of assumptions. Firstly, that there was no degradation of the antibiotic over the 24-hour period. Secondly, that solutes eluted from the scaffold do not effect the absorbance, and thirdly that the amount of antibiotic absorbed by the scaffold enough to cause a detectable change in the concentration of the remaining antibiotic. A future PhD project could investigate in great depth these assumptions and build on the findings of the present study.

CHAPTER 5

MICROBIOLOGICAL TESTING

5.1 SCAFFOLD STERILISATION

Before biological testing was conducted, all samples were sterilised to ensure no contamination. Plain scaffolds were initially sterilised within their package with gamma radiation, before being cut quarters using an aseptic technique so each scaffold measured ~5x5x5mm.

BG-infused and BG-coated scaffolds were subject to a different sterilisation process previously reported in the literature [168]. They were exposed to 20 minutes of UV radiation during which the scaffolds were inverted. This double exposure was to ensure all scaffold surfaces were irradiated. The scaffolds were then submerged in 70% ethanol solution for 20 minutes, before being transferred into phosphate-buffered saline (PBS) for a further 10 minutes. The drying process was similar to dry antibiotic-coated scaffolds, followed by overnight desiccation.

BMG-coated scaffolds were sterilised by exposure to 20 minutes of UV radiation with inversion. Base scaffolds used for coating were pre-sterilised.

Antibiotic-coated scaffolds were not subject to UV or ethanol exposure to prevent degradation of cephazolin sodium. The plain scaffolds had been gamma pre-sterilized prior to coating.

5.2 EVALUATING BACTERIAL ATTACHMENT ON PLAIN SCAFFOLD

5.2.1 Introduction

For the purposes of biological testing, it is necessary for bacteria attach to the base scaffold, in order to determine any effects of the surface modifications.

As mentioned in the literature review, various bacteria types may infect a chronic wound. As such, a preliminary experiment was set up to characterise bacterial attachment to the scaffold with bacterial species including *Staphylococcus aureus*, *Staphylococcus epidermidis* and *Pseudomonas aeruginosa*. These were chosen due to their clinical relevance in infected chronic wounds [13]. However, non-virulent strains were used for the purposes of minimising biological hazards.

5.2.2 Materials & Methods

The bacterial broths were made by inoculating each bacteria in separate jar containing 100% tryptone soy broth (TSB) solution (product no. CM0129, OXOID). These jars were incubated overnight on an incubator shaker platform set at 120 rpm, at 37°C (Innova 42 Incubator Shaker, New Brunswick Scientific). Solutions of 10^6 cfu/ml were made from each bacterial broth via dilution. Twelve sterilised plain scaffolds were submerged in each jar of diluted bacterial broth, and left at room temperature

5.2.2.1 Harvesting Protocol

Triplicate scaffolds were harvested at 24hrs and 48hrs post scaffold submersion as shown in Figure 5.1. Scaffolds from the 24hr harvest were rinsed in PBS solution to eliminate excess bacterial broth. They were then transferred to separate screw-cap vials of 4mL PBS solution. The vials were subject to a 5-minute sonication process to allow bacterial detachment into the surrounding buffer solution. This was done at room temperature in a water-bath sonicator (model no. 80TD, Soniclean). A dilution series then was plated onto horse blood agar (HBA) plates (Micromedia Pty Ltd) for each sample (refer to Appendix). Two to three dilutions were plated to ensure a valid endpoint was reached. The plates were incubated overnight at 37°C. Cell counts were carried out and expected to be between 30 and 300.

A novel scaffold processing protocol was designed for the 48hr harvest in order to optimise the elimination of excess broth. In addition to an initial rinse in PBS, the scaffolds were also subject to a 10 second mixing process in fresh PBS solution, using a vortex mixer (FineVortex, FINEPCR). They were then individually transferred to 1.5mL Eppendorf tubes where excess liquid was removed by flicking the tube. The remaining protocol for processing and plating was the same as for the 24hr harvest.

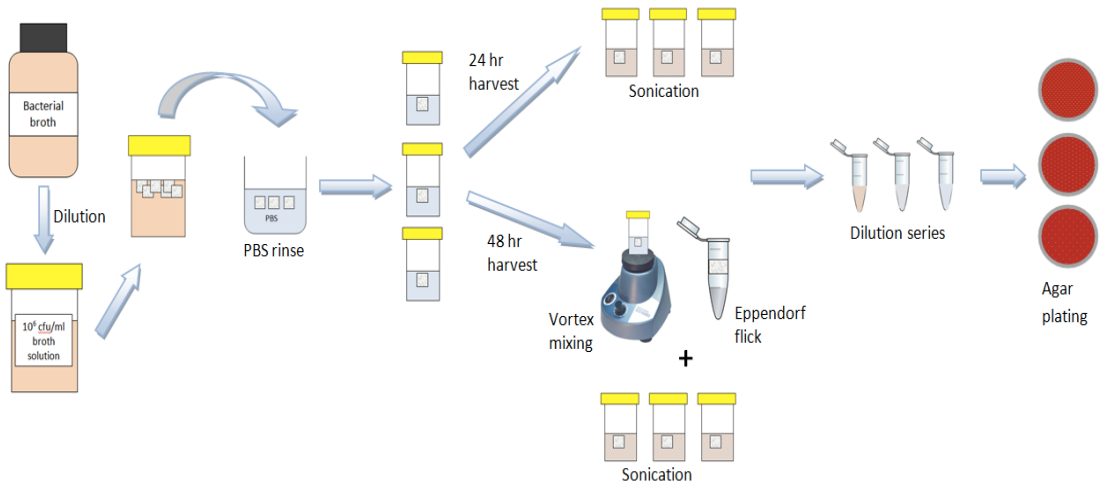

Figure 5.1: Schematic of experimental process for preliminary bacterial attachment tests.

5.2.3 Results & Discussion

All three bacterial species were found to attach onto the scaffolds, as seen in Figure 5.2. The highest attachment is *P. aeruginosa*, followed by *S. aureus*, then *S. epidermidis* for which very little attachment was observed. Slight differences were found between the 24hr and 48hr harvest for all three bacteria. This is contrary to the expected increase of bacterial growth over time. However, this may be due to the different scaffold processing protocol used for the 48-hour harvest. Excess planktonic bacteria may thoroughly be removed prior to plating.

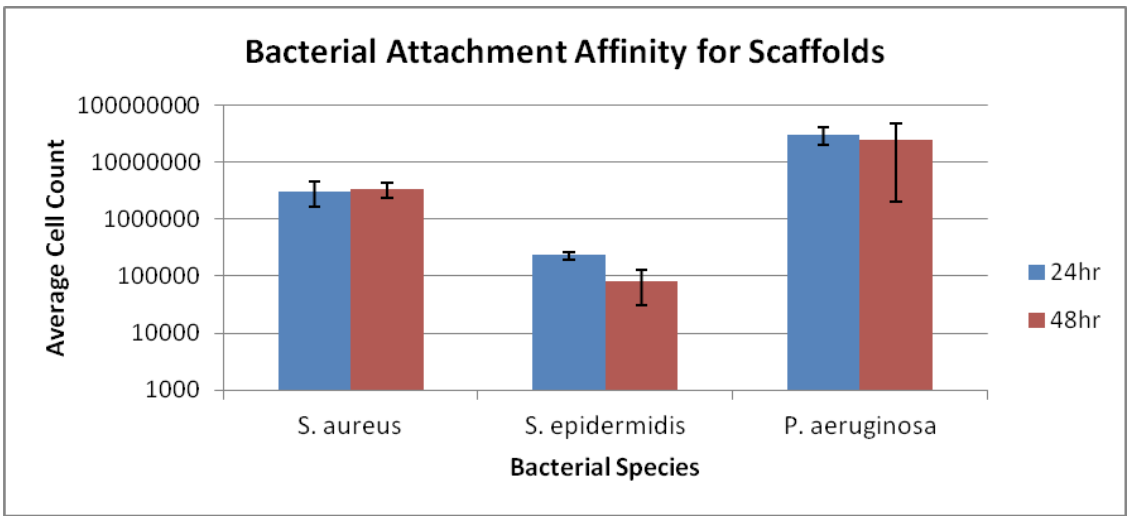

Figure 5.2: Comparison of bacterial attachment capacity of scaffolds with different bacteria relevant to the chronic wound.

The much higher growth of *P. aeruginosa*, an aerobic Gram-negative rod, is representative of its bacterial characteristics as an opportunistic pathogen. It is has a preference for growth in moist environments and is often ubiquitous in soil and water with a flagellum for high motility [169]. As such, the highly porous scaffold architecture provides an advantageous surface for *P. aeruginosa* growth. Additionally, *P. aeruginosa* is known to have simple nutrient requirements [170] , which may have contributed to its comparatively fast growth within 24 hours.

Staphylococcus species, on the other hand, attach to surfaces via adhesion proteins on their cell wall [20]. Their non-motility may thus account for their lower cell attachment count compared to *P. aeruginosa*. It has been shown that adhered *S. epidermidis* on polymeric surfaces take longer to grow than *P. aeruginosa*, with lag times of 4 hours and 1 hour, respectively [171]. Furthermore, *S. aureus* has also been shown, to adhere, at least 5 times longer more than *S. epidermis* on a range of polymeric surfaces [172], which is confirmed by the current results.

5.2.4 Summary of Bacterial Attachment Verification

From the results of this preliminary experiment, it can thus be shown that the scaffold readily acts as a possible surface on which bacteria can grow. Furthermore, different bacteria will display varied growth behaviour. The rinsing process of the scaffolds was found to be critical for an accurate representation of bacterial attachment, where planktonic bacteria must be removed.

5.3 *IN VITRO* WOUND MODELLING

5.3.1 Introduction

The *in vitro* wound model mimics *in vivo* wound environment as closely as possible. The method was established by Ngo et al [161]. A biofilm surface is grown in a moist, perfused environment. Teflon coupons are used as surfaces to grow biofilm. Using this approach, the effects of the scaffold on the experimentally induced bioburden can be investigated with more relevance to clinical settings. *S. aureus* was the chosen bacteria for this wound modeling experiment, given that it is the most prominent pathogen in infected wounds [23].

The principles of this model are based on the surface contact between the scaffold and coupon, and the process of bacterial migration and attachment. It is expected for the bacteria embedded in biofilm to become planktonic and attach to the scaffold surface (Figure 5.3a). As such, the surface modifications are expected to affect and potentially inhibit bacterial activity (Figure 5.3b and Figure 5.3c). It was hypothesised that the scaffold iteration with all modifications would have the most anti-bacterial and anti-biofilm effect.

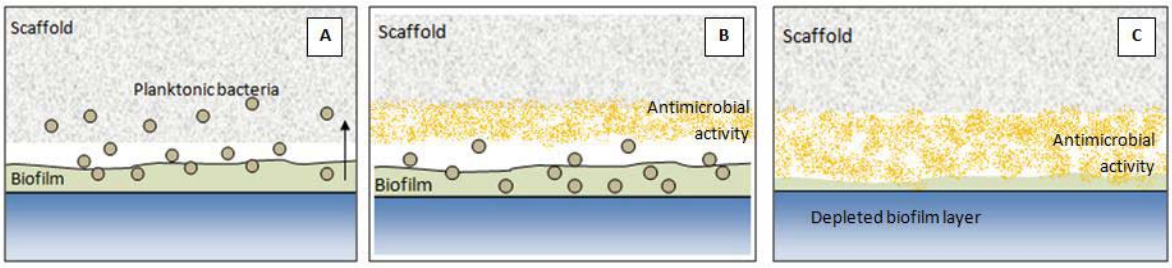

Figure 5.3: Schematic of interaction between scaffold and biofilm layer in an *in vitro* wound model. (a) Planktonic bacteria migrate and attach onto scaffold surface. (b) Antimicrobial activity from scaffold inhibit bacteria migration. (c) Antimicrobial degrade actively biofilm layer.

5.3.2 Methods

5.3.2.1 Biofilm Generation

The main apparatus for biofilm generation was a CDC biofilm reactor (CBR), which consisted of a reactor vessel, a rotating baffle and a cap with three inflow conduits (Figure 5.4). The reactor held 8 polypropylene rods, in which Teflon coupons, measuring 13mm in diameter 4mm depth, were assembled. These coupons provided the surfaces on which the biofilm was grown and for subsequent use in the *in vitro* wound model. Each rod held 3 coupons, thus allowing the generation of 24 biofilm-covered coupons at a time. Since 8 coupons were required for each type of model, so three types of models could be analysed in one set.

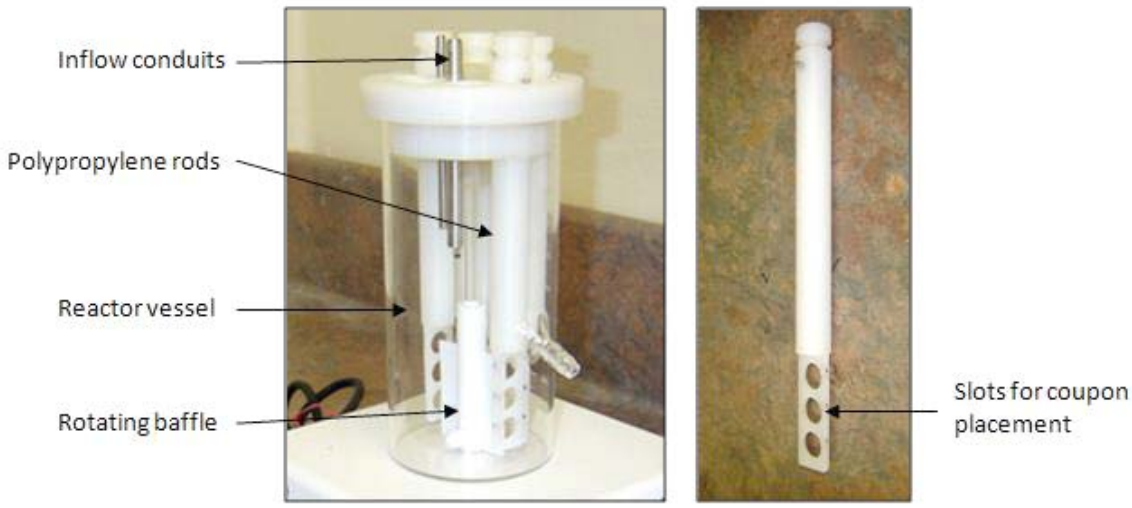

Figure 5.4 CDC biofilm reactor (CBR) apparatus used for biofilm generation.

The *S. aureus* broth was cultured via overnight incubation at 37°C. This was diluted to a 10^8cfu/ml solution, using the method outlined in the Appendix.

An initial static batch-phase, as seen in Figure 5.5, was carried out by inoculating 1ml of the 10^8 cfu/ml *S. aureus* broth into the reactor vessel, via the inoculation port. This also contained 500ml of 100% TSB solution to provide sufficient nutrients for *S. aureus* proliferation and attachment to the coupons. The CBR was kept in a 37°C water bath, on top of a digital magnetic stir plate (IKA RCT Basic, InVitro) set at 120 rpm. The bath was heated using a glass heater (AquaOne). An air pump (AP-750, AquaOne Infinity) was also connected to the CBR, which provided a continuous inflow of air to facilitate aerobic bacterial growth. The batch-phase was maintained for 24 hours.

This was followed by a 24hr dynamic flow-phase of biofilm growth, where 20L of 10% TSB solution was pumped through the CBR system at a rate of 13ml/min. A peristaltic pump

(Masterflex L/S Digital Standard Drive, Cole-Parmer Instrument) was used to connect the TSB reservoir to another inflow conduit on the CBR (Figure 5.5). A waste outflow line from the reactor vessel was connected, which allowed initial evacuation of excess planktonic bacteria, and subsequent continuous waste removal. This was collected in a waste reservoir, which contained 2L of 12.5%w/v sodium hypochlorite to kill incoming bacteria media.

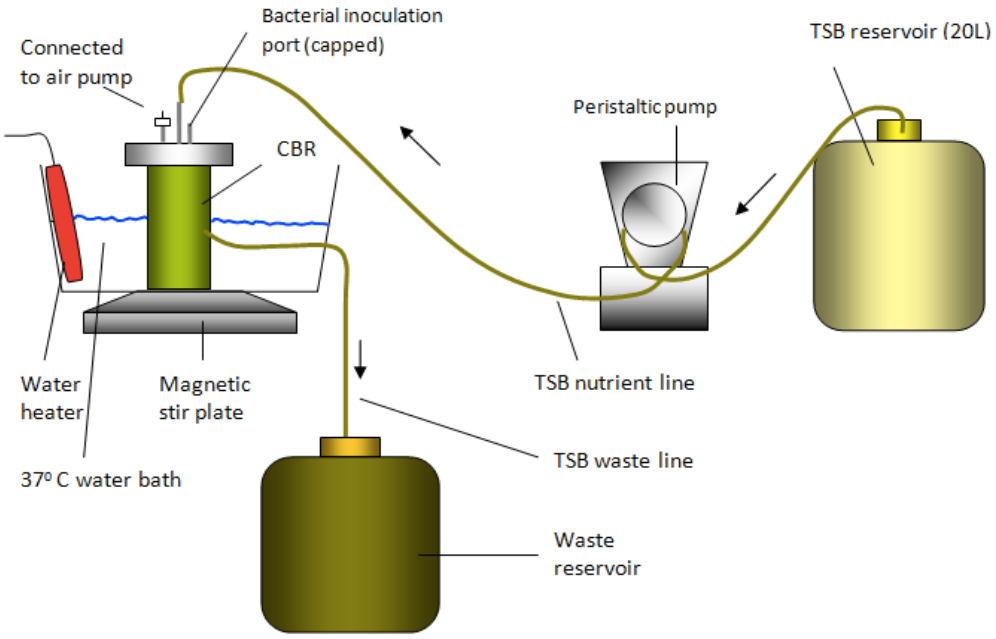

Figure 5.5: Equipment set-up for biofilm generation.

5.3.2.2 Coupon Preparation

The coupon rods were rinsed twice in PBS, before coupon removal and further rinsing to ensure elimination of any residual planktonic bacteria. One surface of biofilm was removed in order to accurately investigate the effects of the scaffold in contact with the remaining layer.

A paper towel moistened with 1.25%w/v sodium hypochlorite solution (APS Ajax Finechem.) was used to wipe one coupon surface (Figure 5.6). Several drops of bovine serum albumin (BSA) (Sigma-Aldrich) were simultaneously placed on the opposite surface to protect against unwanted disinfection. The coupons were then quickly rinsed twice in PBS to remove the BSA and any residual biocide before transferring to a third volume of PBS, until placement into the wound model chamber.

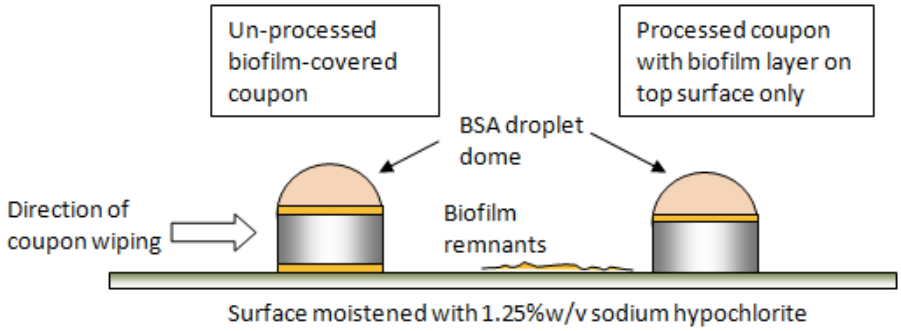

Figure 5.6: Coupon wiping process to rid one surface of biofilm layer.

5.3.2.3 Scaffold Preparation

A total of nine types of wound models were prepared. Three types of scaffolds were examined at a time, with 8 coupons for each type. Scaffolds were prepared as described in Section 3.1 & 3.2.

1. The first set of models contained Control coupons, Plain scaffolds, and BG-infused scaffolds.
2. The second set tested BMG-coated, Ab-infused, and composite BG-infused + Ab-infused scaffolds.
3. The third set tested BG-infused+BMG-coated, BMG-coated+Ab-infused and BG-infused+BMG-coated+Ab-infused composite scaffolds.

Plain scaffolds were used as the control for bacterial attachment. The control coupon was the plain coupon which had not been inoculated with bacteria. This tested whether the inoculation procedure had been successful. Experiments were conducted in triplicate so as to address the accuracy issues

5.3.2.4 Wound Model Chamber Preparation

The wound model chamber housed eight biofilm-covered Teflon coupons, which were embedded in an agar bed for stable placement. The bed was made-up by pouring molten 3% bacteriological agar around glass coupons, of similar size to Teflon coupons, to create the appropriate molds.

The glass coupons were removed once the agar turned to solid, followed by insertion of biofilm-covered coupons into the newly formed molds, with the biofilm surface exposed. This process is illustrated in the schematic of Figure 5.7. Individual scaffolds were then placed on top of the coupons while ensuring complete surface contact between both objects, as shown in Figure 5.7.

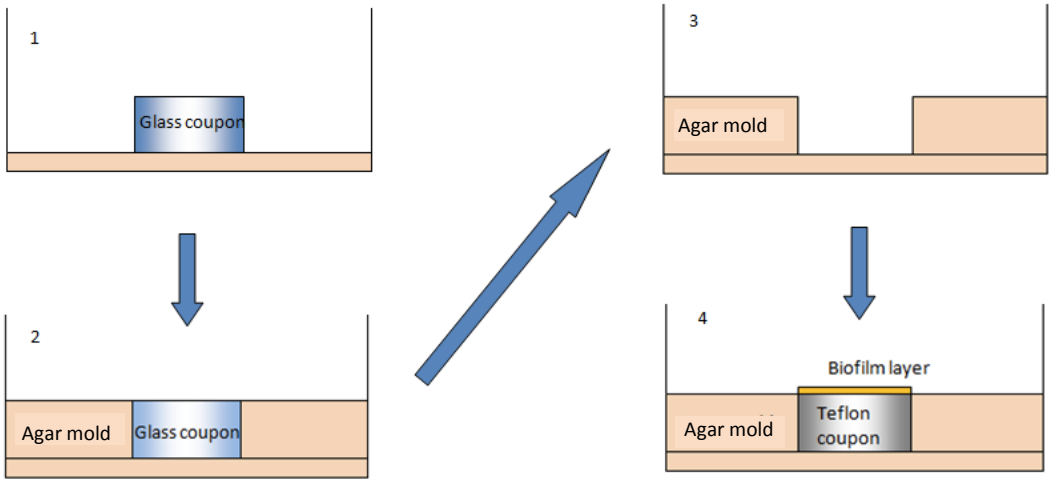

Figure 5.7. Preparation of wound chamber for coupon insertion.

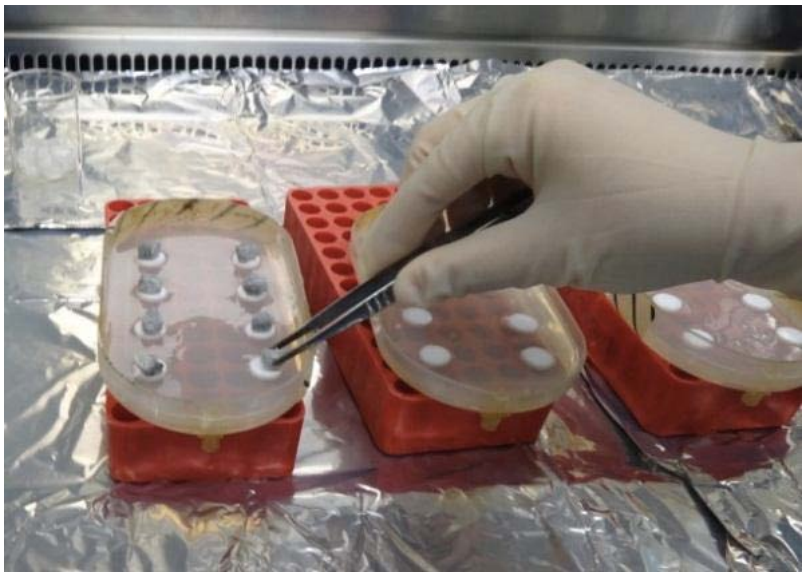

Figure 5.8: Placement of scaffolds into chamber using aseptic technique. Wound model chamber with scaffold samples on top of Teflon coupons (white) sitting in agar platform.

Sterile foam dressing (V.A.C. Vers-Foam Large Dressing, KCI) was cut then carefully placed over the top of the scaffolds in the wound chamber. This step assisted to maintain a moist chamber environment and preventing dislocation of scaffolds. A sterile adhesive drape (V.A.C. Drape, KCI) was then wrapped around the foam and chamber shape to create a fully contained structure with minimal susceptibility to potential contamination. Figure 5.9 & 5.10 illustrates the components within the wound model once completely set up.

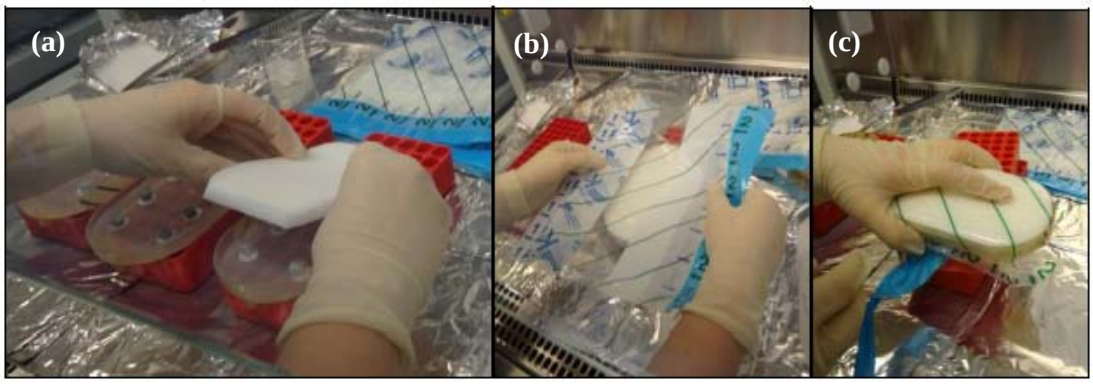

Figure 5.9: (a) Placement of pre-cut sterile foam dressing on top of wound chamber. (b) Positioning of sterile adhesive drape over foam. (c) Drape wrapped around whole chamber to ensure full containment and prevent contamination. The complete process was carried out aseptically in a sterile safety cabinet (HERA Safe KS, Thermo Scientific).

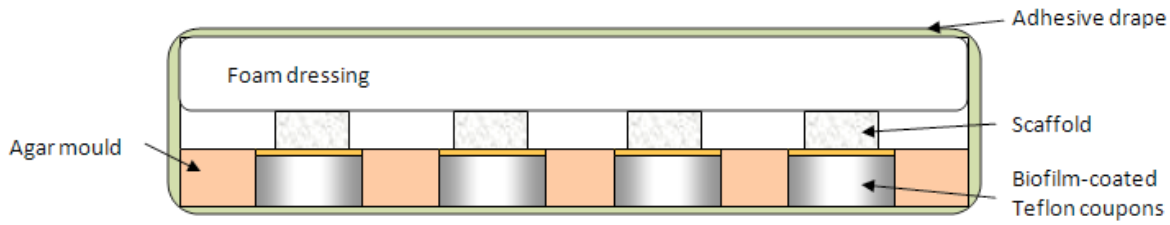

Figure 5.10: A schematic showing the components of a wound model chamber in a cross-sectional view.

5.3.2.5 Perfusion System

A perfusion system was set-up using a standard IV drip (BP Medical Supplies), and a 10% TSB-saline solution for nutrient flow. The perfusion rate was set to approximately 6-8 drips per minute, which was roughly a rate of 10 ml/hr.

The giving-set in-flow tube was connected to the wound model chamber at the top end via a small incision made through the adhesive drape, as depicted in Figure 5.11 & 5.12. The outflow tube connected to a small channel leading from the bottom of the chamber, which was fed into a waste container of 2L 1.25% chlorine solution for disinfection. The solution was replenished as necessary. All procedures were conducted aseptically.

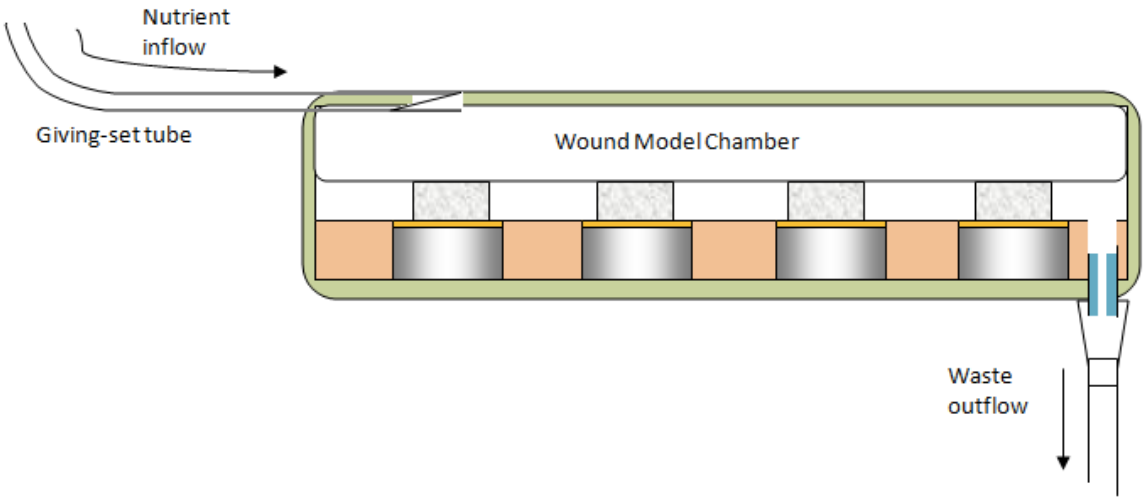

Figure 5.11: Schematic diagram of perfusion inflow and outflow through wound model chamber

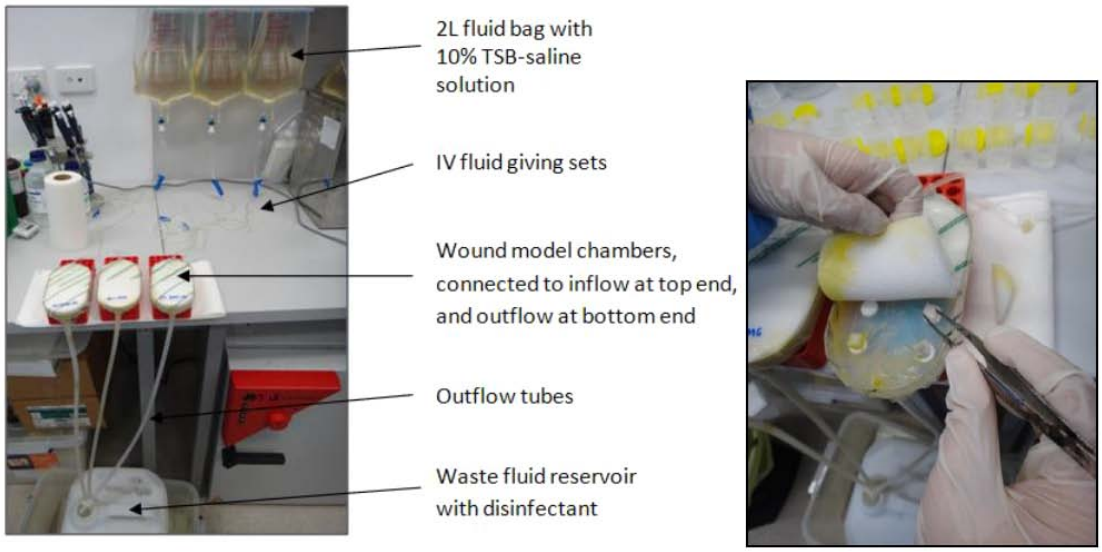

Figure 5.12: Left: Experiment set-up of in-vitro wound models showing the perfusion system in operation. Right: Sample harvesting process.

5.3.2.6 Harvesting Protocol

Triplicates of both scaffolds and coupons were harvested from the wound models. This was done at two time points; 4 and 6 days post scaffold-coupon contact. These times were chosen to allow adequate time for planktonic bacteria release from the biofilm and attachment onto the scaffold.

The harvesting process was carried out in an aseptic manner, sterile equipment was used. Access to the wound model chamber interior was achieved by firstly slicing through the adhesive dressing around the chamber perimeter, then peeling back the foam dressing to reveal the samples (Figure 5.12; right). These were then extracted and placed in individual vials of 5mL PBS, before sonication.

A dilution series then was plated onto horse blood agar (HBA) plates (Micromedia Pty Ltd) for each sample (refer to Appendix). Two to three dilutions were plated to ensure a valid endpoint was reached. The plates were incubated overnight at 37°C.

5.3.2.7 SEM Sample Preparation

An extra scaffold was also harvested for use in SEM imaging. These were transferred directly into 5mL of 3% glutaraldehyde solution for primary fixation and left for at least 2 hours at room temperature. The scaffold samples were then transferred into 5mL sterile deionised water and stored in a refrigerator at 5°C.

The remaining protocol for biological sample preparation and imaging was carried out by Alex Baume (USYD) at the Australian Centre for Microscopy & Microanalysis as described in section 3.2.3.2.

5.3.2.8 Statistical Analyses Method

Raw cell counts from each wound model were taken initially after 4 days and 6 days. Each wound model has one type of modified scaffold but three samples were taken for each harvest. So the result was an average of 3 samples. Cell counts across scaffolds and coupons were separately analysed using Kruskal-Wallis One Way Analysis of Variance (Kruskal-Wallis ANOVA) on Ranks, evaluating differences in median values. All Pairwise Multiple Comparison Procedures (Dunn's Method) were then carried out for each possible pair of scaffolds, then coupons. If results were insignificant, t-tests were carried out using sample pairs that showed largest difference on ranks. The power of these were calculated with $\alpha = 0.05$.

T-tests were similarly used to compare differences between the two harvesting time points for scaffolds and coupons. The program SigmaPlot 11 was used.

5.3.4 Results & Discussion

5.3.4.1 Cell Counts of Bacterial and Biofilm Attachment

Cell attachment was seen for most scaffold iterations at both time points. However, there were some exceptions.

Figure 5.13 shows the results from the first set of wound models. The control coupons demonstrated bacteria was successfully transferred and inoculation did occur. Without the scaffolds, bacteria inoculated successfully around 10^6 – 10^9 cfu/ml. At 4 days, the cell count on the BG-infused scaffolds and corresponding coupons is less than that of the plain scaffolds. This suggests a possible antimicrobial effect of the Bioglass on *S. aureus* attachment and biofilm, in accordance with literature [110].

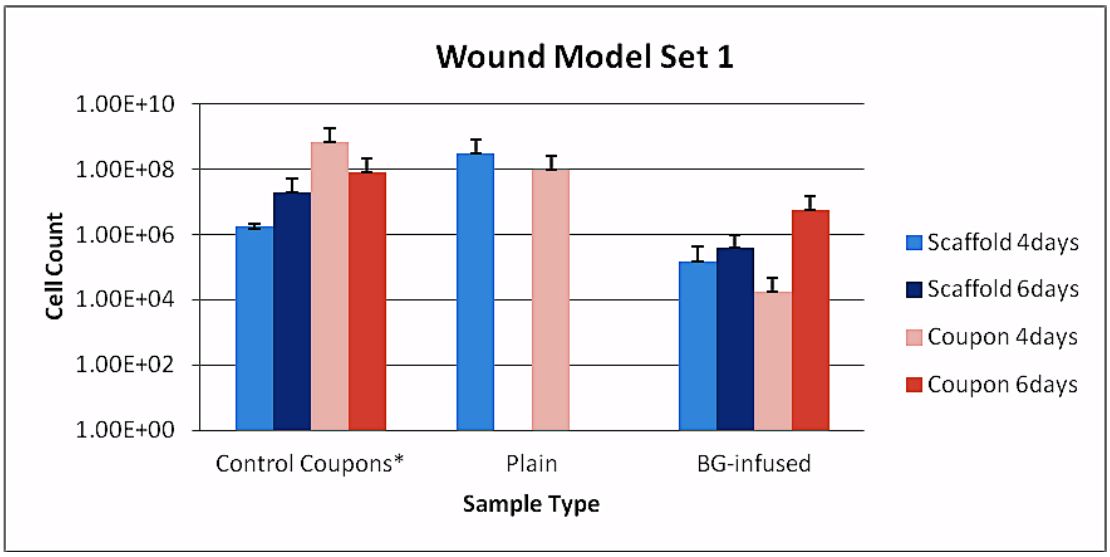

Figure 5.13. *S. aureus* cell counts for scaffolds and corresponding coupons of wound model set 1.

Figure 5.14 depicts the results for the second set of wound models. At 4 days, there were zero cells for all scaffolds for these Wound Models. This may imply effective antimicrobial activity, however, this result must be interpreted with caution. It is more likely to be a result of insufficient sonication or mixing, where the small amount of bacterial attachment may have been missed.

After 6 days, the scaffold with the least level of bacterial attachment was the BMG-coated scaffold. The BMG appears to have had a substantial effect on resisting biofilm attachment. This can be further reinforced by the low cell count on the corresponding coupon at day 4 ($8.17x10^2$ cfu). This is in comparison to the initial cell seeding number of $1x10^7$ cfu. This value was taken from a protocol adapted from Ngo et al [161].

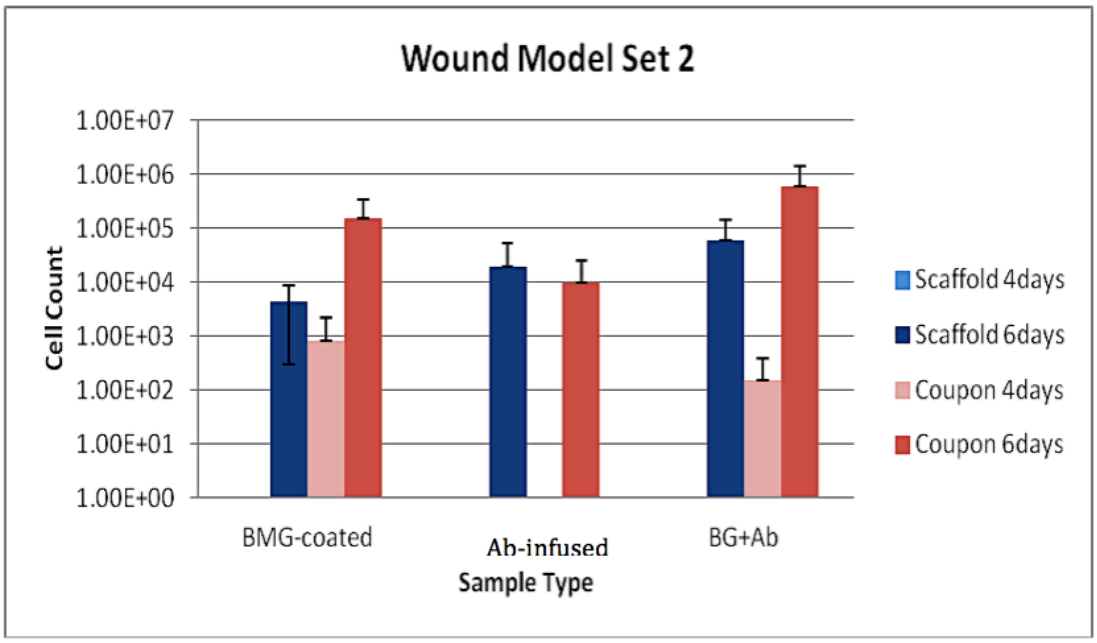

Figure 5.14. *S. aureus* cell counts for scaffolds and corresponding coupons of wound model set 2.

The antimicrobial effect of BMG is largely due to the metal ions and oxide by-products. Both magnesium and zinc oxides have been shown to inhibit *S. aureus* growth and attachment [116,117].

The 4 day time point was not used for the wound model set 2 as wound model set 1 was the primary experiment

The effect of BMG on bacterial attachment did have a limit, however, as evident by the increased average cell count on the coupons at 6 days. The elution of surface BMG may account for this. This excess BMG would have been subsequently flushed from the chamber by the flow of perfusion. However, residual BMG still remains as shown in Figure 5.21a.

The antibiotic-infused scaffold demonstrated a notably increased bacterial growth at the 6 day time-point compared to the BMG-coated scaffold. However, after 4 days, the number of bacteria on both the coupon and scaffold had been less than other scaffold types. This result may be explained by the antibiotics initially having an effect but they may have degraded over time. Alternately, this result may indicate an error in either the sonication or dilution steps.

Figure 5.5 shows the results for the third set of wound models. The scaffold with the highest antibacterial action appears to be the BG+BMG+Ab scaffolds. This was the trend for both the 4 day and 6 day timepoints. Furthermore, a similar trend for the corresponding coupons demonstrates anti-biofilm activity. It is proposed that the three modifications together create a synergistic antimicrobial effect, which otherwise cannot be achieved on their own or in pairs.

The formation of a hydrated silica gel layer by the infused Bioglass may entrap BMG particles and antibiotics, and thus delay their elution. This surface change is depicted in Figure 5.17.b. Consequently, their antimicrobial activity is prolonged, as seen after 6 days. This promising trend should be confirmed with further in-vitro testing with larger sample sizes.

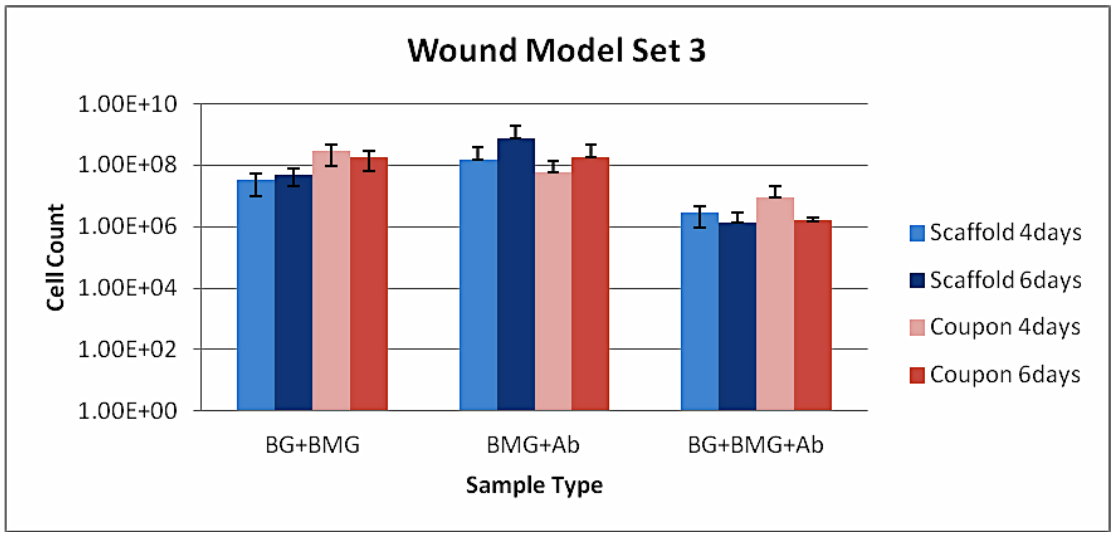

Figure 5.15. *S. aureus* cell counts for scaffolds and corresponding coupons of wound model set 3.

5.3.4.2 SEM Imaging of Bacterial Attachment

In order to certify bacterial attachment onto modified scaffold, SEM imaging has been undertaken. The results are shown in Figure 5.16 & 5.17.

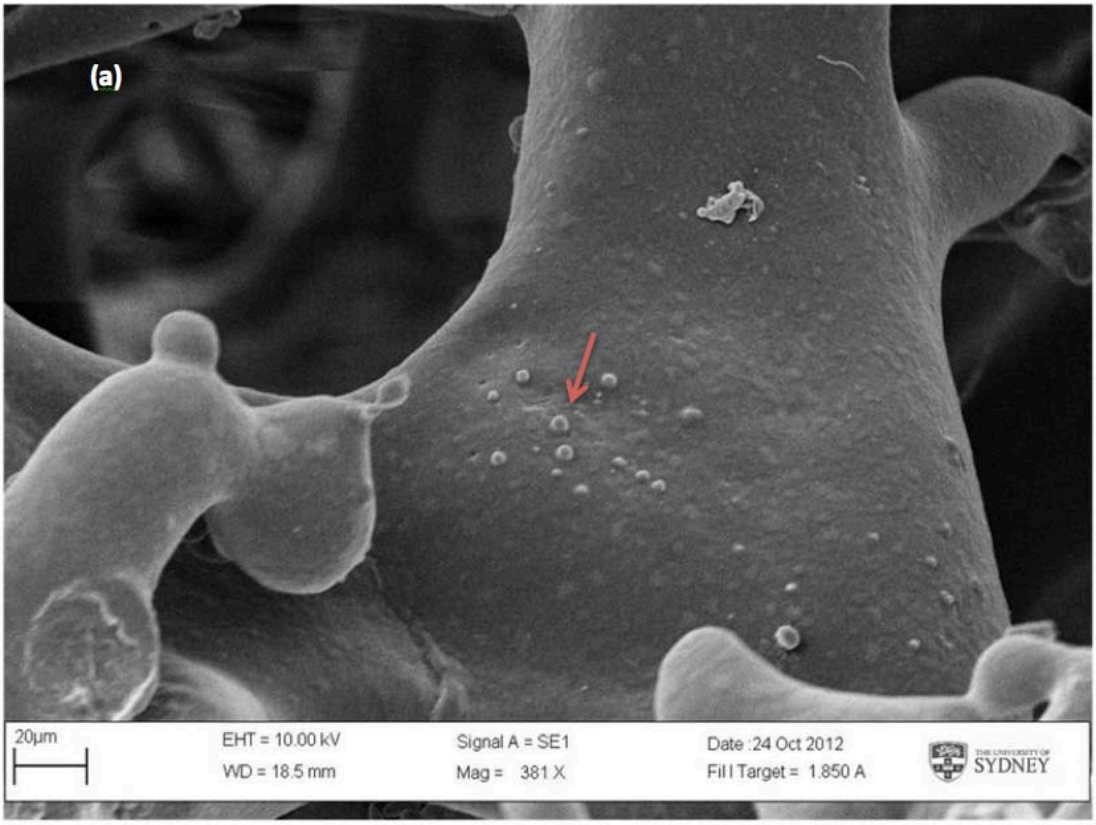
(a)
20µm
EHT = 10.00 kV
WD = 18.5 mm
Signal A = SE1
Mag = 381 X
Date :24 Oct 2012
Fil I Target = 1.850 A
THE UNIVERSITY OF SYDNEY

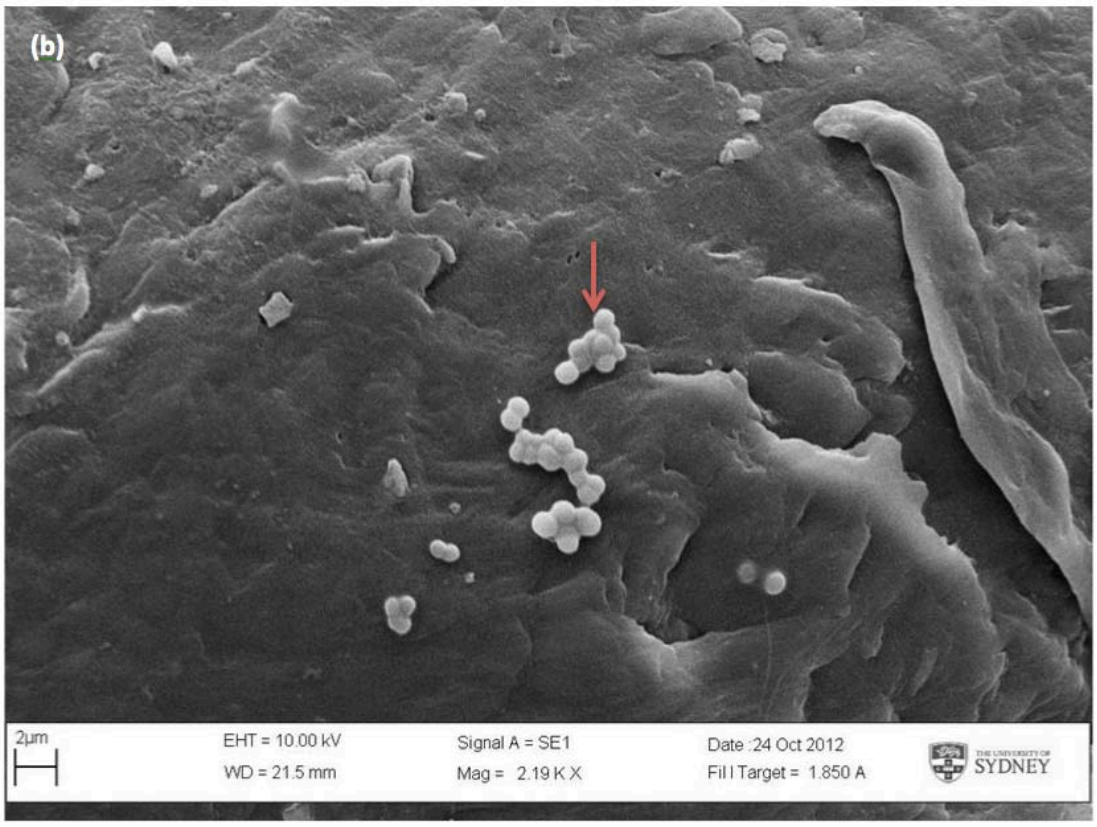
(b)
2µm
EHT = 10.00 kV
WD = 21.5 mm
Signal A = SE1
Mag = 2.19 K X
Date :24 Oct 2012
Fil I Target = 1.850 A
THE UNIVERSITY OF SYDNEY

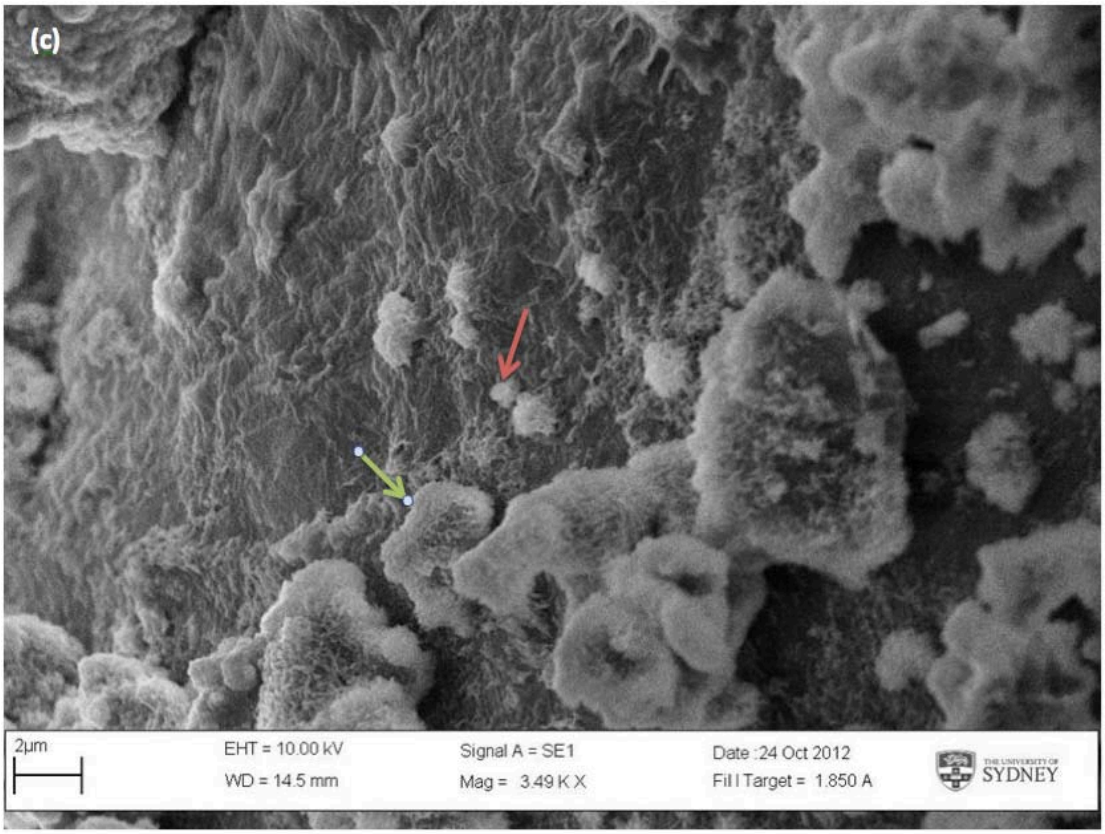

Figure 5.16. Magnified surface morphologies of scaffolds with none or one modification: (a) Plain Scaffold: Smooth surface with evidence of S. aureus attachment (red arrows) (x381), (b) BG-infused Scaffold: Clusters of S. aureus (red arrows) found on relatively smooth surface (2190x), (c) BMG-coated Scaffold: Highly textured surface with BMG particles (green arrows), and compromised bacterial remnants (red arrow) (3490x)

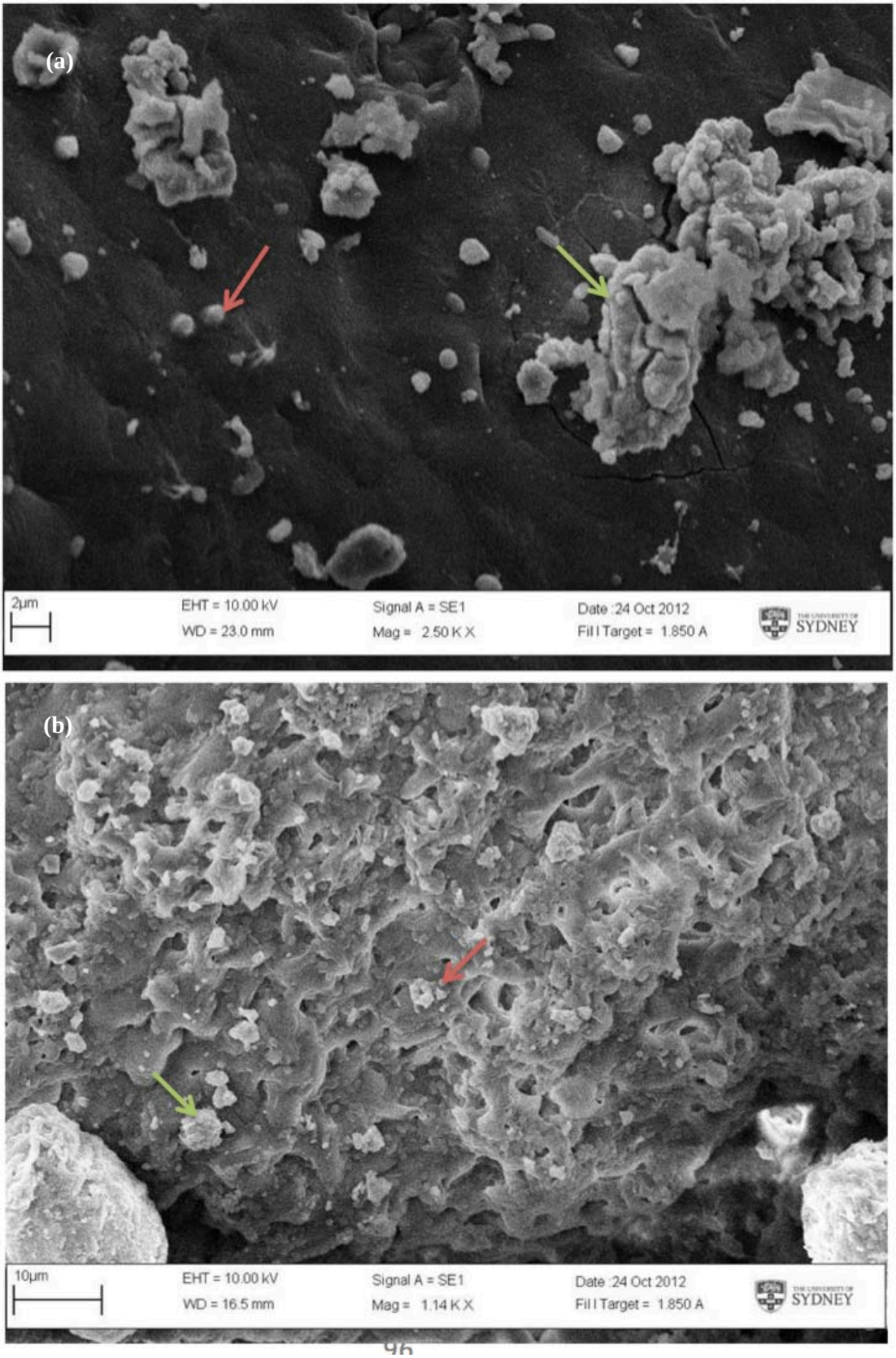

Figure 5.17. Magnified surface morphologies of scaffolds with combined modifications: (a) BG-infused + BMG-coated (2500x). Clumps of BMG remnants (green arrows) and individual S. aureus cocci (red arrows) amongst other debris can be found on top of a relatively smooth surface. (b) BG-infused + BMG-coated + antibiotic-coated (1140x). Highly roughened surface with S. aureus clusters (red arrow) and BMG precipitates (green arrow).

5.3.4.3 General Analysis of Wound Model

The t-tests comparing cell counts across harvests recorded negative results. This suggests that the prolonged wound model incubation time did not affect the bacterial growth on scaffolds or the biofilm layer on coupons. This insignificant difference, however, may again be accounted for by the high variability within triplicate cell counts for the same sample type. A general trend can still be distinguished amongst mean scaffold cell counts, with a general increase over the 6 day incubation period except BG+BMG+Ab scaffolds as shown in Figure 5.15.

The highest scaffold cell count was found for plain scaffolds ($3.03x10^8$ cfu) and for BMG-coated + Ab-infused ($7.35x10^8$ cfu), at 4 and 6 days respectively. Coupon cell counts were highest for control coupons ($6.70x10^8$) at 4 days, and for corresponding BMG-coated + Ab-infused coupons ($1.86x10^8$ cfu) at 6 days.

The zero cell count for scaffolds and corresponding coupons at 4 days is unexpected. In Section 5.2.3 the presence of bacteria attachment onto scaffolds had been confirmed. The primary explanation for this may be error in processing of coupon preparation for the wound model. Factors which may have caused biofilm elimination included excess sodium hypochlorite solution (biocide) for wiping or insufficient rinsing. Furthermore, moving of the scaffolds within the wound chamber may have scratched the biofilms. This may have occurred during placement of the foam dressing.

The Kruskal-Wallis ANOVA found significant differences amongst medians of both scaffold and coupon groups for each harvest, however, pairwise comparisons were mostly insignificant. Only coupons used with BG-infused+BMG-coated scaffolds were found to have significantly more bacteria than corresponding plain coupon ($P < 0.05$).

Subsequent t-tests found no significant differences between any scaffold pair at 4 days. However, the low power of the tests (0.408) suggests caution to be taken when interpreting negative results. Figure 5.16 and Figure 5.17 are SEM images revealing bacterial attachment onto the scaffolds. For the 6 day harvest of scaffolds, BG-infused+BMG-coated scaffolds were found to have significantly higher cell counts than plain ones ($P = 0.042$), however the power was also relatively low (0.553). This result may seem contradictory, as it was expected for modified scaffolds to introduce and encourage an antibacterial effect.

Despite the lack of significant differences between most scaffold types, which may be attributable to the variability in cell counts, general trends can still be drawn. For instance, the cell count on BG-infused scaffolds and corresponding coupons at 4 days is less than that of the plain scaffolds (Figure 5.13). However, the presence of Bioglass may lessen the effect of

cephazolin sodium. This effect was also seen in Figure 5.14, where there was an increased cell count on BG-infused+Ab-infused scaffolds compared to Ab-infused scaffolds. This may be due to a destructive interaction between the two substances, where Bioglass may inactivate the antibiotic, or vice versa by affecting the hydration products of Bioglass.

A further speculation is that the perfused TSB solution, as a protein source, may have affected antibiotic potency. In contrast, TSB enables bacterial growth, an activity required by antibiotics to have effect. In this instance, the potency of antibiotics may be indirectly increased. Further investigation would be required for a conclusive finding.

Although combine BMG+BG+Ab has seen the most effective (Figure 5.15) the increase in cell attachment for the remaining scaffold types does not necessarily dismiss antimicrobial effects of other modifications. As previously documented, the elution of antibiotics may account for the absence of their effects. The bacteria may simply have reattached and regrown within the first 4 days of inoculation. As such, higher concentrations of additives or perhaps a lower initial biofilm bioburden are acquired in future investigations.

An alternative viewpoint is that hydrated Bioglass may encourage bacterial growth. A hydrated silica gel may also provide a larger and optimum surface for bacteria to attach. The existence of both pro- and anti-bacterial activities of these substances are reasonable, thus a balance must be achieved in order to induce the desired effect.

5.3.4.3 Experimental Variations and In-vitro Wound Model Assessment

While interpreting these results, caution must be assigned upon drawing comparisons across all 8 scaffold types tested. As noted previously, the *in-vitro* wound model experiments were carried out in different groups, where slight variations in methodology as well as biological alteration may have affected the relative outcomes. As such, it may not be warranted to draw direct comparisons between combinations of scaffold modifications and the effects of their individual types. Cross comparisons within experimental sets, however, are more reasonable but still subject to experimental variation.

One possible explanation for various results is that there may have been different local pressures within the wound model chambers when applying the foam and adhesive dressing. This is an inherent design issue of this wound model system. This would have induced inconsistent scaffold-coupon contact areas, where higher bacterial attachment may be an indirect result of a greater compressive pressure. The greater exposure of the scaffold surface may have thus allowed more relative bacterial attachment. Furthermore, the decreased distance between the biofilm layer and scaffold struts may have contributed to more effective bacterial transfer. Alternatively, scaffold displacement from the coupon, during chamber

constructing, would have prevented bacterial attachment altogether. Any potential antibacterial effects would then have been overlooked. This variation would have to be controlled for manually, where consistent performance is required.

Variations in the perfusion system may also greatly influence the results. While this system is capable of replicating the perfused environment in a wound, the use of an IV fluid drip set invariably brings about inconsistencies, as it can only be controlled by hand with approximations to perfusion rate for each set. This system can be improved by using of peristaltic pumps, where perfusion rates can be accurately quantified and maintained.

A further cause of variation can be related to inconsistent scaffold geometries. This may have been due to inconsistent cutting, or distortion when handling with forceps. Thus, it is likely that different surface areas may have been exposed to the biofilm, leading changes in relative cell attachment. Therefore, the relative amounts of antimicrobial substances on the scaffolds would have been affected, in addition to the inherent variations during scaffold modification. To control for this error, scaffold sectioning may be automated or cutting guides used, or alternatively be manufactured to size to eliminate the need for quartering.

Larger sample sizes or customizing coupon number in each model can also be studied to reduce the variability.

5.34.4 Summary of Wound Model Tests

From this *in vitro* wound modelling experiment, it can be said that the combined antimicrobial effects of Bioglass, BMG and antibiotics were achieved, thus fulfilling a key user requirement defined for the scaffold. This modification on its own can induce activity against bacteria. However, the concentrations used may not have been high enough to induce prolonged effects. There is also the possibility of these substances inducing bacterial growth, either on each type or within a pair. There is still potential, however, to maximize resistance ability to bacteria and activity against biofilms. There need to used adequate concentrations and application techniques of antimicrobial substances.

It can thus be said that this novel experimental procedure has revealed the highly complex interactions between biological media and biomaterials. There is a need to carry out further *in vitro* testing in order to fully assess the interactions and effects of developed scaffolds on wound-like bioburdens. The incorporation of a perfusion system and presence of biofilm are particularly important experimental variables that allow a more clinically relevant assessment, and thus the novelty of this investigation.

5.4 PRIMARY BACTERIAL ATTACHMENT TESTS

5.4.1 Introduction

In order to further characterise the antibacterial potential of modified scaffolds in a simpler experimental model, planktonic bacterial attachment tests were developed. This was carried out to more directly exhibit the interaction between *S. aureus* and the modified scaffolds. Furthermore, the experimental outcome may have clinical significance for infected wounds devoid of biofilm.

5.4.3 Methods

5.4.2.1 Scaffold Test Samples

The following scaffold samples were used, and the hypothesised outcome in term of bacterial attachment:

BG-infused + BMG coated < BMG-coated< BG-coated< BG-infused< Plain scaffolds.

5.4.2.2 Primary Bacterial Attachment Protocol

S. aureus was again used in this experiment, where the broth and a dilute techinque 10^5cfu/ml solution were made using the same harvesting protocol.

Twelve scaffolds and four silicone samples of each type were placed into individual plastic specimen vials, containing 20mL of diluted *S. aureus* broth (Figure 5.18 & 5.19). These were left at room temperature. Samples were harvested at two time-points; 7 hours and 24 hours, including triplicate scaffold and duplicate silicone samples.

Samples were processed similarly to the optimised rinsing protocol set out in Section 5.2.2. However, instead of flicking, scaffolds were centrifuged at 1200rpm in Eppendorf tubes. This was to remove excess broth solution. Silicone samples were rinsed twice in PBS only. All scaffolds were placed into 5mL PBS solution for sonication, followed by a dilution series and plating onto HBA plates for overnight incubation at 37°C. Cell counts were subsequently recorded.

An extra sample of each scaffold type was also harvested at the 7-hour time-point for processing for confocal imaging. A live-dead stain was applied to the scaffold surface for 1 hour, followed by a 1-hour fixation process with 3% paraformaldehyde. The samples were then rinsed 3 times with PBS for 10 minutes and left in the final rinse for storage at 4°C until imaging. Tubes containing samples were covered in aluminum foil throughout the process. Dr's A. Jacombs and H. Hu at the Australian School of Advanced Medicine, Macquarie University, carried out the sample preparation and imaging.

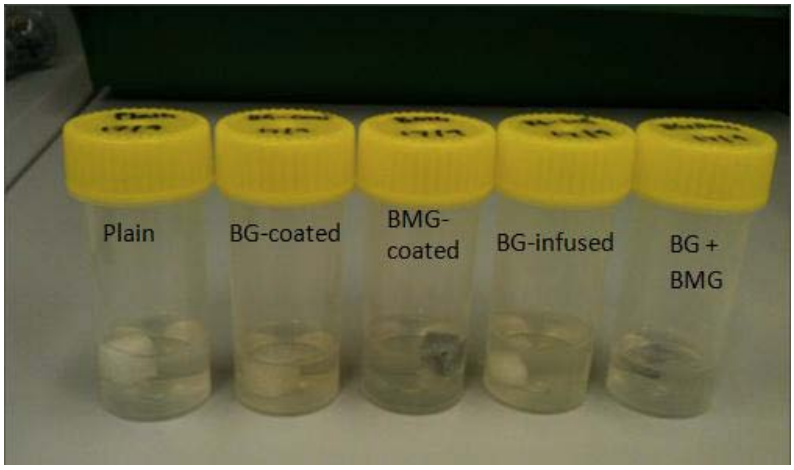

Figure 5.18: Scaffold samples after harvesting and sonication.

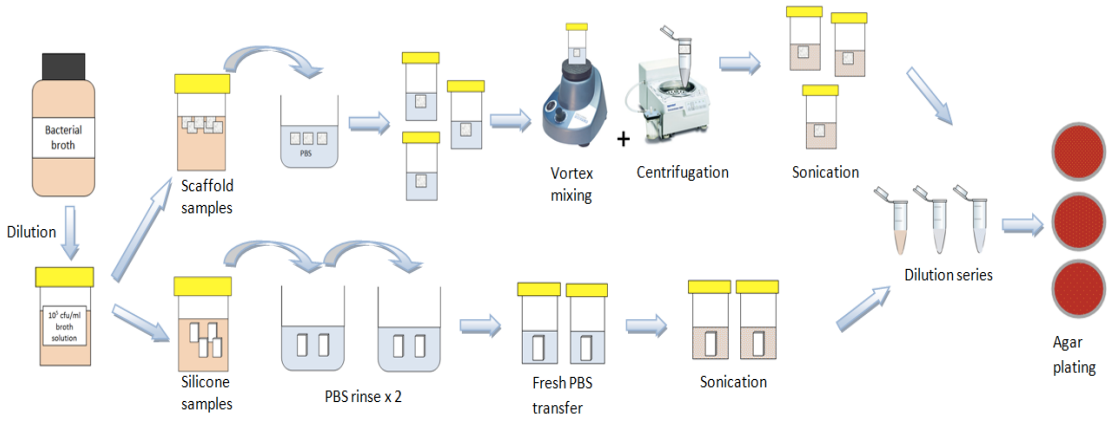

Figure 5.19: Schematic of experimental process for primary bacterial attachment test.

5.4.4 Results & Discussion

S. aureus was found to attach onto all sample types, with highest attachment counts on Bioglass-infused scaffolds and 100%w/v Bioglass coated silicone samples, at both harvesting time-points. Cell counts were also found to increase between the first and second harvest, as shown in Figure 5.20.

Statistical analysis showed that BG+BMG samples had bacterial attachment significantly higher ($p<0.05$) than plain, Bioglass-coated or BMG-coated samples at 7 hours. At 24 hours, Bioglass-coated scaffolds had significantly higher counts ($p<0.05$) than all other scaffold types, excepting BG+BMG samples, and similarly for Bioglass-infused scaffolds.

These results deviate widely from what was hypothesised, which was based on findings in literature that establish antimicrobial effects of Bioglass. The level of bacterial attachment or resistance by Bioglass is highly dependent on the amount it has dissolved into the media. In longer time courses, a higher level of resistance to microbial growth may have be evident for Bioglass. However at the 7 and 24hr timepoints, it appears the Bioglass infusion and coatings

change the scaffold surface morphology, particularly when Bioglass becomes hydrated to form a silica gel layer. This results in an increased surface area, which actually encourages bacterial attachment.

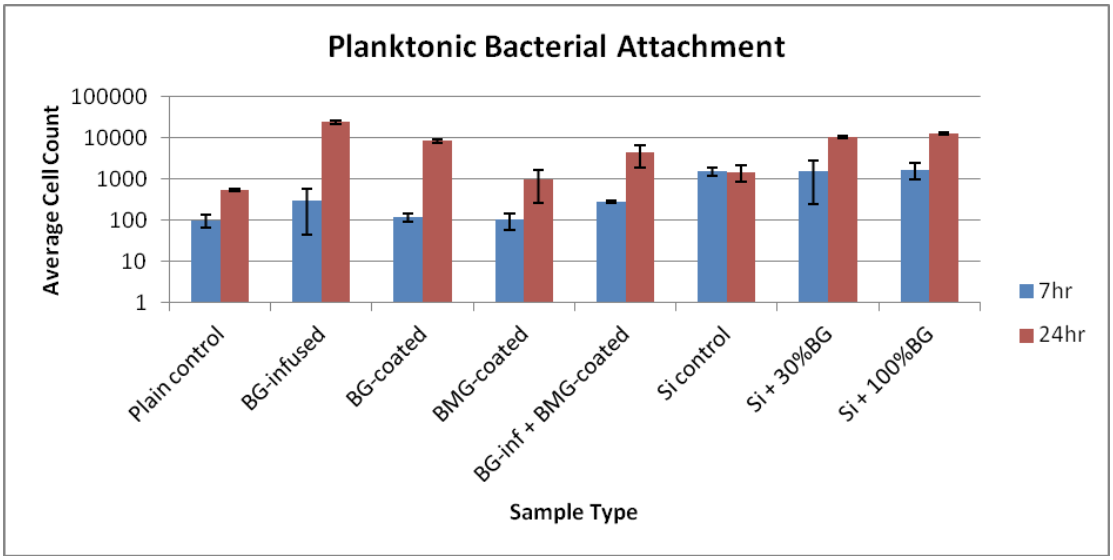

Figure 5.20: Average cell count of S. aureus attachment to scaffold and silicone samples submerged in planktonic bacterial broth for 6hrs and 24hrs.

This explanation could also be applied to Bioglass-coated silicone samples. After 24hr culture, there was more *S. aureus* attachment to BG-coated silicone than plain silicone. Similarly, a Bioglass coating can increase surface area due to increased surface roughness, and thus create more sites flat to bacterial attachment.

Differences to results reported in literature are likely to be due to variations in experimental protocol. Antimicrobial studies in the literature often test single Bioglass granules in higher concentrations than would be coated or infused onto scaffolds [110]. Current scaffold samples are highly interconnected, which contributes to a much larger surface area and a favourable microstructure on which bacteria can attach.

Furthermore, Bioglass particles are embedded in the polymeric struts of BG-infused scaffolds, thus reducing their exposure to the surrounding medium and overall concentration. Bacteria in samples with Bioglass in this experiment are therefore much higher than that of literature studies.

A different situation applies to Bioglass-coated scaffolds, as Bioglass particles here are not subject to the lack of bacterial exposure. Instead, detachment and elution of Bioglass may be the contributing factor to increased bacterial attachment. The eluted Bioglass will again be in the presence of much higher bacterial concentrations, thus any antimicrobial action may be reduced. This is particularly relevant for the 24-hour harvest where bacterial growth is known

to increase exponentially, which is confirmed by the increased cell counts (Figure 5.20). As such, the potential antimicrobial activity of Bioglass is greatly impeded due to these conditions.

The lack of expected antimicrobial effects of BMG-coated samples, as compared to the plain scaffold, is highly attributable to its elution into the surrounding TSB medium. This can be verified by observation of BMG particulate accumulation within the sample container (Figure 5.21a), as well as the loss of the characteristic grey discolouration of BMG-powder coating (Figure 5.21b) at the 7-hour harvest.

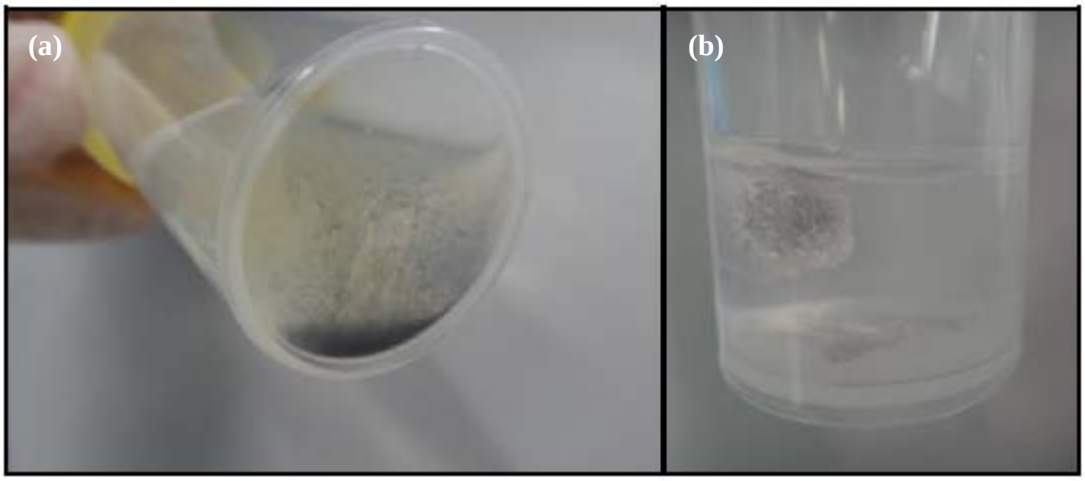

Figure 5.21: (a) Residual BMG powder accumulated from BMG-coated scaffold in sample vial. (b) Discolouration of BMG coated scaffolds from the surface, indicating BMG detachment.

Confocal images of all five scaffold types verify the attachment of bacteria, as seen by the green fluorescent staining (Figure 5.22). This staining is indicative of live bacteria, which suggest that *S. aureus* can still readily attach and grow on the scaffolds despite the presence of Bioglass and BMG. However, coverarge of live bacterial coverage may conceal any stained dead bacteria. Furthermore, dead bacteria may have detached from the scaffold, thus are absent in the images. These images remain a qualitative means of exhibiting confluent surface coverage by *S. aureus*, whereupon scaffold microstructure can also be represented.

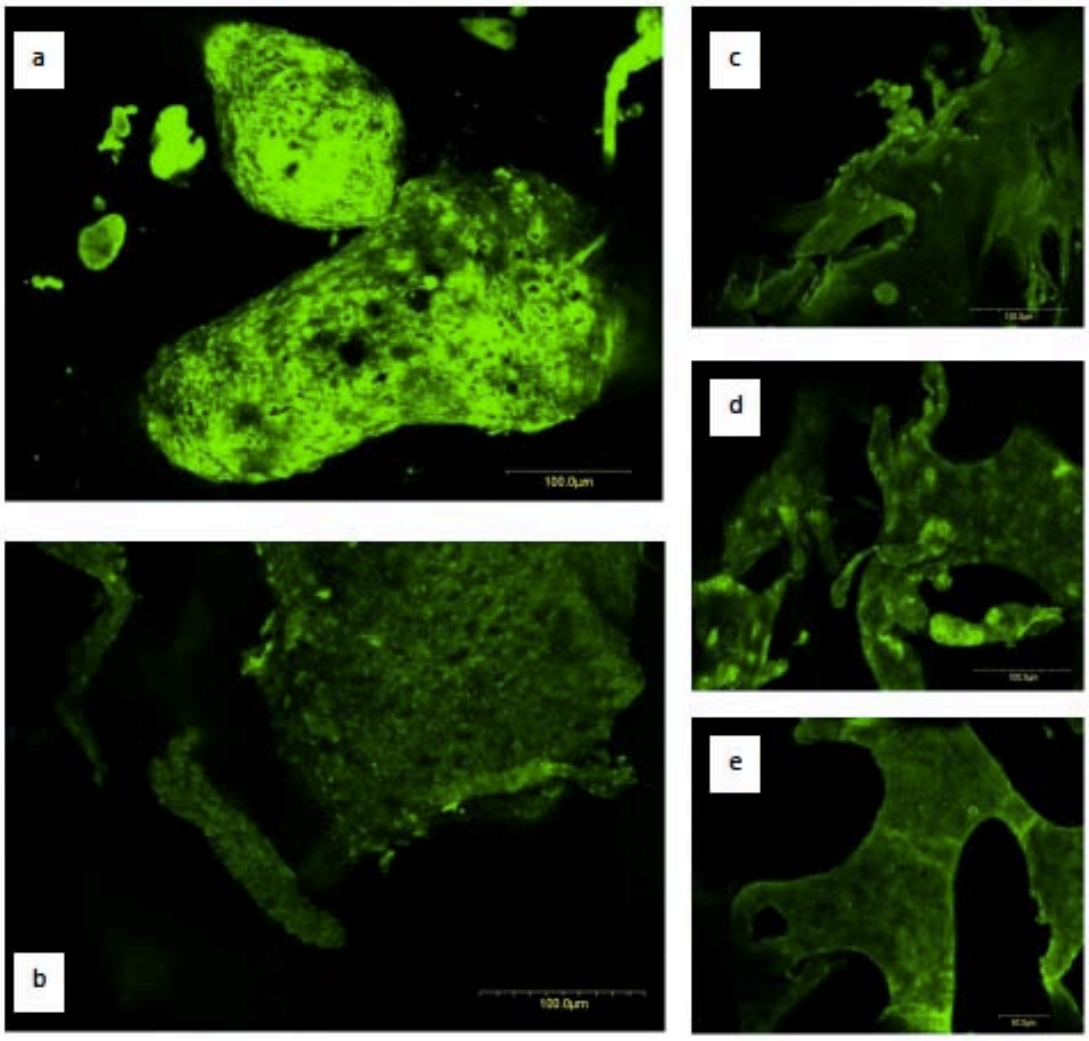

Figure 5.22. Confocal images of bacterial attachment onto scaffolds of the following types: a. Plain, b. BG-infused + BMG-coated, c. BG-coated, d. BG-infused, e. BMG-coated.

5.4.5 Summary of Bacterial Attachment

The result of this experiment provides preliminary evidence that Bioglass may encourage bacterial growth and attachment, contrary to several findings in literature [110]. This is a clinically relevant finding, which can help bring about a wider understanding of Bioglass-composite behaviours and may have a larger influence on its future applications.

With that, however, it must also be said that the experimental protocol plays a significant role in determining the result. This is particularly relevant to the highly dynamic and flexible nature of biological environments. Thus, this planktonic bacterial attachment experiment may be used to provide opposite insight into the complex interactions explored by more clinically relevant *in vitro* protocols, such as the *in vitro* wound modelling system.

CHAPTER 6

DISCUSSION & CONCLUSION

6.1 DISCUSION

Soft elastomeric polycaprolactone and bioactive glass composite scaffolds were reliably fabricated using an established method as outlined in Chapter 2 [132]. A thermal coating method was used to adhere MgZnCa BMG particles to the scaffold. Scaffolds has been verified by SEM image (Figure 3.8) to observe interconnected and porous structure. When viewed on a sectioned surface, bioactive particles were found to consistently cover and adhere to the scaffold structure. The scaffold's strut array was maintained, vital for hosting granular tissue infiltrated with neo-vasculature carrying infection fighting cells.

Staph. aureus biofilm was generated using bioreactor (10^6-10^9 cfu/ml each coupon) after 4 days. This is compared to a value previously experiment by Ngo et al [161]which generated 1.8 x10^7 cfu/ml after 5 days. Inoculation was carried out via a new wound model. The token carrying the biofilm was situated within an agar dish and flow of body fluids was replicated using a IV. Bacteria was only allowed to infect the scaffold residing above the biofilm token in its planktonic phase of its life cycle.

As seen in Figure 5.16, BG+BMG+Ab scaffolds had more antibacterial activity than other modified scaffolds. It is proposed that the three modifications together create a synergistic antimicrobial effect, which cannot be achieved on their own or in pairs. The formation of a hydrated silica gel layer by the infused Bioglass may allow adsorption and ingress of metallic cations/salts and antibiotics, and thus slow the release of these antibacterial agents from the proximity of the scaffold. The MgZnCa BMG releases magnesium and zinc cations and related salts/oxides that are known to inhibit S.aureus growth [116,117]. Their antimicrobial activity was observed after 6 days. These finding need to be replicated.

From bacterial attachment test (Section 5.4), statistical analysis showed that BG+BMG samples had bacterial attachment significantly higher ($p<0.05$) than plain, Bioglass-coated or BMG-coated samples at 7 hours. At 24 hours, Bioglass-coated scaffolds had significantly higher counts ($p<0.05$) than all other scaffold types. While

biomaterials chemistry is critical in understanding antibacterial activity, this is also dependent on surface roughness and morphology. Bioactive glass infused and BMG coated scaffolds were observed to have additional porosity or surface roughness, providing additional binding sites for bacterial cells with good media access.

Work carried out in Section 5.4 with 30%, 100% bioactive glass coated silicone, demonstrated that bacterial attachment was enhanced by bioactive glass. While bioactive glass may be beneficial for soft and hard tissue attachment [95,105] and provide some minor antibacterial activity [110], this is not the case for all types of bacteria and all situations. It is speculated that both bioactive glass infusion and coatings change the scaffold surface morphology, particularly when bioactive glass becomes hydrated to form a silica gel layer. Increasing surface area by adding rough coating would normally increase bacterial attachment.

This results in an increased surface area, which thus encourages bacterial attachment. While some studies have shown silver in Bioglass can improve antibacterial effect [111-113], silver is cytotoxic to wound tissues. Zinc on the other hand, can be antibacterial without being cytotoxic to granular tissue. Increasing zinc component and released cation may be beneficial for future studies.

Antimicrobial studies in literature often test single bioactive glass granules in higher concentrations than would be coated or infused onto the current scaffolds [110]. Current scaffold samples are highly interconnected, which contributes to a much larger surface area and a favourable microstructure on which both tissue and bacteria can attach. By enhancing tissue attachment using hydrated-silicate surfaces a scaffold can become more prone to bacterial infection, and yet, healthy vascularized tissue attachment can exclude bacterial attachment that would occur if a scaffold were isolated from blood contact due to a fibrous capsule. The optimum balance is proposed to be reached in ensuring vascularized tissue infiltration using a high interconnected porosity scaffold, using a soft tissue attachment medium such as bioactive glass.

6.2 CONCLUSION

Bioactive soft tissue scaffolds that can improve granular tissue infiltration and integration could assist wound healing even aside from the incorporation of antibacterial and antibiotic agents into the scaffold. To mitigate against persisting infection a new scaffold configuration was developed in this work. While bioactive glass particulates have been shown to have a slight anti-bacterial response, the main benefit afforded is for soft tissue attachment.

A cross-disciplinary review of relevant literature on wounds, biomaterials and scaffolds. Scaffold prototype and test design inputs were identified. Requirements were identified in chapter 2 then utilised and verified in subsequent chapters.

A novel iteration of scaffold design was successfully fabricated that incorporated a particulate bioactive glass infusion, and a particulate MgZnCa BMG and antibiotic infusion. This was characterized alongside variations and with controls using a bacterial attachment study and novel perfusion-biofilm model. The scaffold design demonstrated antibacterial and anti-biofilm activity that exceeded other variants and may be attributable to a synergistic effect arising from the combination of BMG, bioactive glass and antibiotic infusion.

Specific findings and contributions of this thesis include:

- Producing a polymer synthesis material which suit design requirement.
- Not only bacteria but also biofilm was created to test antibacterial possibility of scaffolds.
- Bioglass, BMG, and Cephazolin sodium can act synergistically to enhance antimicrobial and anti-biofilm action against *S. aureus* bacteria.
- Bioglass coated silicone and scaffolds, and infused scaffolds may encourage bacterial growth. This may be due to increased surface area and hydrated silicate surface chemistry that is desirable for soft tissue attachment.
- A novel *in vitro* scaffold-wound model was developed that can be used for pre-clinical development of wound treatments. It may also be applicable to investigating implant microbe, implant-biofilm interactions even approach to animal testing.

6.3 RECOMMENDATIONS

- Test other clinically relevant bacterial species with the same configuration (E Coli etc)

- Increase sample numbers used in microbiological evaluation

- Validate scaffold efficacy in in-vivo murine studies

- Apply this in vitro approach to other wound and biofilm relevant microbes

- Investigate the scaffold design in an infected in vitro skin cell culture model, before a subsequent animal infection model.

In conclusion, this thesis provides a some preliminary evidence for a platform for which further development could result in a safe and efficacious solution for treating serious chronic wounds.

REFERENCES

1. Rúben F Pereira, C.C.B., Pedro L Granja, Paulo J Bartolo, *Advanced Biofabrication Strategies for Skin Regeneration and Repair*. Nanomedicine, 2013. **8**(4): p. 603-621.
2. Silver, F.H., L.M. Siperko, and G.P. Seehra, *Mechanobiology of force transduction in dermal tissue.* Skin Res Technol, 2003. **9**(1): p. 3-23.
3. Proksch, E., J.M. Brandner, and J.M. Jensen, *The skin: an indispensable barrier.* Exp Dermatol, 2008. **17**(12): p. 1063-72.
4. Pomahac, B., et al., *Tissue engineering of skin.* Crit Rev Oral Biol Med, 1998. **9**(3): p. 333-44.
5. L, N., Chapter 29. Dermatologic Principles: Skin Anatomy and Physiology, M.-H. Medical, Editor 2011.
6. Fore, J., A review of skin and the effects of aging on skin structure and function. Ostomy Wound Manage, 2006. **52**(9): p. 24-35; quiz 36-7.
7. Marks, J.G.M., Jeffery Lookingbill and Marks' Principles of Dermatology. 2006. Elsevier Inc.
8. Sanders, J.E., B.S. Goldstein and D.F.Leotta, Skin response to mechanical stress: adaptation rather than breakdown - a review of the literature. J Rehabil Res Dev, 1995. **32**(3): p. 214-26.
9. Madison, K.C., Barrier function of the skin: "la raison d'être" of the epidermis. J Invest Dermatol, 2003. **2**: p. 121.
10. Robson, M.C., *A Failure of Wound Healing Caused by an Imbalance of Bacteria.* Surgical Clinics of North America, 1997. **77**(3): p. 637-650.
11. Robert D.Galiano , T.A.M., *Chapter 3: Wound care*. sixth ed. Grabb and Smith's Plastic Surgery, ed. C.H. Thorne2007: Lippincott Williams & Wilkins. 23-32.
12. Stephens, P., et al., Anaerobic cocci populating the deep tissues of chronic wounds impair cellular wound healing responses in vitro. British Journal of Dermatology, 2003. **148**(3): p. 456-466.
13. James GA, S.E., Wolcott R, et al, *Biofilms in chronic wounds. Wound Repair Regen.* 2008. **16**(1): p. 37-44.
14. Rhoads, D.D., R.D. Wolcott, and S.L. Percival, *Biofilms in wounds: management strategies.* J Wound Care, 2008. **17**(11): p. 502-8.
15. Lynch, A.S.a.G.T.R., *Bacterial and fungal biofilm infections.* Annual Review of Medicine, 2008. **49**: p. 415-428.
16. Anderson GG, O.T.G., *Innate and induced resistance mechanisms of bacterial biofilms.* Curr Top Microbiol Immunol, 2008. **322**: p. 85-105.
17. Suh, J.R., V.; Palmer, JN., *Biofilms.* Otolaryngologic Clinics of North America, 2010. **43**(3): p. 521-530.
18. Davies CE, H.K., Wilson MJ, et al. , se of 16S ribosomal DNA PCR and denaturing gradient gel electrophoresis for analysis of the micro- floras of healing and nonhealing chronic venous leg ulcers. J Clin Mi- crobiol 2004;42:3549–57., 2004. **42**(35): p. 49-57.
19. Boughton, E.A., Development of bioactive soft tissue scaffold systems, in University of Sydney2011, University of Sydney.

20. L.G. Harris, S.J.F., R.G. Richards, An Introduction to Staphylococcus Aureus, and Techniques for Identifying and Quantifying S. aureus Adhesins in Relation to Adhesion to Biomaterials: Review. European Cells and Materials, 2002. **4**: p. 39-60.

21. Smith's, G.a., *Plastic surgery*. 6th ed, ed. Charles H. Thorne2007.

22. Lipsky, B.A.a.C.H., *Topical Antimicrobial Therapy for Treating Chronic Wounds.* Clinical Infectious Diseases, 2009. **49**(10): p. 1541-1549.

23. Rayner C, M.W., Antibiotics currently used in the treatment of infections caused by Staphylococcus aureus. Intern Med J., 2006. **36**(2): p. 142-3.

24. Limited, N.N.Z., *Cefazolin Sandoz.* N.N.Z. Limited, 2009.

25. Veronese FM, B.R., Boccù E, Benassi CA, *Drug-protein interaction: the binding of cephalosporins to albumins.* Farmoco Sci, 1977. **32**(4): p. 303-10.

26. Rojanarata, T., et al., Stability of Fortified Cefazolin Ophthalmic Solutions Prepared in Artificial Tears Containing Surfactant-Based Versus Oxidant-Based Preservatives. Journal of Ocular Pharmacology and Therapeutics,, 2010. **26**(5): p. 485-490.

27. S., P., Advanced textile materials and biopolymers in wound management. Dan Med Bull, 2008. **55**(1): p. 72-7.

28. Jones, S.M., P.E. Banwell, and P.G. Shakespeare, *Advances in wound healing: topical negative pressure therapy.* Postgraduate Medical Journal, 2005. **81**(956): p. 353-357.

29. Jeff, C., Fewer wound complications seen with incisional negative pressure wound therapy. Orthopedics Today, 2011. **31**(11): p. 59-60.

30. Gregor, S., et al., *Negative pressure wound therapy - A vacuum of evidence?* Archives of Surgery, 2008. **143**(2): p. 189-196.

31. Patrick S. Murphy, G.R.D.E., *Advances in Wound Healing: A Review of CurrentWound Healing Products.* Plastic Surgery International, 2012: p. 1-8.

32. Mark, B., Using human skin equivalents to heal chronic wounds. Nursing, 2003. **33**(3): p. 68-69.

33. Sophocles H. Voineskos, O.A.A., Leslie McKnight, Achilleas Thoma, *Systematic Review of Skin Graft Donor-Site Dressings.* Plastic and reconstructive surgery, 2009. **124**(1): p. p.298-306.

34. Reza Miraliakbari, D.R.M., *Skin Grafts.* Operative Techniques in General Surgery, 2006. **8**(4): p. p.197-206.

35. Guan J, F.K., Sacks MS, Wagner WR., Preparation and characterization of highly porous, biodegradable polyurethane scaffolds for soft tissue applications. Biomaterials, 2005. **26**(18): p. 71-3961.

36. Jones AC, A.C., Hutmacher DW, Milthorpe BK, Sheppard AP, Knackstedt MA, The correlation of pore morphology, interconnectivity and physical properties of 3D ceramic scaffolds with bone ingrowth. Biomaterials, 2009. **30**(7): p. 51-1440.

37. Hench, L.L., *The story of Bioglass.* J Mater Sci: Mater Med, 2006. **17**: p. 22.

38. Hench LL, P.J., *Third-generation biomedical materials.* Science, 2002. **295**(5557): p. 1014-1017.

39. Jones JR, H.L., Factors affecting the structure and properties of bioactive foam scaffolds for tissue engineering. J Biomed Mater Res B Appl Biomater, 2004. **68**(1): p. 36-44.

40. Park WC, H.S., Kim NJ, Chung TY, Khwarg SI, Effect of basic fibroblast growth factor on fibrovascular ingrowth into porous polyethylene anophthalmic socket implants. Korean J Ophthalmol, 2005. **19**(1): p. 1-8.

41. LL, H., *Bioceramics and the origin of life.* J Biomed Mater Res, 1989. **23**(7): p. 685-703.

42. Jones JR, E.L., Hench LL., *Optimising bioactive glass scaffolds for bone tissue engineering.* Biomaterials, 2006. **27**(7): p. 964-73.

43. MacNeil, S., *Biomaterials for tissue engineering of skin.* Materials Today, 2008. **11**(5): p. 26-35.

44. Supp, D.M. and S.T. Boyce, *Engineered skin substitutes: practices and potentials.* Clinics in Dermatology, 2005. **23**(4): p. 403-412.

45. Priya, S.G., H. Jungvid, and A. Kumar, *Skin tissue engineering for tissue repair and regeneration.* Tissue Eng Part B Rev, 2008. **14**(1): p. 105-18.

46. Bottcher-Haberzeth, S., T. Biedermann, and E. Reichmann, *Tissue engineering of skin.* Burns, 2010. **36**(4): p. 450-60.

47. Clark, R.A., K. Ghosh, and M.G. Tonnesen, *Tissue engineering for cutaneous wounds.* J Invest Dermatol, 2007. **127**(5): p. 1018-29.

48. Metcalfe, A.D. and M.W. Ferguson, Tissue engineering of replacement skin: the crossroads of biomaterials, wound healing, embryonic development, stem cells and regeneration. J R Soc Interface, 2007. **4**(14): p. 413-37.

49. Joshaua S. Boateng, K.H.M., Howard N. E. Stevens, Gillian M. Eccleston, *Wound Healing Dressings and Drug Delivery Systems: A Review.* Journal of Pharmaceutical Sciences, 2008. **97**(8): p. 2892-2923.

50. Gaurav Tiwari, R.T., Birendra Sriwastawa, L Bhati, S Pandey, P Pandey, and Saurabh K Bannerjee, *Drug delivery systems: An updated review.* International Journal of Pharmaceutical Investigation, 2012. **2**(1): p. 2-11.

51. Montserrat Colilla, M.M., María Vallet-Regí, *Recent advances in ceramic implants as drug delivery systems for biomedical applications.* International Journal of Nanomedicine, 2008. **3**(4): p. 403-414.

52. Wood, D.A., *Biodegradable Drug Delivery System.* International Journal of Pharmaceutics, 1980. **7**: p. 1-18.

53. B. Huet de Barochez , F.L., A. Cuine Ardix , rue E. Vignat, *Oral Sustained Release Dosage Forms Comparison Between Matrices and Reservoir Devices.* Drug Development and Industrial Pharmacy, 1989. **15**(6&7): p. 1001-1020.

54. Siepmann, J. and F. Siepmann, *Modeling of diffusion controlled drug delivery.* J Control Release, 2012. **161**(2): p. 351-62.

55. Ronald S. Harland, N.A.P., *Accessibility Factors for Diff usion-Controlled Drug Delivery Systems.* Journal of Pharmaceutical Sciences, 1989. **78**(2): p. 146-148.

56. Komei Okabe, H.K., Junko Okabe, Aki Kato, Noriyuki Kunou, and Yuichiro Ogura, Intraocular Tissue Distribution of Betamethasone after Intrascleral Administration Using a Non-biodegradable Sustained Drug Delivery Device. 44, 2003. **6**: p. 2702-2707.

57. Patel, K., Design of Diffusion Controlled Drug Delivery System, in Rensselaer Polytechnic Institute., 2008, Rensselaer Polytechnic Institute: New York. p. 142.

58. Blazek, A., NMR imaging investigations of swelling-controlled drug delivery, in Department of Chemical1998, University of Victoria.

59. A. Martínez-Ruvalcaba, J.C.S.-D., F. Becerra, L. E. Cruz-Barba, A. González-Álvarez, *Swelling characterization and drug delivery kinetics of polyacrylamide-co-itaconic acid/chitosan hydrogels.* eXPRESS Polymer Letters, 2009. **3**(1): p. 25-31.

60. Cherng-Ju Kim, P.I.L., *Hydrophobic Anionic Gel Beads for Swelling-Controlled Drug Delivery.* Pharmaceutical Research 1992. **9**(2): p. 195-199.

61. Fariba Ganji, E.V.-F., *Hydrogels in Controlled Drug Delivery Systems.* Iranian Polymer Journal, 2009. **18**(1): p. 63-78.

62. Yihua Yin, Y.Y., Huibi Xu, *Swelling Behavior of Hydrogels for Colon-Site Drug Delivery.* Journal of Applied Polymer Science, 2001. **83**: p. 2835-2842.

63. Santosh Shep, S.D., Sandeep Lahoti, Rahul Mayee, *Swelling System: A Novel Approach Towards Gastroretentive Drug Delivery System.* Indo-Global Journal of Pharmaceutical Sciences, 2011. **1**(3): p. 234-242.

64. Giancarlo Santus, R.W.B., *Osmotic drug delivery: a review of the patent literature.* Journal of Controlled Release, 1995. **35**: p. 1-20.

65. Sapna N. Makhija, P.R.V., Controlled porosity osmotic pump-based controlled release systems of pseudoephedrine I. Cellulose acetate as a semipermeable membrane. Journal of Controlled Release, 2003. **89**: p. 5-18.

66. Irene S. Tobias, H.L., George C. Engelmayr Jr., Daniel Macaya, Christopher J. Bettinger, Michael J. Cima, *Zero-order controlled release of ciprofloxacin-HCl from a reservoir-based, bioresorbable and elastomeric device.* Journal of Controlled Release, 2010. **146**: p. 356-362.

67. Rajesh A. Keraliya, C.P., Pranav Patel, Vipul Keraliya, Tejal G. Soni, Rajnikant C. Patel, M.M. Patel, *Osmotic Drug Delivery Systemas a Part of Modified Release Dosage Form.* ISRN Pharmaceutics, 2012: p. 1-9.

68. Wright, J.C., Critical Variables Associated with Nonbiodegradable Osmotically Controlled Implants. The AAPS Journal, 2010. **12**(3): p. 437-442.

69. S.M. Herbig, J.R.C., R.W. Korsmeyer, K.L. Smith, *Asymmetric-membrane tablet coatings for osmotic drug delivery.* Journal of Controlled Release, 1995. **35**: p. 127-136.

70. Yu-Hsien Li, Y.-C.S., *Miniature osmotic actuators for controlled maxillofacial distraction osteogenesis.* Journal of Micromechanics and Microengineering, 2010. **20**: p. 8.

71. Shuaifei Zhao, L.Z., Chuyang Y. Tang, Dennis Mulcahy, *Recent developments in forward osmosis: Opportunities and challenges.* Journal of Membrane Science, 2012. **396**(1-21).

72. Ahmed Abd-Elbary, M.I.T., Ahmed Adel Alaa-Eldin, *Development and In Vitro/In Vivo Evaluation of Etodolac Controlled Porosity Osmotic Pump Tablets.* AAPS PharmSciTech, 2011. **12**(2): p. 485-495.

73. Teija Niittymaki, E.B., Evelina Laitinen, Anna Leisvuori, Pasi Virta, Harri Lonnberg, Zn2+ Complexes of 3,5-Bis[(1,5,9-triazacyclododecan-3-yloxy)methyl]phenyl Conjugates of Oligonucleotides as Artificial RNases: The Effect of Oligonucleotide Conjugation on Uridine Selectivity of the Cleaving Agent. Helvetica Chimica Acta, 2013. **96**(1): p. 31-43.

74. Ronit Satchi-Fainaro, W.W., Holger N. Lodec, Doron Shabata, Synthesis and Characterization of a Catalytic Antibody–HPMA Copolymer-Conjugate as a Tool for Tumor Selective Prodrug Activation. Bioorganic & Medicinal Chemistry, 2002. **10**: p. 3023-3029.

75. Jayant Khandare, T.M., *Polymer–drug conjugates: Progress in polymeric prodrugs.* Prog. Polym. Sci. , 2006. **31**: p. 359-397.

76. Zhiping Zhang, L.M., Si-Shen Feng, *Paclitaxel drug delivery systems.* . Expert Opinion Drug Delivery, 2013. **10**(3): p. 325-340.

77. Ping-Shan Lai, P.-J.L., Cheng-Liang Peng, Chin-Ling Pai, Wei-Nen Yen, Ming-Yi Huang, Tai-Horng Young, Ming-Jium Shieh, *Doxorubicin delivery by polyamidoamine dendrimer conjugation and photochemical internalization for cancer therapy.* Journal of Controlled Release, 2007. **122**: p. 39-47.

78. Rebecca M. Broyer, G.N.G., Heather D. Maynard, *Emerging Synthetic Techniques for Protein-Polymer Conjugations.* Chem Commun (Camb), , 2011. **47**(8): p. 2212-2226.

79. Shashi Ravi Suman. Rudrangi, R.R., Vijaya Kumar. Bontha, Samatha Rudrangi, *Progress: Legendary 'Magic Bullets' for delivery of Therapeutics.* International Journal of Pharmaceutical Sciences Review and Research, 2011. **11**(2): p. 7-12.

80. Toshiyuki Sakaeda, Y.T., Tamio Sugawara, Touko Ryu, Fumiaki Hirose, Takayoshi Yoshikawa, Koichiro Hirano, Lidia Kupczyk-Subotkowska, Teruna J. Siahaan, Kenneth L. Audus, Valentino J. Stella, *Conjugation with L-Glutamate for in vivo Brain Drug Delivery.* Journal of Drug Targeting, 2001. **9**(1): p. 23-31.

81. Kosasih, Conjugation of methotrexate to gelatin and its characterization, in Pharmacy and Science, 1997, Philadelphia College: UMI Dissertation Publishing. p. 103.

82. Lakshmi S. Nair, C.T.L., *Biodegradable polymers as biomaterials.* Progress in Polymer Science, 2007. **32**: p. 762-798.

83. F. Braye, J.L.I., E. Jallot, H. Oudadesse, G. Weber, N. Deschamps, C. Deschamps, P. Frayssinet, P. Tourermet, and S.T. H. Tixier, J. Lefaivrell and A. Amirabad, *Resorption kinetics of osseous substitute: natural coral and synthetic hydroxyapatite.* Biomaterials 1996. **17**: p. 1345-1350.

84. Friederike von Burkersroda, L.S., Achim G.opferich, *Why degradable polymers undergo surface erosion or bulk erosion.* Biomaterials, 2002. **23**(4221-4231).

85. Gopferich, A., *Polymer Bulk Erosion.* Macromolecules, 1997. **30**: p. 2598-2604.

86. MingPing Zhang, Z.Y., Li-Ling Chow, Chi-Hwa Wang, *Simulation of Drug Release from Biodegradable Polymeric Microspheres with Bulk and Surface Erosions.* Journal of Pharmaceutical Sciences, 2003. **92**(10): p. 2040-2057.

87. Elsie S. Place , J.H.G., Charlotte K. Williamsc and Molly M. Stevens, *Synthetic polymer scaffolds for tissue engineering.* The Royal Society of Chemistry, 2008. **38**: p. 1139-1151.

88. Negoro, S., *Biopolymers Online*. Biodegradation of Nylon and other Synthetic Polyamides2005: Wiley Online Library.

89. Langer, R., *Drug Delivery and Targeting.* Nature, 1998. **392**: p. 5-10.

90. Davis, B.K., Control of Diabetes with Polyacrylamaide Implants Containing Insulin. . Experientia, 1972. **28**(3): p. 348.

91. Robert Langer, J.F., Polymer for the sustained release of proteins and other macromolecules. Nature, 1976. **263**: p. 797-800.

92. Terasaka S, I.Y., Shinya N, Uchida T, Fibrin glue and polyglycolic Acid nonwoven fabric as a biocompatible dural substitute. Neurosurgery, 2006. **58**(134-139).

93. Peter B. Maurus, C.C.K., *Bioabsorbable implant material review.* Operative Techniques in Sports Medicine, 2004. **12**(3): p. 158-160.

94. Y. Lu, S.C.C., *Micro and nano-fabrication of biodegradable polymers for drug delivery.* Advanced Drug Delivery Reviews, 2004. **56**(11): p. 1621-2643.

95. Sinha VR, B.K., Kaushik K, Kumria R, Trehan A, *Poly-e-caprolactone microspheres and nanospheres: an overview.* Int J Pharm, 2004. **278**: p. 1-23.

96. Sung, H.J., et al., The effect of scaffold degradation rate on three-dimensional cell growth and angiogenesis. Biomaterials, 2004. **25**(26): p. 5735-5742.

97. Maria Ann Woodruff, D.W.H., *The return of a forgotten polymer—Polycaprolactone in the 21st century.* Progress in Polymer Science, 2010. **35**(10).

98. Vogel M, V.C., Gross UM, Müller-Mai CM., *In vivo comparison of bioactive glass particles in rabbits.* Biomaterials, 2001. **22**(4): p. 357-62.

99. Bhattarai N, G.J., Zhang M., *Chitosan-based hydrogels for controlled, localized drug delivery.* Adv Drug Deliv Rev, 2010. **62**(1): p. 83-99.

100. Takahashi Y, Y.M., Tabata Y., Osteogenic differentiation of mesenchymal stem cells in biodegradable sponges composed of gelatin and beta-tricalcium phosphate. Biomaterials, 2005. **26**(17): p. 3587-96.

101. Dumbleton J, M.M., Hydroxyapatite-coated prostheses in total hip and knee arthroplasty. J Bone Joint Surg Am, 2004: p. 2526-40.

102. Kotani Y, A.K., Shikinami Y, Takahata M, Kadoya K, Kadosawa T, Minami A, Kaneda K., Two-year observation of artificial intervertebral disc replacement: results after supplemental ultra-high strength bioresorbable spinal stabilization. J Neurosurg, 2004: p. 337-42.

103. Shikinami Y, K.H., Potential application of a triaxial three-dimensional fabric (3-DF) as an implant. Biomaterials, 1998. **19**(7): p. 617-35.

104. De Aza PN, L.Z., Martinez A, Anseau MR, Guitian F, De Aza S., *Morphological and structural study of pseudowollastonite implants in bone.* J Microsc, 2000: p. 69-7.

105. Kharaziha M, F.M., Improvement of mechanical properties and biocompatibility of forsterite bioceramic addressed to bone tissue engineering materials. J Mech Behav Biomed Mater, 2010. **3**(7): p. 530-7.

106. Mohamed N. Rahaman, D.E.D., B. Sonny Bal, Qiang Fu, Steven B. Jung, Lynda F. Bonewald, Antoni P. Tomsia, *Bioactive glass in tissue engineering.* Acta Biomaterialia, 2011. **7**: p. 2355-2374.

107. Tai BJ, B.Z., Jiang H, Greenspan DC, Zhong J, Clark AE, Du MQ., *Anti-gingivitis effect of a dentifrice containing bioactive glass (NovaMin) particulate.* J Clin Periodontol, 2006. **33**(2): p. 86-91.

108. Oonishi H, H.L., Wilson J, Sugihara F, Tsuji E, Kushitani S, Iwaki H., *Comparative bone growth behavior in granules of bioceramic materials of various sizes.* J Biomed Mater Res, 1999. **44**(1): p. 31-43.

109. Jones JR, L.P., Hench LL, *Hierarchical porous materials for tissue engineering.* Philos Trans A Math Phys Eng Sci, 2006. **364**(1838): p. 81-263.

110. Sheng Hu, J.C., Mingqiu Liu, Congqin Ning, *Study on antibacterial effect of 45S5 Bioglass.* Journal of Materials Science Materials in Medicine 2008. **20**(1): p. 281-6.

111. Vernè E, D.N.S., Bosetti M, Appendino P, Brovarone CV, Maina G, Cannas M, *Surface characterization of silver-doped bioactive glass.* Biomaterials., 2005. **26**(25): p. 5111-9.

112. Luo SH, X.W., Wei XJ, Jia WT, Zhang CQ, Huang WH, Jin DX, Rahaman MN, Day DE., *In vitro evaluation of cytotoxicity of silver-containing borate bioactive glass.* J Biomed Mater Res B Appl Biomater, 2010. **95**(2): p. 441-8.

113. S Simon, A.V., V Simon, H Ylanen, Development and in vitro assessment of bioactive glass/polymer nanostructured composites with silver. Journal of Composite Materials, 2012.

114. Brindley, L. *Fixing bones with dissolvable glass*. physicsworld.com, 2009.

115. Gu, X., et al., Corrosion of, and cellular responses to Mg–Zn–Ca bulk metallic glasses. Biomaterials, 2010. **31**(6): p. 1093-1103.

116. Tamai, H., et al., Antibacterial activated carbons prepared from pitch containing organometallics. Carbon, 2001. **39**(13): p. 1963-1969.

117. Sawai, J., Quantitative evaluation of antibacterial activities of metallic oxide powders (ZnO, MgO and CaO) by conductimetric assay. Journal of Microbiological Methods, 2003. **54**(2): p. 177-182.

118. Ochiai, T., Staphylococcus aureus requires increased level of Ca(2+) or Mn(2+) to grow normally in a high-NaCl/low-Mg(2+) medium. Microbiology and Immunology, 2001. **45**(11): p. 769-76.

119. W.J.E.M. Habraken, J.G.C.W., J.A. Jansen, *Ceramic composites as matrices and scaffolds for drug delivery in tissue engineering.* Advanced Drug Delivery Reviews, 2007. **59**: p. 234-248.

120. H.-W. Kim, J.C.K., H.-E. Kim, Hydroxyapatite and gelatin composite foams processed via novel freeze-drying and crosslinking for use as temporary hard tissue scaffolds. J. Biomed. Mater, 2004. **72**: p. 136-145.

121. Zilberman M, E.J., *Antibiotic-eluting medical devices for various applications.* J Control Release 2008. **130**(3): p. 15-202.

122. Stemberger A, G.H., Bader F, Local treatment of bone and soft tissue infections with the collagen-gentamicin sponge. Eur J Surg Suppl 1997. **578**: p. 17-26.

123. Rutten HJ, N.P., Prevention of wound infection in elective colorectal surgery by local application of a gentamicin-containing collagen sponge. Eur J Surg Suppl, 1997(578): p. 5-31.

124. M., W., Developing bioactive composite materials for tissue replacement. Biomaterials, 2003. **24**(13): p. 2133-51.

125. Corden TJ, J.I., Rudd CD, Christian P, Downes S, McDougall KE., Physical and biocompatibility properties of poly-epsilon-caprolactone produced using in situ polymerisation: a novel manufacturing technique for long-fibre composite materials. Biomaterials, 2000. **21**(7): p. 713-24.

126. Shea LD, S.E., Bonadio J, Mooney DJ., *DNA delivery from polymer matrices for tissue engineering*. Nat Biotechnol, 1999. **17**(6): p. 551-4.

127. Mikos AG, H.S., Ochareon P, Elisseeff J, Lu HH, Kandel R, Schoen FJ, Toner M, Mooney D, Atala A, Van Dyke ME, Kaplan D, Vunjak-Novakovic G., *Engineering complex tissues.* Tissue Eng, 2006. **12**(12): p. 3307-39.

128. Zalfen AM, N.D., Jérôme C, Jérôme R, Frankenne F, Foidart JM, Maquet V, Lecomte F, Hubert P, Evrard B., *Controlled release of drugs from multi-component biomaterials.* Acta Biomater, 2008. **4**(6): p. 1788-96.

129. James D. Kretlow, L.K., Antonios G. Mikos, *Injectable matrices and scaffolds for drug delivery in tissue engineering.* Advanced Drug Delivery Reviews, 2007. **59**: p. 263-273.

130. Avi Domba, A.G.M., *Matrices and scaffolds for drug delivery in tissue engineering.* Advanced Drug Delivery Reviews, 2007. **59**((4-5)): p. 185-186.

131. Mikirova NA, C.J., Riordan NH, Ascorbate inhibition of angiogenesis in aortic rings ex vivo and subcutaneous Matrigel plugs in vivo. J Angiogenes Res, 2010. **2**(2).

132. Wang HL, G.H., Fiorellini J, Giannobile W, Offenbacher S, Salkin L, Townsend C, Sheridan P, Genco RJ; Research, Science and Therapy Committee., *Periodontal regeneration.* J Periodontol, 2005. **76**(9): p. 1601-22.

133. Stosich MS, M.E., Wu JK, Lee CH, Rohde C, Yoursef AM, Ascherman J, Diraddo R, Marion NW, Mao JJ., *Bioengineering strategies to generate vascularized soft tissue grafts with sustained shape.* Methods, 2009. **47**(2): p. 21-116.

134. Wang DA, V.S., Sharma B, Strehin I, Fermanian S, Gorham J, Fairbrother DH, Cascio B, Elisseeff JH., *Multifunctional chondroitin sulphate for cartilage tissue-biomaterial integration.* Nat Mater, 2007. **6**(5): p. 385-392.

135. Kimura Y, I.T., Tabata Y., *Adipose tissue formation in collagen scaffolds with different biodegradabilities.* J Biomater Sci Polym Ed, 2010. **21**(4): p. 463-476.

136. Schantz JT, H.D., Lam CX, Brinkmann M, Wong KM, Lim TC, Chou N, Guldberg RE, Teoh SH., Repair of calvarial defects with customised tissue-engineered bone grafts II. Evaluation of cellular efficiency and efficacy in vivo. Tissue Eng, 2003. **9**: p. 127-39.

137. Navarro M, M.A., Castaño O, Planell JA., *Biomaterials in orthopaedics.* J R Soc Interface, 2008. **5**(27): p. 1137-58.

138. Q. Z. Chen, K.R., D. Armitage, S. N. Nazhat, A. R. Boccaccini, *The surface functionalization of 45S5 Bioglass-based glass-ceramic 73 scaffolds and its impact on bioactivity.* J Mater Sci: Mater Med, 2006. **17**: p. 979-987.

139. Martina Ka¨ llrot, U.E., A.-C. Albertsson, *Surface functionalization of degradable polymers by covalent grafting.* Biomaterials, 2005. **27**: p. 1788-1796.

140. Chau D. Y. S., A., K., Shakesheff K. M., *Microparticles as tissue engineering scaffolds: manufacture, modification and manipulation: MST MST.* Materials Science and Technology, 2008. **24**(9): p. 1031-1044.

141. ChangYou Gao, X.H., Yi Hong, Jianjun Guan, Jiacong Shen, Photografting of poly(hydroxylethyl acrylate) onto porous polyurethane scaffolds to improve their endothelial cell compatibility. J. Biomater. Sci. Polymer Edn,, , 2003. **14**(9): p. 937-950.

142. Jeremy M. Grace, L.J.G., *Plasma Treatment of Polymers.* JOURNAL OF DISPERSION SCIENCE AND TECHNOLOGY, 2003. **24**(3 & 4): p. 305-341.

143. Ming-Hua Ho, L.-T.H., Chen-Yuan Tu, Hsyue-Jen Hsieh, Juin-Yih Lai, Wei-Jung Chen, Da-Ming Wang, *Promotion of Cell Affinity of Porous PLLA Scaffolds by Immobilization of RGD Peptides via Plasma Treatment.* Macromolecular Bioscience, 2005. **6**(1): p. 90-98.

144. Q. F. Wei, H.Y., D. Y. Hou, H. B. Wang, W. D. Gao, *Surface Functionalization of Polymer Nanofibers by Silver Sputter Coating.* Journal of Applied Polymer Science, 2005. **99**(5): p. 2384-2388.

145. Darilis Suárez-González, K.B., Francesco Migneco, Colleen Flanagand, Scott J. Hollisterd, William L. Murphy, *Controllable mineral coatings on PCL scaffolds as carriers for growth factor release.* Biomaterials, 2012. **33**(2): p. 713-721.

146. Kundu B, N.S., Dasgupta S, Datta S, Mukherjee P, Roy S, Singh AK, Mandal TK, Das P, Bhattacharya R, Basu D., Macro-to-micro porous special bioactive glass and

ceftriaxone-sulbactam composite drug delivery system for treatment of chronic osteomyelitis: an investigation through in vitro and in vivo animal trial. J Mater Sci Mater Med, 2011. **22**(3): p. 705-20.

147. Ghosh SK, N.S., Kundu B, Datta S, De DK, Roy SK, Basu D., In vivo response of porous hydroxyapatite and beta-tricalcium phosphate prepared by aqueous solution combustion method and comparison with bioglass scaffolds. J Biomed Mater Res B Appl Biomater, 2008. **86**(1): p. 217-27.

148. Zhang X, J.W., Gu Y, Xiao W, Liu X, Wang D, Zhang C, Huang W, Rahaman MN, Day DE, Zhou N, *Teicoplanin-loaded borate bioactive glass implants for treating chronic bone infection in a rabbit tibia osteomyelitis model.* Biomaterials, 2010. **31**(22): p. 5865-74.

149. Zhang Y, Z.M., Calcium phosphate/chitosan composite scaffolds for controlled in vitro antibiotic drug release. J Biomed Mater Res, 2002. **62**(3): p. 378-86.

150. Chang HI, P.Y., Coombes AG., Delivery of the antibiotic gentamicin sulphate from precipitation cast matrices of polycaprolactone. J Control Release, 2006. **110**(2): p. 414-21.

151. Kim, H.W., et al., *Degradation and drug release of phosphate glass/polycaprolactone biological composites for hard-tissue regeneration.* Journal of Biomedical Materials Research Part B-Applied Biomaterials, 2005. **75B**(1): p. 34-41.

152. Zamani, M., et al., Controlled release of metronidazole benzoate from poly epsilon-caprolactone electrospun nanofibers for periodontal diseases. European Journal of Pharmaceutics and Biopharmaceutics, 2010. **75**(2): p. 179-185.

153. Otto S Kluin , H.C.v.d.M., Henk J Busscher , Daniëlle Neut *Biodegradable vs non-biodegradable antibiotic delivery devices in the treatment of osteomyelitis.* Exp Opin Drug Delivery, 2013. **10**: p. 341-351.

154. A.M. Hoang, T.W.O., Dr. D.L. Cochran, *In Vitro Wound Healing Responses to Enamel Matrix Derivative.* Journal of Periodontology, 2007. **71**(8): p. 1270-77.

155. Hill, K.E., et al, An in vitro model of chronic wound biofilms to test wound dressings and assess antimicrobial susceptibilities. Journal of Antimicrobial Chemotherapy, 2010. **65**(6): p. 1195-1206.

156. Roth, C., et al., Response Analysis of Stimulating Efficacy of Polihexanide in an in vitro Wound Model with Respiratory Ciliary Epithelial Cells. Skin Pharmacology and Physiology, 2010. **23**: p. 35-40.

157. Woods, J., et al, *Development and application of a polymicrobial, in vitro, wound biofilm model.* Journal of Applied Microbiology, 2012. **112**(5): p. 998-1006.

158. Lin, W., et al, Toxicity of nano- and micro-sized ZnO particles in human lung epithelial cells. Journal of Nanoparticle Research, 2009. **11**(1): p. 25-39.

159. Sun, Y., et al, *In vitro multispecies Lubbock chronic wound biofilm model.* Wound Repair and Regeneration, 2008. **16**(6): p. 805-813.

160. Assadian, O., et al, Bacterial growth kinetic without the influence of the immune system using vacuum-assisted closure dressing with and without negative pressure in an in vitro wound model. International Wound Journal, 2010. **7**(4): p. 283-289.

161. Ngo, Q.D., K. Vickery, and A.K. Deva, *The effect of topical negative pressure on wound biofilms using an in vitro wound model.* Wound Repair and Regeneration, 2012. **20**(1): p. 83-90.

162. Pitt, C.G., T.A. Marks, and A. Schindler, Biodegradable drug delivery systems based on aliphatic polyesters: application to contraceptives and narcotic antagonists. NIDA Res Monogr, 1981. **28**: p. 232-53.

163. Hu, S., et al., *Study on antibacterial effect of 45S5 Bioglass*. J Mater Sci Mater Med, 2009. **20**(1): p. 281-6.

164. Allan, I., H. Newman, and M. Wilson, Antibacterial activity of particulate bioglass against supra- and subgingival bacteria. Biomaterials, 2001. **22**(12): p. 1683-7.

165. Verrier, S., et al., PDLLA/Bioglass (R) composites for soft-tissue and hard-tissue engineering: an in vitro cell biology assessment. Biomaterials, 2004. **25**(15): p. 3013-3021.

166. Goldstein, J., Scanning electron microscopy and x-ray microanalysis2003: Kluwer Adacemic/Plenum

167. Chow, B., Development of a Bioactive Skin Graft in School of AMME 2001, University of Sydney.

168. Li, O.Y.H., Development of an Injectable Soft Tissue Scaffold for Restoration of Facial Form and Function, in School of AMMW2010, University of Sydney.

169. Drake, D.a.M., T.C.,, *Flagella, Motility and Invasive Virulence of Pseudomonas aeruginosa.* Journal of General Microbiology, 1988. **134**: p. 43-52.

170. Vasil, M.L., Pseudomonas aeruginosa: Biology, mechanisms of virulence, epidemiology. The Journal of Pediatrics, 1986. **108**: p. 800-805.

171. Bart Gottenbos, H.C.v.d.M., Henk J. Busscher, *Initial adhesion and surface growth of Staphylococcus epidermidis and Pseudomonas aeruginosa on biomedical polymers.* Journal of Biomedical Materials Research Part B-Applied Biomaterials, 1999. **50**(2): p. 208-14.

172. Verheyen, C.C.P.M., et al, Adherence to a metal, polymer and composite by Staphylococcus aureus and Staphylococcus epidermidis. Biomaterials, 1993. **14**(5): p. 383-391.

APPENDIX

SCAFFOLD MODIFICATION DATA

BMG-coating mass verification: raw data

	No. of scaffolds weighed	$M_{initial}$ (g)	M_{final} (g)	M_{BMG}/scaffold (mg)
Plain	23	0.97051	1.08435	4.949565
			average:	**4.949565**
BG-infused	14	0.50672	0.52647	1.410714
	6	0.18748	0.19447	1.165
	16	0.57309	0.59145	1.1475
			average:	**1.241071**

Equation for Calculating Total Mass of Antibiotics

$$\frac{Absorbance}{Std\ Curve\ Slope} \times Dilution\ factor \times Initial\ Sample\ Volume$$

Where;

Standard curve slope = 0.0109

Dilution factor = 50 for antibiotic loading (since 20uL sample in 1mL cuvette volume)

= 5 for elution profile (since 200uL sample in 1mL cuvette volume)

Initial Sample Volume = volume in sample vial prior to sampling

MICROBIOLOGICAL EVALUATION DATA

Average counts and standard deviations

	Wound Model Set 1			Wound Model Set 2			Wound Model Set 3		
Average	Control Coupons	Plain	BG-infused	BMG-coated	Ab-coated	BG+Ab	BG+BMG	BMG+Ab	BG+BMG+Ab
Scaffold 4days	1.75E+06	3.03E+08	1.50E+05	0.00E+00	0.00E+00	0.00E+00	3.24E+07	1.53E+08	2.85E+06
Scaffold 6days	1.95E+07	0.00E+00	3.75E+05	4.43E+03	1.88E+04	5.88E+04	4.88E+07	7.35E+08	1.39E+06
Coupon 4days	6.70E+08	9.40E+07	1.75E+04	8.17E+02	0.00E+00	1.50E+02	2.84E+08	5.85E+07	8.75E+06
Coupon 6days	7.74E+07	0.00E+00	5.38E+06	1.49E+05	9.87E+03	5.75E+05	1.79E+08	1.86E+08	1.70E+06

Stdev	Control Coupons	Plain	BG-infused	BMG-coated	Ab-coated	BG+Ab	BG+BMG	BMG+Ab	BG+BMG+Ab
Scaffold 4days	2.83E+05	5.25E+08	2.60E+05	0.00E+00	0.00E+00	0.00E+00	2.26E+07	2.36E+08	1.92E+06
Scaffold 6days	3.04E+07	0.00E+00	5.65E+05	4.14E+03	3.22E+04	8.01E+04	2.88E+07	1.27E+09	1.43E+06
Coupon 4days	1.15E+09	1.61E+08	2.82E+04	1.41E+03	0.00E+00	2.18E+02	1.87E+08	7.97E+07	1.24E+07
Coupon 6days	1.32E+08	0.00E+00	9.19E+06	1.96E+05	1.44E+04	8.09E+05	1.14E+08	2.61E+08	2.12E+05